UNIVERSITY OF BIRMINGHAM

THE SCALE UP OF AIR FILLED EMULSION PRODUCTION

by

LIAM JOHN CRITCHLEY

A thesis submitted to the University of Birmingham for the degree of MASTERS BY RESEARCH

Supervised by DR PHILIP COX

School of Chemical Engineering

College of Engineering Physical Sciences

The University of Birmingham

ABSTRACT

An Air Filled Emulsion (AFEs) is a dispersion of particles, of colloidal size, that are generally characterised from sub-micron to ten microns in diameter. They are produced by unfolding proteins so that the disulphide bonds in the protein react with superoxide radicals. The radicals are formed from injecting air into a sonochemical reactor where the cavitation bubbles produce enough energy to create these radical species, which in turn template the reaction to form 'air cells'. These air cells are what form the non-aqueous phase in AFEs. AFEs can be used as formulation agents in whipped toppings to reduce the fat content in such foods. The aim of this project was to see if the production of AFEs could be scaled up from bench to pilot scale, potentially making the production more viable at an industrial level and therefore more likely that AFEs will be used in the near future as healthier alternatives to fats. The backbone of the project focused around whether that waste and excess precursors to AFE (protein solutions) could be recycled, therefore minimising wastage and maximising the output. Results showed that recycle methods produced up to 98.7 % AFE yield with two out of three top-up methods (STUM) producing >90 % AFE yield. Other methods which were non-top-up (NoTUM) did not produce a high yield, but showed that air cells are robust enough to withstand multiple passes of sonication waves and heating. These methods also yielded the first continuous method of AFE production. This was adapted to produce a novel way of isolating and concentrating AFE ready for formulation, which concentrated the AFE up to 6 times previously found using a cross flow filtration module. Work on the pilot scale produced the first AFE sample beyond the bench scale, and combined with the novel methods it provides a promising benchmark to take the production to larger scales in the future.

COLLABORATORS

Academic:

DR PHILIP COX (The University of Birmingham, Senior Lecturer) ALISTAIR JOHN GREEN (The University of Birmingham, EngD student)

Industrial:

MIKE PIATKO (Rich Products, Principal Scientist)

COLETTE JERMANN (Campden BRI, Food Scientist)

TECHNOLOGY STATEGY BOARD (Innovate UK)

Students Supervised:

Heloisa Didier (The University of Birmingham, Student)

Milton Junior (The University of Birmingham, Student)

ACKNOWLEDGEMENTS

I would like to thank all of my family and friends for their continued support throughout my studies. I would especially like to thank my fiancée Emma and my son Luke for helping me through hard and stressful times. I would also like to thank Emma for being selfless and for continuing to put up with me whilst I continue to be a student. I'd also like thank both my parents (and their partners) and my grandparents, whom have supported me right throughout my studies and encouraged me to achieve the best that I can.

A very big thank you goes out to my supervisor Dr Philip Cox, for his continued support throughout my studies and for giving me the opportunity to undertake this research. I hope the research I have done has made it as worthwhile for him as it has for me. I would also like to thank Alistair Green for his help throughout my MPhil and providing both technical and ideological insight. Especially for when the equipment failed and he managed to sort out the problems every time. I would also like to thank him for driving me down to Campden BRI on multiple occasions. I would like to thank them both in helping to transition from a chemist to a chemical/formulation engineer. I would also like to thank Sarah Santos-Murphy for help with day to day issues.

I would like to thank the Technology Strategy Board (Innovate UK) for funding the project, without which I wouldn't be writing this. I would also like to thank Mike Piatko and the rest of the people at Rich's Products for providing the research project. I would also like to thank Campden BRI for letting me to use their facilities to do my pilot scale research. I would especially like to thank Collete Jermann for helping out with the research down at Campden BRI.

I would like to thank Elaine Mitchell, Dave French, Ronnie Baglin and Zarmina Butt, the support staff in the Chemical Engineering and Bio-Chemical Engineering departments at The University of Birmingham, for backline help with equipment and the general running of everyday things, which helped in many ways. I'd also like to thank Lynn Draper who helped

out on the administrative side and has printed off lots of documents for me when my student card was experiencing problems.

ABBREVIATIONS AND DEFINITIONS

AFE	Air Filled Emulsion
AFEs	Air Filled Emulsions (plural)
EWP	Egg White Protein
WPI	Whey Protein Isolate
BSA	Bovine Serum Albumin
EWP-AFE	Air Filled Emulsion produced from Egg White Protein
BSA-AFE	Air Filled Emulsion produced form Bovine Serum Albumin
HCl	Hydrochloric Acid
Air Cell	Air particles encased by a protein shell
Quality of AFE	Quality relates to the amount of air cells present in solution
STUM	Solution Top-Up Method
NTUM	Non Top-Up Method
NTUCeM	Non Top-Up Centrifugal Method
NTUCoM	Non Top-Up Continuous Method
WBH	Water Bath Heating
HE	Heat Exchanger
O/W	Oil in Water (Emulsion)
W/O	Water in Oil (Emulsion)
A/O/W	Air in oil in water (Emulsion- tri-phasic/double)

CFF	Cross-Flow Filtration
**	Experiments assisted by students Heloisa and Milton

CONTENTS

ABSTRACT 2
COLLABORATORS 3
ACKNOWLEDGEMENTS 4
ABBREVIATIONS AND DEFINITIONS 6
CHAPTER 1- INTRODUCTION 11
1.1. Context of the study 11
1.2. Aims of the Project 12
1.3. Thesis Structure 12
1.4. Publications 13
CHAPTER 2- LITERATURE REVIEW 14
2.1. Air-Filled Emulsions (AFEs) 14
2.2. Proteins 18
2.2.1. Egg White Protein (EWP) 18
2.2.2. Protein Unfolding and Denaturation 24
2.3. Sonochemistry 29
2.3.1. Cavitations 29
2.3.2. Ultrasonic Cavitation Parameters 31
2.3.3. Ultrasonic Probes 33
2.4. Experimental Parameters 35
2.4.1. Centrifugation 35
2.4.2. Mixing Methods 35
2.4.3. Concentration Gradients 36
2.4.4. Flow rates and Residence Time 37
2.4.5. Recycle Methods 38
CHAPTER 3- MATERIALS AND METHODS 41
3.1. Introduction 41
3.2. Materials and equipment used 41
3.2.1. Materials 41
3.2.2. Equipment 41
3.3. Experimental Methods 42
3.3.1. Air Filled Emulsion Production 42
3.3.2. Air Filled Emulsion Analysis 43
3.3.3. Experimental Variable Parameters 44
3.3.4. Critchley-Green Recycling Methods 45
3.4. Experimental Flow Schematics 48
3.5 Control Experiments 51
3.5.1 Dry Weight Analysis 51
3.5.2 Centrifuge 53
3.5.3. Amplitude vs Energy 55

CHAPTER 4- PREVIOUS AND INITIAL STUDIES (BATCH MODE WITH NO RECYCLES) 58
4.1. Previous Studies 58
4.2. Parallel Studies 58
4.3. Initial Project Studies 59
4.3.1 Introduction 59
4.3.2. Reheating 59
4.3.3 Testing Various Amplitudes 61
4.4.4 Conclusion 65
CHAPTER 5- THE CRITCHLEY-GREEN RECYCLE METHODS 66
5.1 Introduction 66
5.2 The Solution Top-Up Method (STUM) - Water Bath Heating (WBH) 66
5.2.1 Quantitative analysis 66
5.2.2 Qualitative Analysis 73
5.3. The Solution Top-Up Method (STUM) With a Heat Exchanger (HE) 75
5.3.1. Introduction 75
5.3.2. Ambient Starting Temperature 76
5.3.3. Cold Starting Temperature 82
5.3.4. Summary of STUM Methods 86
5.4. Non Top-Up Recycle Methods (NoTUM) 87
5.4.1. Non Top-Up Centrifugal Method (NoTUCeM) 88
5.4.2. Non Top-Up Continuous Method (NoTUCoM) 92
5.4.3 Conclusion of NoTUM's 97
5.5 Energy output of NoTUM against STUM 98
5.6. Critchley-Green Recycling Method Conclusions 99
CHAPTER 6- CROSS-FLOW FILTRATION (CFF) OF AFEs 100
6.1. Introduction 100
6.2. Two Stage Process 101
6.3. One Stage Process 104
6.4. CFF Conclusion 109
CHAPTER 7- PILOT SCALE WORK (CAMPDEN BRI) 110
7.1. Introduction 110
7.2. Methods 110
7.2.1. Equipment and Materials 110
7.2.2. Method for AFE Production 111
7.2.3. Design of Experiments 112
7.3. Problems and Solutions 116
7.3.1 Problems 116
7.3.2. Solutions 118
7.4. Results 121
7.4.1 Optimisation Analysis 121
7.4.2. Statistical Analysis 123

7.4.3. Performing a Recycle on the Pilot Scale 125
7.5. Conclusion 127
Chapter 8- Conclusion and Future Work 128
8.1. Conclusion 128
8.2 Future Work 131
REFERENCES 139
APPENDIX..... 146

CHAPTER 1- INTRODUCTION

1.1. Context of the study

Large amount of foods these days contain a significant portion of unhealthy fats. There is a constant demand and pressure from governments and the general public to reduce the fat content of many products to fit in with today's healthy lifestyle and obesity crisis. One of the worst contenders for being unhealthy is foods of the sweet variety. New ways of combating obesity are being implemented but because people can still eat what they want, the fundamental solution will come from food industries to replace saturated fat with trans-fat or other alternatives. These alternatives however have to have the same textural feel as fats but also have to have a high stability [1-2].

The project is with Rich Product, a large American food company who specialise in sweet food such as cakes. The product in question within this project is whipped toppings for cakes. This project does not deal with the formulation of the food product itself. But, it ran in conjunction with another project (EngD) in the school led by Alistair Green.

The EngD project was undertaken by Alistair to replace fat content in whipped topping by replacing a portion of the fats with Air Filled Emulsions (AFEs). A lot of work has been previously undertaken on the production of AFES, characterising their stability and the ability to be used in foodstuffs, (*Tchuenbou-Magaia et al, 2009-2011*). However, for AFEs to be used in food, the production on a larger scale needs to maximised otherwise the concept of using AFE as a fat replacement would be economically unviable. This is where this project comes in. Where Ali undertook the formulation side of the product, this project was designed to optimise the small scale production and especially identify a method to re-use waste. This is the strongest factor to make the process economic because finding a way to use waste material means, less starting material and less waste which ultimately means more efficiency and profit. The project was not intended to just utilise the bench scale, upon fining a way to optimise on the small scale, the aim was to use the facilities at Campden BRI (Food

and Drink Innovation Centre) to scale up the process to the pilot scale. If this was to be successful, then it could pave a way for many more projects to look into optimising the industrial/factory scale.

1.2. Aims of the Project

The main aims of the project were to start research into recycling methods and adapt them to maximise the output of AFE whilst minimising waste which is to minimise the overheads for industry. The other main aim of the project was to see if production on the pilot scale was possible, and if the production process is feasible for industry to take the production beyond the bench scale.

1.3. Thesis Structure

This section (chapter 1) is concerned with giving an introduction to the project and the reasons for research into this area. Following on from this is Chapter 2, which is a literature review of the topics concerned with this project. The literature review centres around four main topics: Air Filled Emulsion (AFEs), Proteins, Sonochemistry and Experimental Parameters.

Chapter 3 details what materials and equipment were used during the experiments. It also describes the experimental methods used in the project and includes schematic/flow diagrams for each experimental setup.

Chapter 4 gives examples of studies which have been previously undertaken in this department that are related to this project and shows the initial testing results.

Chapter 5 is the main chapter of the thesis and details the results of the Critchley-Green Recycling Methods including all the methods associated with re-concentrating the waste solution (STUM) and those that are not (NoTUM) and gives an explanation into the possible outcomes of the scalability based on the findings from the bench scale.

Chapter 6 is concerned with the final work on the bench scale. It describes the use of a cross-flow filtration module to extract and concentrate AFE samples.

Chapter 7 is the section on the pilot scale work at Campden BRI. This chapter describes all of the work undertaken on the larger pilot scale.

Chapter 8 is a conclusion/summary of the work produced in this project and any future work that can be undertaken in this field following this project.

Following Chapter 8, there is a list of references which are in the format of the Royal Society of Chemistry (RSC) referencing system. The Appendix at the end of report shows the raw data obtained for the Mastersizer, the data tables and the dry weight analysis raw data.

1.4. Publications

There are no current publications associated with the project as the aim is to patent after the project has finished.

CHAPTER 2- LITERATURE REVIEW

2.1. Air-Filled Emulsions (AFEs)

A standard emulsion consists of either two or three phases and are termed bi-phasic and tri-phasic, respectively. Standard emulsions are formed from two or more immiscible liquids with varying degrees of hydrophobicity. Standard emulsions generally contain an oil phase and a water phase. An Air-Filled Emulsion however is different to a normal emulsion. Rather than the standard oil-in-water (o/w) or water-in-oil (w/o), an Air-Filled Emulsion only contains a protein stabilised air phase and an aqueous (water) phase and contains no oil phase, so hence it has great potential for incorporation into low fat emulsions for the food industry [1-3]. An Air Filled Emulsion (AFE) is a dispersion of particulates, of colloidal size, that are generally characterised from sub-micron to ten microns in diameter. They are produced under sonochemical irradiation using a cysteine rich protein solution which has been both pH and temperature adjusted. The reaction occurs due to cavitation's which cause bubble collapse within the solution [4]. The cavitation's are of high energy and are what form the template for the formation of 'air cells' within the AFE. Upon exposure to the sonochemical energy, the oxygen from the air supply form superoxide radical species and template within the cavitational voids produced by the sonicator. The di-sulphide bonds within the cysteine residues in the Egg White Protein (EWP) solution form a cross link with the radical species to form a 'cage-like' structure. This in turn forms the protein coat under self-assembly (non-native conformation) and hence the closure of the molecules to form the air cells [1,5]. These air cells are what form the non-aqueous phase in AFEs.

Air-Filled Emulsions were originally produced using cysteine rich hydrophobins. But due to the lack of availability and cost of the hydrophobins, the process was not viable from an industrial standpoint [1,6]. Hydrophobins are a group of small cysteine rich proteins consisting of around 100 amino acids. Hydrophobins work by lowering the surface tension, allowing

smaller droplets or ‘air cells’ to be produced within the desired range of 0.5 to 10 microns. As well as reducing the surface area, they also enhance stability in the form of quick self-assembly around the radical oxygen species which minimises emulsion instabilities such as coalescence, flocculation, Ostwald ripening and creaming [7]. Hydrophobins are formed in solution from a monomeric form to form dimers and tetramers. These forms protect the hydrophobins from polar conditions so that large aggregates do not occur. As water is a weak electrolyte and can form H^+ and OH^- ions simultaneously, the hydrophobin is therefore protected from the electrolyte screening the electrostatic forces of repulsion between monomers and therefore no excessive aggregation occurs. Hydrophobins can self-assemble into films, and it is these protein films that can self-assemble around oxygen radicals, solidify and in turn produce the hydrohobic protein coat. The solidified protein coat is also found to have elastic properties in which it has a relaxation state that it will return to, after being subjected to stress and strain forces. It is believed that the elasticity of the protein coat is what gives the air cells their enhanced stability and robustness and allows them to be formulated efficiently; as they are able to withstand stresses and strains in various industrial environments.

Because the main application for Air-Filled Emulsions, be it from hydrophobins or otherwise, is for the replacement of fats in food products [3,8-11], then the emulsion needs to have both the same textural and rheological feel in the mouth that fat does [1]. Whilst the primary aim and the focus on this project is for low fat foods, Air-Filled Emulsions alongside other protein-based microbubble formulations are now widely becoming used in variety of applications such as biomedical research [12-14] and the treatment of decontaminant waste [15].

From hydrophobins, cheaper alternatives have been explored which have similar mechanical and physical properties that interact with the superoxide radicals in the same way that hydrophobins do. These include proteins which are rich in cysteine residues such as Egg White Protein (EWP) and Bovine Serum Albumin (BSA) [6]. The research into these two

proteins by *Tchenbou-Magaia et al* [1] allowed for a new class of Air-Filled Emulsions to be produced from both EWP (EWP-AFE) and from BSA (BSA-AFE). EWP-AFEs have found to have good stability and turbidity, [6] and the proteins can self-assemble under sonochemical conditions just like hydrophobins. They have also been found to be texturally and rheologically comparable to hydrophobins, creating a class of AFEs that is cheap, accessible and works as well as any AFE currently produced today [1]. The egg white protein forms the outer shell whilst the oxygen radical occupies the core of the air cell. This is shown in Figure 1. The production of EWP-AFEs depend on numerous factors which have to be optimised in order to yield a 'good' emulsion. These include keeping the solution within a desired pH range (3.8 ± 10), ionic strength, temperature of the solution (50 ± 5 °C) and the concentration of the stating protein solution (5 %w/v). Some of these factors, predominantly pH and temperature have a large influence of the production of AFEs. It has been found by *Tchuenbou-Magaia et al* that above pH 4, the process does not work properly and the yield is lower. This is due to the protein not being able to unfold (see section 2.2.2.1.). It has also been shown that at temperatures above 50 °C, especially for large periods of time is counterproductive to AFE formation as the proteins start to denature (see section 2.2.2.2.), and start to aggregate together rendering them unusable. Air cells that have been formed outside of the optimal conditions show a much greater instability than their counterparts produced at specific optimised conditions. However, with the conditions known, it is very easy to tune the conditions towards optimal production and those air cells are inherently stable and can survive thermal treatments greater than 120 °C [6]. This makes them robust enough to survive food processing plants and is useful because the presence of AFE can enhance the stability of whipped topping products compared to solely oil-based counterparts.

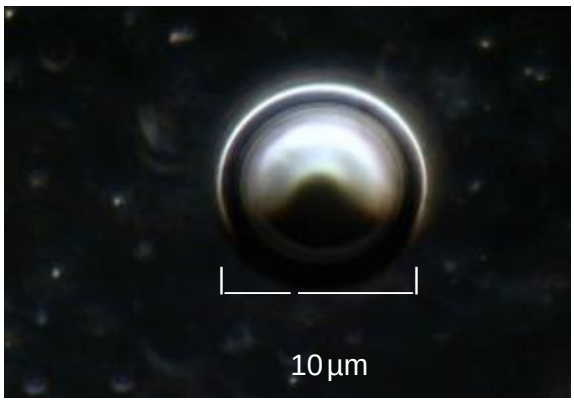

Figure 2-1. An air cell imaged using a Motic Imaging Camera showing the two main phases: - the self-assembled protein coat and the core consisting of oxygen species.

Because they are comparable to hydrophobin based AFEs, they have been used as a fat replacement in tri-phasic emulsions consisting of an air in oil in water (A/O/W) emulsion. The air phase acts as a replacement for some of the oil present in the formulation. These A/O/W emulsions are being tested in the food industry for low-fat whipped toppings. The different structures of EWP-AFE and A/O/W are shown in Figure 2. In the same way that AFEs need certain concentrations and conditions to make the emulsion stable, A/O/W need certain concentrations to make the formulations stable. To obtain a stable formulation it has been found that a 28 % A/O/W emulsion composed of 10 % Air and 18 % oil is needed in these quantities. This allows for the tribological and rheological behaviour to behave in the mouth as if it were fat. Other quantities have been tested and worked, but it was found that additional stabilisers were needed in the form of xanthan gum and Whey Protein Isolate (WPI) to stabilise the formulations [1,2]. This is due to the air cells in the air phase causing increased coalescence compared to its O/W counterparts. The air cells cause a reduction in the friction co-efficient and enhance lubrication of the A/O/W emulsion. This allows the particles to move more freely and collide together, which in turn causes the electrostatic forces between the droplets to breakdown and merge into larger droplets and form a polydisperse emulsion. This can cause the rheological properties of the emulsion to change due to the increased size of the emulsion droplets. Lubricating properties of the air cells can also be attributed to a varying degree of other factors such as the protein shell absorbing

onto surfaces and droplet spreading (causing hydrophilicity of the drops and reducing their contact angle at the three-phase interface of surface, air and fat) [1,2,16].

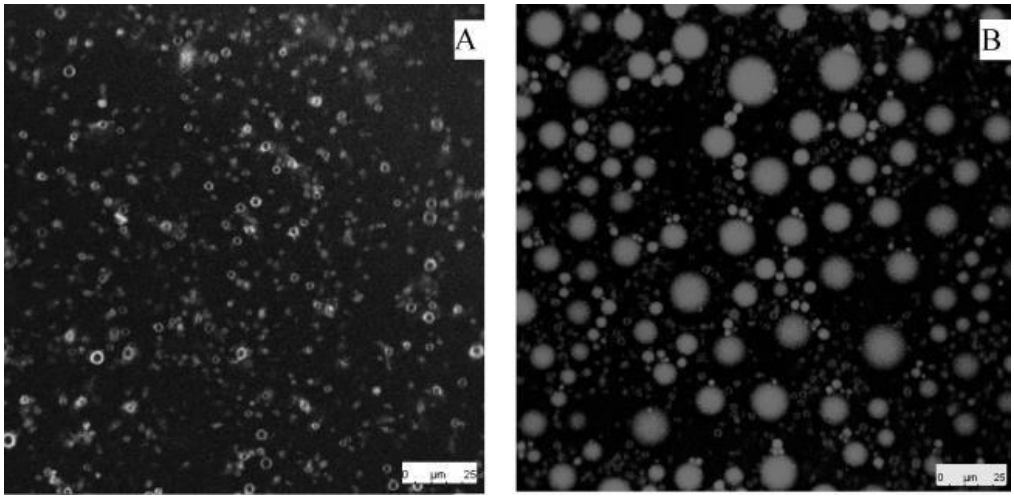

Figure 2-2. "TYPICAL MICROGRAPHS OF AFEs (A) and (B) are confocal micrographs of the AFE stabilised with egg white proteins (AFE_EWP) and an air based A/O/W emulsion respectively." Taken by TchuenbouMagaia F. [1-2]

So in using AFEs as formulation agents in food, many factors need to be considered including relative concentrations, lubricating and rheological properties as well as limiting the amount of emulsion-based instabilities present in the formulation.

2.2. Proteins

2.2.1. Egg White Protein (EWP)

An egg consists of three main regions: - The outer shell- which is a semi-porous calcium carbonate material that protects the internal components. The yolk- which roughly makes up a third of the egg and contains virtually all of the lipids in the egg, as well many different types of vitamins. And egg white- which is low in lipids but contains over half of the total proteins found in an egg. The proteins in egg white make up between 9 and 11 % by weight of the total composition of the egg white. The rest is made up of water and is an alkaline solution [17-18]. Egg White Protein (EWP) consists of a multitude of different proteins and has a high concentration of cysteine rich proteins with the highest concentration being ovalbumin making up 54 % of all the proteins in egg white. This is followed by ovotransferrin at 12 %, ovomucoid (11 %), ovomucin (3.5 %) and lysozyme (3.4 %). These are the top five highest

occurring proteins in EWP but it also consists of other proteins including ovoglobulin, ovoinhibitor, and ovoglycoprotein, all of which have a concentration of at least 1 %, plus many more with negligible concentrations [17].

2.2.1.1 Ovalbumin

As previously mentioned, it is the most abundant protein in egg white, so when reactions take place involving egg white, then the majority of reactions will take place with ovalbumin plus the other four highest concentrated proteins. Because of this, it is important to understand how the various proteins interact and how they differ as they can be involved in the reaction processes simultaneously. Ovalbumin is a member of the serpin family and has a very similar structure to Bovine Serum Albumin [19] (BSA). It has a molecular weight of 42.7 kDa. A Dalton (Da) is equivalent to $1/12^{th}$ of a carbon atom. Due to the size of the protein molecule it is easier to define the molecular weight in Da/kDa rather than $gmol^{-1}$. The structure consists of a sequence of 385 amino acids which assemble together to form a monomeric phosphoglycoprotein. It is a cysteine rich protein with four sulphur bonding regions and a disulphide bridge. These sulphur binding points are only available upon unfolding of the protein, making them an ideal candidate for AFE formation via a superoxide template mechanism. The secondary structure is mainly composed of α-helix (41 %) and β-pleated sheets (34 %) as well as β-turns and random coils [20]. It also has a well ordered 3-D heterogeneous structure with a reactive outcrop from the main body of the protein, which allows for a multitude of binding reactions including phosphorylation and glycosylation [21].

In addition to ovalbumin, S-ovalbumin is also found naturally in egg white and is thought to contribute to the heterogeneous nature of the molecule. S-ovalbumin has a greater thermal stability and has a higher denaturing temperature by 8 °C (92.5 °C compared to 84.5 °C of ovalbumin) [18]. Other factors including its crystallinity, amount of sulphur residues, and molecular weight are the same as ovalbumin. The reason for the increase in thermal stability is due to the structure being more compact and therefore more tightly bound. This compact

structure also increases the hydrophobicity of the surface due to less surface area interactions with the more hydrophilic groups of the protein, promoting hydrophobicity [22]. There has been no mechanism confirmed for the interconversion of ovalbumin and S-ovalbumin, however it is known that pH and the age of the protein have an effect on the ratios of ovalbumin and S-ovalbumin found in a sample. It has been found that for a fresh egg white sample, the amount of S-ovalbumin present is around 5 % compared with 81 % after 6 months stored under cool conditions [22-23].

Both ovalbumin and S-ovalbumin are able to unfold, denature and aggregate. Denaturation for ovalbumin can be calculated by equation (1) [24]:

$$N_1 \underset{k_{-1}}{\overset{k_1}{\rightleftharpoons}} U_1 \overset{k_2}{\rightarrow} D_1 \rightarrow A \qquad (1)$$

Where N, U, D and A correspond to native, unfolded, denatured and aggregated conformations of the protein and k_1, k_2, and k_{-1} equate to the rate constants for the reactions. It is assumed that D can only form aggregates after the protein is denatured. U corresponds to the reversible unfolding of the protein and not irreversible unfolding [25-27]. Under denaturation, the thiol groups can become exposed due to the increase of hydrophobic interactions. The exposure of thiol groups exposes the sulphur atoms and can form disulphide bridges with other denatured proteins, which are of the same nature. In the same way that superoxide radicals can react with the disulphide bridges to form air cells (section 2.2.1), to give an irreversible reaction, the same occurs and therefore an irreversible aggregation can occur, rendering the protein unusable [28]. Irreversible protein unfolding/denaturation involves two different steps. The first is the reversible unfolding of the original protein which is followed by altering of the unfolded protein into a denatured state via an irreversible process. If k_2 is of a much greater value than k_1 then the majority of the unfolded proteins will be converted into denatured protein. This results in a first order

reaction with the rate determining step (r.d.s) and the limitations being k_1. This can be then shown in the form of equation (2) [29]:

$$N \xrightarrow{k} D \quad (2)$$

2.2.1.2. Ovotransferrin

Ovotransferrin makes up 12 % of the total protein contained in egg whites and is the second largest abundant protein. It is a type of monomeric glycoprotein with a molecular weight of 77.7 kDa and consists of 686 amino acids. As the name suggests, it is a protein which has an affinity for iron binding [22,30]. Ovotransferrin is known to have antimicrobial properties and it is the binding efficiency to iron that is thought to produce this effect. Ovotransferrin folds into two lobes denoted as the C and N lobes, with an iron binding site located within each of the two regions associated with each lobe. Per protein molecule two Fe^{3+} ions can be accommodated into the binding sites as can two carbonate (CO_3^{2-}) ions. The binding sites consist of histidine residues as well as tyrosine and aspartic acid molecules [31].

Ovotransferrin contains fifteen disulphide bridges between the two lobes with six being found in the N-lobe and nine found in the C-lobe. Each lobe contains four domains which are composed of two α-domains and two β-domains. These are linked with strands that are β-antiparallel strands and act as a hinge. The large amount of sulphur bridges makes it a good candidate for AFE formation as there is plenty of binding sites for the superoxide radical species, resulting in a high binding efficiency [32]. Ovotransferrin can isolate iron ions and is thought that this is what gives it its antimicrobial properties, as it can isolate the iron required for the growth of microorganisms and cause iron deprivation. It is believed that this iron binding and isolation is what gives egg white in general its antimicrobial properties, which is an important factor to consider when producing products for the food industry [33].

2.2.1.3. Ovomucoid

Ovomucoid accounts for 11 % of the total amount of protein in egg white and is known to be one of the most highly glycosylated proteins in the composition of egg white [34]. The molecular weight of ovomucoid is 28 kDa and 25 % of the proteins are present as carbohydrates, which are bound to aspartic acid residues. The tertiary structure is composed of three regions which are linked by disulphide bridges, of which there are nine in total in one ovomucoid protein molecule [35]. Out of the three regions, two of them contain carbohydrate chains and one is absent of carbohydrates. The carbohydrates present in the chains are mannose, galactose and acetyl glucosamine. The secondary structure consists mainly of β-pleated sheets at which 46 % of amino acids adopt this conformation. 26 % adopt a α-helix conformation and 18 % and 10 % of amino acids adopt random coils and β-turns, respectively. Due to the presence of the disulphide linkages, the structure of ovomucoid is very stable and can survive acidic conditions at temperatures up to 100 °C for an extended period of time [22]. One negative aspect for consideration in the food industry, is that it is known to be a trypsin inhibitor (protease enzyme in the digestive system). Under extreme conditions, the inhibitory properties can be lost due to reducing and alkylating of the disulphide linkages [18]. Ovomucoid also has the ability to control microorganisms, making it a useful molecule as an antimicrobial agent in food products [32].

2.2.1.4. Ovomucin

Ovomucin makes up roughly 3.5 % of all proteins in egg white, and is a viscous glycoprotein. Ovomucin consists of both soluble and insoluble regions. The soluble regions are much smaller in comparison to the insoluble regions where the soluble component has a molecular weight of 8300 Da compared to the molecular weight of the insoluble component which ranges between 220 and 270 kDa [36]. Because of this, ovomucin is insoluble in water unless it is subjected to high electrolyte concentrations or a high alkaline pH [18]. It is one of the largest protein molecules containing carbohydrate moieties and is the reason why egg

whites adopt a gel-like structure [37]. Ovomucin consists of two sub-regions- α and β. α-ovomucin is homogenous and is composed of acidic amino acids such as aspartic and glutamic acid and contains a lower concentration of carbohydrates (15 %). β-ovomucin is different in nature in that it is heterogeneous and is mainly made up of serine and threonine residues, and it contains a much higher concentration of carbohydrates (50 %) [38]. There are multiple carbohydrates present including galactose, sialic acid and hexose, where carbohydrates make up a total of 33 % of the ovomucin composition [39]. Complexing of the α and β regions results in an insoluble protein and composes of both thick and thin egg white. The α:β ratio of the thick and thin egg whites varies drastically. The ratio for thin egg white (soluble) is 40:3 and is compared with 84:20 of thick (insoluble) egg white. Thinning of the egg white can occur, which is due to the separation of the α-ovomucin from the insoluble protein structure [18].

2.2.1.5. Lysozyme

Lysozyme was the first egg white protein to be sequenced and is one of the most studied to date and consists of around 3.4 % of the total proteins found in egg whites. There are many forms found but the lysozyme in the egg is more stable than its counterparts. Lysozyme is an enzyme that can break down the β-linkages in a bacterial cell wall [40]. Unlike some of the other proteins found in egg white, it is small in nature and consists only of a single polypeptide chain made up of 129 amino acids, with a molecular weight of only 14.3 kDa. The three-dimensional structure contains four disulphide bridges and has a similar structure to α-lactalbumin found in milk. It has been postulated that they both have been evolved from the same protein as they share 40 % of the same base sequence. An α-helix in the form of a helix-loop-helix moiety connects two different domains. One domain is predominantly composed of α-helices, whilst the other is mainly composed of anti-parallel β-sheets [41]. The presence of the disulphide linkages in a small protein gives lysozyme a great thermal stability and has a preference to binding with negatively charged/anionic proteins such as ovomucin [42]. However, if more than two of the sulphide linkages undergo reduction, then the

lysozyme protein results in a loss of bioactivity, but the functional properties of the protein are improved with regards to gel and foam formation. In addition to helping to form the gel like structure of egg white and foaming (when solubilised), it is thought that the protein also contributes to the thinning of the egg white due to electrostatic interactions with ovomucin[18,32].

2.2.2. Protein Unfolding and Denaturation

As mentioned in section 2.2.1.1., proteins can undergo conformational changes which enable their native state (N) to change into a reversible unfolded state (U), or an irreversible denatured state (D), which can turn into an aggregated state (A) [29]. Many factors within the protein environment can aid in protein unfolding and denaturation. These include, but are not limited to, temperature, pH, protein concentration and electrolyte concentration. Changing the protein conformations from their native form can result in a multitude of characteristic changes including the loss of biological activity, a decrease in solubility, an increase in the reactivity and an increase of hydrodynamic size. The driving force behind reversible protein unfolding is due to thermodynamic contribution, whereas the kinetic contributions are responsible for the irreversible denaturation of the protein structure [43].

2.2.2.1. Protein Unfolding

In addition to the physical factors affecting the unfolding and denaturation of the protein, thermodynamic and kinetic contributions play a major role in the conformational changes of the protein structure. The thermodynamics can be determined by a dynamic equilibrium. These two reactions occur from the native to the unfolded state (N→U), and from the native to the denatured state (N→D). The change between these two states can be determined by analysing both the hydrodynamic properties and spectroscopic properties of the protein. The results are determined by the fractional change between the states and generally give identical results. The dynamic equilibrium of the changes can be calculated by equation (3) [44].

$$(\Delta_{N\rightarrow U}G/RT) = (\Delta_{N\rightarrow U}H/RT) - (\Delta_{N\rightarrow U}S/R) = \ln([N]/[U]) = \ln K \quad (3)$$

Where K is equal to K_F/K_U and is the equilibrium constant. K_U is synonymous of the rate constant for the unfolding (N→U) reaction and K_F is the rate constant for the re-folding (N→D) denaturation assembly. The Gibbs Free Energy change (ΔG) of the system gives two different temperature values for when ΔG=0. This shows that [N]=[U] and these values are the denaturation temperatures. The ΔG values in this equation can be thought of as a function of the conformational stability of the protein, which is generally found to be small. Other variables depend on thermodynamic contributions, including temperature. The unfolding due to temperature involves both enthalpic (ΔH) and entropic (ΔS) terms. These are generally hard to deduce for calculation purposes. One way is by using equation (3) and plotting the R and ln K terms against 1/T in a Van't Hoff plot. The ΔH can be extrapolated from the curve and the ΔS term can by determined by the intercept.

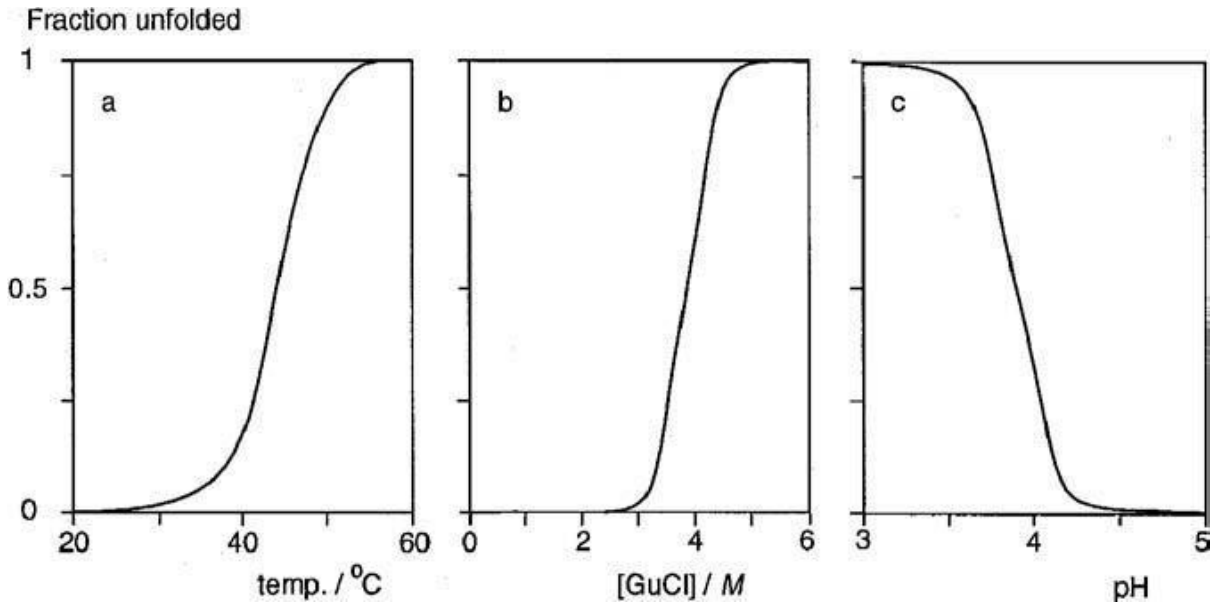

Figure 2-3. "Transition of proteins from the native to the unfolded state or vice versa." a= with respect to temperature change, b= with respect to concentration change, c= with respect to pH change. Taken from [44].

Figure 2-3 shows the transition states as a function of the variable and the fraction of protein unfolded. The graphs show that for temperature, proteins start to unfold around 25 °C and are completely unfolded around 55 °C. Beyond this is when reversible protein unfolding

starts to turn into irreversible denaturation. The ‘b’ graph shows the lysozyme protein (part of egg white) as a function of GuCl concentration. It shows that above 3 M, the proteins start to unfold and are fully unfolded at a concentration of 5 M. The pH curve shows that at acidic pH’s below 4.5, the proteins start to unfold are completely unfolded by pH 3. What the graph does show is that there is a very small range for each of the variables for the N→U transition. This type of transition is a cooperative transition and involves the breaking of multiple bonds simultaneously. This means that the protein is found in either a fully native state or a fully unfolded state. Both of the variables for unfolding via temperature or pH dependence rely on different thermodynamic contributions. Because temperature dependence is governed by the Gibbs free energy of the system, a high temperature is required to provide a significant ΔH term, which is the driving factor behind temperature dependence unfolding. The unfolding of the protein structure due to pH is however due to ionisation of the side chains of the protein molecule. The transition pH range is much smaller compared to small and simple ions, meaning that there could be hidden histidine moieties. If the protein molecule unfolds then the histidine residues become ionised, this has been found to occur at pH 3.8. At pH’s below 4 it has been found to promote unfolding due the hydrophobic interactions and extra H^+ neutralising the surface charges of the protein, making the molecule more stable as there is less charge separation and therefore less compensation mechanisms. This is not the case for proteins above pH 4 (when also subject to temperature dependant unfolding) as the carboxylic acid groups become deprotonated due to a lack of H^+ ions in solution and therefore, there is competition to bind to water, which causes more protein aggregation [6,43].

Many of the conformational changes associated with the unfolding of proteins are due to thermodynamic effects, which correspond to the breaking of multiple bonds and intermolecular forces within the protein structure. Four of the interactions exhibit a negative free energy stabilisation contribution and therefore promote the native conformation. These are hydrogen bonds, hydrophobic interactions, van der Waals attraction and salt bridges. Other forces exhibit a positive free energy stabilisation contribution and promote the

unfolded conformation. These are conformational entropy, hydration of polar side groups and peptide linkages, electrostatic repulsion of charged groups on the surface of the protein and the stretching and bending of the covalent bonds holding the protein structure together.

There are compensation mechanisms that proteins adopt that promote and enhance the conformational stability. These mechanisms include the formation of sulphide bridges between cysteine residues, pairing the domains of the protein together and the general bridging of ligands. The mechanisms and stabilisation contributions are not without complications. Because proteins are composed of domains, each domain can unfold independently causing partial unfolding. There is also the possibility of the protein adopting an intermediate structure between the native and the unfolded states, which leads to a very unstable structure. After a protein has unfolded, re-folding can become incomplete without the help of a secondary 'helper' protein. Once the unfolding conditions are removed, the protein can refold into a 'near-native' state, if not aided. This could cause minor changes in the conformation but could have a much larger impact on the activity of the protein, rendering it unusable due to loss of function [43].

2.2.2.2. Protein Denaturing

As mentioned in section 2.2.2.1, proteins can unfold in a multitude of ways, under a number of varying conditions. This process produces a reversible unfolding of the protein molecule. If the conditions causing the unfolding are removed, irreversible denaturing can occur if the protein if does not refold itself into its native form, and can exhibit a permanent conformational change. The transition of re-folding back to the native state may not occur due to a number of reasons. The process involved with protein denaturation is largely kinetic in nature, compared to reversible unfolding which involves thermodynamic contributions. Aggregation of the unfolded proteins is the main reason behind the prevention of refolding, and occurs due to the exposure of the hydrophobic residues leading to a decrease in the solubility of the protein. This causes the re-folding process to be slow, but in addition to this, cross-linking of side groups and reshuffling of sulphur bridges occur much quicker, causing

bonded aggregates before the protein can refold itself. The inability to refold itself can also be contributed to other chemical reactions; the change from trans- to cis- isomers in the peptide bonds. The ratio of trans and cis bonds are the same in the unfolded state but trans is more prominent in the native state due to increased stability from less steric strain around the double bonds. Cooling of the unfolded proteins can lock the cis conformations, rendering the protein unable to return to its original native state due to a change in the conformational ratio in the peptide bonds. At high temperatures, the asparagine residues within the protein can undergo a de-amidation reaction forming aspartic acid. It can also occur with the reaction of glutamine to glutamic acid. This reaction is faster under a low pH and results in a non-native conformational refolding. In addition to these reactions, the lack of 'helper' proteins (as mentioned in 2.2.2.1.) known as chaperonins, can also cause the failure of refolding back to the native conformation [45].

As well as various reactions taking place within the protein structure, the denaturation of proteins is also environment dependant. Various conditions can promote the denaturation of proteins, as can the presence of certain reagents. Extreme temperatures, whether it be high or low can break down the weak hydrophobic bond within the protein molecules. At high temperatures, the main driving force is the entropy of conformational change and irreversible changes can occur. This is less likely at lower temperature where kinetic effects are the main driving force. Extremes of pH, on either side of the isoelectric pH of proteins can induce instability in the molecule. This stems from the inability of the protein to form salt bridges and the electrostatic repulsion of like charges. At a low pH, the effects can be reversible, however at high pH's, the sulphur bridges break down and can cause irreversible denaturing of the protein. A combination of the extremes of both pH and temperature can be used to induce conformational changes where each denaturing agent enhances the other, causing the sum effect to be greater than the individual parts. Solvent quality and specific reagents can play a big part in the destabilisation of the native form. If a reaction mixture contains reactants deigned to reduce a sulphur bridge (even at low concentrations), then the protein would not return to its native conformation due to the protein now containing –SH groups

instead of –S–S- bonds. This is the most common type of destabilising reagent. When various solutes are added to a solvent in high concentrations, it can have a direct effect on the solvent quality which relates to both the solubility and conformation of the protein molecules. Because proteins are complex molecules containing both polar and apolar regions, it is not as straightforward with regards to causing unfolding or retaining the native state, as different regions could work in opposite ways to each other. High pressure can have an effect on the conformations and unfold proteins, and in some cases denature them. This is an important factor as high pressure heat processing is common for the food industry to eradicate microbial growth. The pressure required depends on other factors such as temperature but occurs over a short pressure range. High pressures greater than 1000 bar are required to unfold proteins. Mid-range pressures have been known to stabilise the native conformation due to formation of intermolecular forces as a result of the molecule being forced together under pressure. These forces include electrostatic interaction, van der Waals and hydrogen bonds which have a negative ΔG promoting native conformation stability. At high pressures, it is the breaking of the hydrophobic bonds which causes destabilisation. Under high pressures, ovalbumin can be destabilised to instantly produce aggregation. Because proteins are surface active, they can adsorb to a multitude of interfaces with great efficiency, which can cause irreversible self-assembly. This is true for the formation of AFE, as the protein self-assembles itself around the air-water interface of the radical species, changing its conformation to form air cells. The only conditions where this isn't the case, is when a stable globular protein comes into contact with a solid interface which carries the same charge and is hydrophilic in nature [45].

2.3. Sonochemistry

2.3.1. Cavitations

Acoustic cavitation bubbles are produced in solutions under sonochemical conditions. Ultrasound is transmitted in waves by compressing and stretching the space of which the waves pass through. The waves cause oscillations through the medium and when a

negative pressure is large enough, the distance between the molecules exceeds the molecular distance which is required to keep the liquid medium intact and causes the liquid to break down and create voids. It is these voids that are known as the cavitation bubbles [46,48]. There are two different behaviours exhibited from the compression and stretching of the liquid. One is a low intensity bubble called a stable cavitation and the other is of a much greater intensity, and is known as a transient cavitation. Transient cavitations are the most common and can double in radius after a few acoustic cycles and then collapse on themselves, releasing a high amount of energy [49]. This is shown diagrammatically in Figure 2-4.

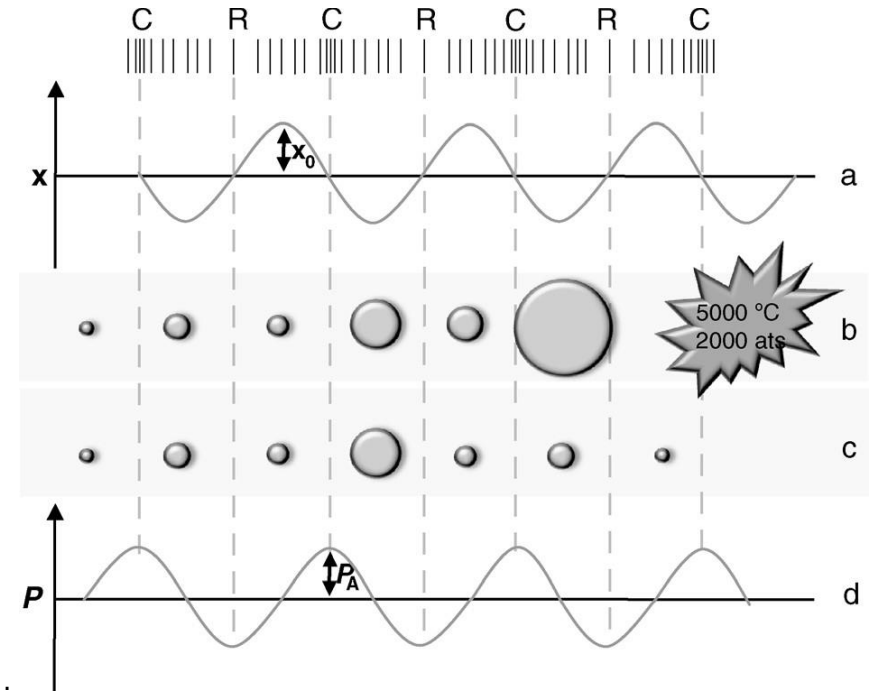

Figure 2-4. "Creation of stable cavitation bubbles and creation and collapse of transient and stable cavitation bubbles. (a) Displacement (x) graph; (b) transient cavitation; (c) stable cavitation; (d) pressure (P) graph" [49].

The energy released from a collapsed bubble can be phenomenal for a transient cavitation. Temperatures can reach up to several thousand °C and pressures greater than 1000 atmospheres can be created in the instant the bubble collapses. Each cavitation bubble can be categorised as an individual reactor and can form reactive radical species causing the medium the bubble is suspended in to become highly reactive. Solid particles under these

conditions are disassembled from each other and give an increased surface to liquid medium contact area ratio [50-52].

2.3.2. Ultrasonic Cavitation Parameters

Frequency can have an impact on the amount of cavitation bubbles a sonication device produces. Low frequencies (kHz) provide a higher concentration of cavitation bubbles compared to high frequencies (MHz). Increasing the frequency requires an increase in the intensity of the sound waves to ensure that the forces acting upon the liquid are in correct proportions to create collapse and voids within the liquid medium. Cavitations are less likely to occur at higher frequencies because the compression and stretching forces caused by the sound waves become so short that the liquid molecules cannot be separated, so no collapsing of the solution occurs and therefore no voids are created [49].

Intensity of the sonochemical device can have an impact on the liquid medium as it is proportional to the amplitude produced by the sonochemical source. The amplitude equates to the amount of energy input into the system and a minimum intensity is required to reach the cavitation threshold. Higher amplitudes are not always required for efficient cavitation production, as at higher levels of sonication amplitude, the sonic transducer can undergo rapid deterioration. This can result in a solution being agitated as opposed to producing the desired cavitation, due to insufficient compression and stretching of the medium. With regards to high viscosity samples, high amplitudes and intensities are required (regardless of transducer degradation) to produce sufficient vibrations to penetrate the viscosity of the sample [49].

For most experiments, water is the preferred solvent of choice due to its low viscosity and surface tension. However, in some cases apolar liquids such as organics solvents can be used providing that the surface tension and viscosity are low, as these are the main limiting factors for solvents. High surface tensions and viscosities increase the cohesive forces,

causing the intermolecular distance between molecules to be shorter, decreasing the likelihood of cavitations [47].

Temperature can work in two different ways when applied to ultrasonic waves. High temperature can interfere with the intermolecular forces such as van der Waals forces, hydrogen bonds and dipolar interactions between the medium and the solute. Interference occurs within the active sites of the liquid medium and faster diffusion rates can occur at higher temperatures. Lower temperatures produce a greater amount of cavitation bubbles within a liquid medium under constant sonication. Higher temperatures produce more energy into the surrounding medium causing the vapour pressure to rise. This increase in vapour pressure gives a higher affinity for liquid diffusion into the cavitation bubbles, meaning that the collapse is less violent in nature, producing less energy upon collapse [48].

External pressure can have an effect on cavitation production within a medium. If the pressure is increased, the molecules will be forced closer together, meaning that a higher energy input from the ultrasonic source will be required to produce cavitation's. There is an optimum external pressure where the intermolecular distances produce a high amount of cavitation's, but most experiments are performed at atmospheric pressure [47].

Ultrasonic energy can be introduced into a sample via both directly and indirectly. Direct application is applied through an ultrasonic probe. These are submerged directly into the sample and are in direct contact with the solution. The advantages of using direct sonication is that there is no barrier other than the solution itself for the ultrasonic waves, but metal detachment from the probe itself into the sample has been recorded, which is a potential disadvantage of the direct approach. However, this can be overcome with the use of glass probes [51,53]. Indirect approaches generally involve the use of an ultrasonic bath, where the sound waves have to travel through the liquid in the bath followed by travelling through the sample container itself to reach the desired sample. Indirect approaches are of less intensity and power compared to direct approaches, so are limited in their use to produce sufficient

caviatation's. Many indirect experiments effects are based off heating the liquid within the bath, and not the ultrasonic waves itself, causing heating of the sample and not acoustic cavitations [53-54].

2.3.3. Ultrasonic Probes

An ultrasonic probe is submerged directly into the sample and can provide a much higher intensity (up to 100 times greater) compared to indirect approaches. The probes are generally made of a titanium alloy, making them resistant to thermal degradation and corrosion. The disadvantage of an ultrasonic probe is that metal ions such as aluminium or chromium can contaminate the solution. Other sonication probes have been developed, including silica glass probes, spiral probes (made of titanium, vanadium or aluminium) and multiple probes, all of which come with their own advantages and disadvantages [51,55].

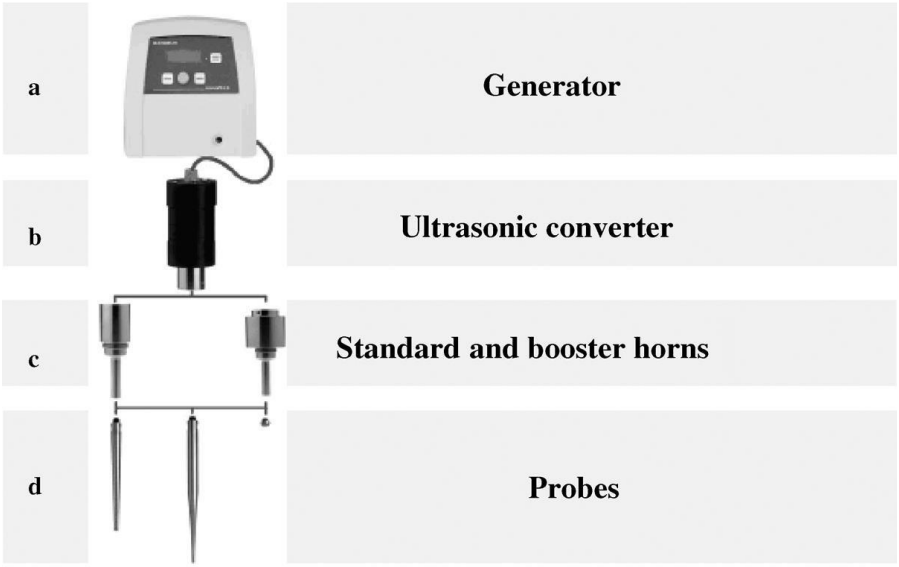

Figure 2-5 An ultrasonic probe. (a) is the generator, (b) the ultrasonic converter, (c) the standard and booster horns, and (d) is the probe [49].

Figure 2-5 shows the different components of an ultrasonic probe, which contains four main parts- the generator, ultrasonic convertor, standard and booster horns and the probe itself. The generator is responsible for converting voltage from a mains source into electrical energy with high frequencies (generally around 20 kHz). The ultrasonic converter converts the high frequency electrical energy into ultrasonic vibrations with a defined frequency. Both sets of horns are used to increase the ultrasonic amplitude. The probe, which is also

considered to be a detachable horn, is used to transmit the ultrasonic waves into the sample. Probe sizes are designed to fit specific volumes with tips that complement the probe size. The probe is the important part of the sonication device as it allows the boosted vibrations to travel through a greater length, magnifying the wave signal and allowing for direct submersion into the sample.

The higher the amplitude applied by the probe, the more intense the sonication energy becomes, and therefore the greater the number of cavitation's produced. In addition to this, the shape of the probe itself affects the magnification of the ultrasonic waves produced. Each shape has a defined use and the different shapes are shown in Figure 2-6. The stepped probe gives the highest amplitude magnification and the exponential shape is useful for microvolumes as it has a small diameter at the tip [49].

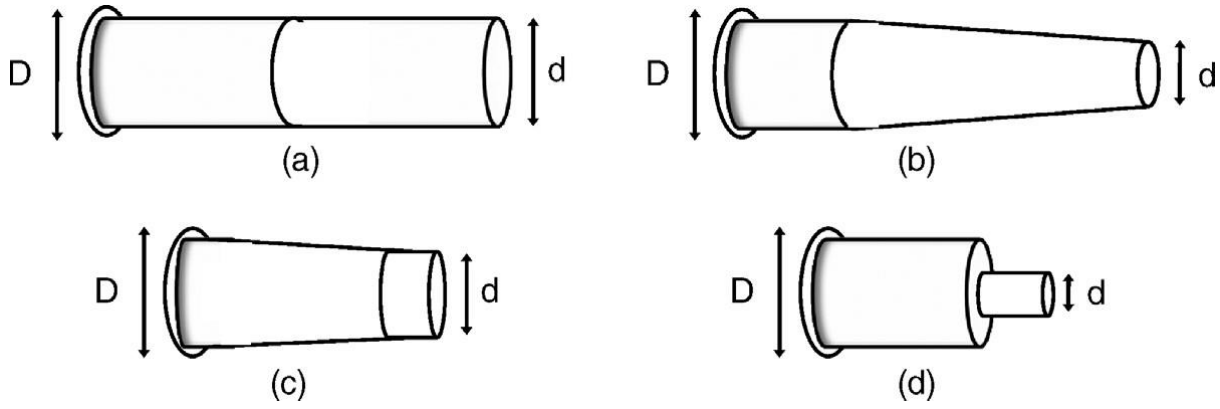

Figure 2-6. "Probe shapes: (a) uniform cylinder; (b) exponential taper; (c) linear taper or cone; (d) stepped" [49].

Once the ultrasonic waves are emitted from the probe tip, they spread throughout the sample and rapidly decrease away from the source, in both radial and axial directions. Areas where the cavitation's will not reach the sample in the container are known as dead zones. To reduce the dead zone area, the distance between the probe and the container wall should be kept to a minimum. However, the distance should not be so close that the probe and container are touching as this could cause the probe to break. Minimisation of the dead zones within the sample is crucial to ensuring maximum interaction between sample and cavitation's. So the choice of container that the sample is in can be important in obtaining good sample-cavitation interactions [49,56].

2.4. Experimental Parameters

2.4.1. Centrifugation

Centrifugation is the process of separating a heterogeneous mixture of two immiscible phases by applying force to a sample. The rotor rotates around a central axis, where the denser phase(s) settle out away from the axis, at the bottom of the centrifuge tubes is generally a solid component (known as a pellet), or in cases where it is liquid mixture, the denser liquid. The less dense liquid that the pellet has been removed from is known as the supernatant settles closer to the axis, and can be decanted so that none of the sediment is present in the liquid. Many variables contribute to the centrifugal process and these include the rotor speed measure in revolutions per minute (RPM), brake setting, temperature setting and an over-temperature. The temperature setting is the desired temperature setting for the process and the over-temperature is the limit where the centrifuge's safety setting will turn the centrifuge off, if the temperature inside the centrifuge goes above this value. The force acting upon the centrifuges is measured in g-force (g) and needs to be evenly balanced on opposite sides of rotor as to not cause an imbalance in the centrifuge [57].

2.4.2. Mixing Methods

Mixing relies on turbulent mixing of two or more phases to achieve complete mixing to a single solubilised phase. This is achieved by providing a turbulent flow rate within a given volume, where small volumes provide the best conditions for turbulent flow. At the highest efficiencies, the flow can intersperse two phases down to μm distances. The main factor to achieve complete solubilisation relies within the diffusion of molecules to produce a homogenous mixture down to the molecular scale. Diffusion time relies upon distance^2, which is the distance at which the molecules have to diffuse [58].

For food grade applications, the reactants are best mixed in either a magnetic stirrer (hot) plate or a large food grade mixer dependant on the scale of production. A Teflon coated

magnetic stirrer hot plate works by implementing a rotating magnetic field with a solution that contains a magnetic stirrer bar. It is the rotating stirrer bar that mixes the solution and rotates in line with the magnetic field. The stirring produced is fast and forms a whirlpool in the solution under high speeds promoting efficient mixing. This stems from a high flow speed with a relatively low volume, providing high turbulence. The maximum capacity to achieve mixing is low (≤ 4 litres), so can only be used for bench scale experiments [59]. The second type of mixing is in a large food grade mixer. These mixers have a much higher volume capacity and are operated by a motorised stirrer. These mixers do not produce a high turbulence, due to both the high volume and slow mixing speed. This can lead to complications with regards to mixing efficiency and complete dispersion to a single phase. Due the scale of production, rotational magnets would not penetrate the solution far enough to completely mix the solution, so a less turbulent mixer would have to be used, but the mixing time would have to be adjusted accordingly due to slower diffusion rates of phases [60].

2.4.3. Concentration Gradients

Concentration gradients are the difference in concentration between two different areas. Concentration gradients are a product of the diffusion of molecules and act generally in one of two ways. The most common is passive diffusion, which is the movement from a high concentration to a low concentration following a concentration gradient until the diffusion equilibrium has been reached, and the concentration gradient is removed. The second way is active diffusion, from a low concentration to a high concentration against a concentration gradient. Because active diffusion goes against the gradient, an energy input is required to make a solution more concentrated. Diffusion of molecules in a solution (such as EWP solution), is important for the mixing process, as effective diffusion down a concentration gradient results in effective mixing [61].

2.4.4. Flow rates and Residence Time

2.4.4.1. Flow Rates

Flow rates can be divided into two main types: these are fluid volumetric flow rate and mass flow rate. The fluid volumetric flow rate is concerned with solutions and the SI unit of measurement is m^3s^{-1}. Mass flow rate is concerned with the amount of mass movement that flows past a given point and is measured in kgs^{-1}. Because the project is concerned with solution movement per time where the total mass of solution components is known, mass flow is not appropriate.

Fluid volumetric flow rates are defined by the amount of solution passing past a defined point at a given time. The flow rate (defined as Q) can be expressed as a product of the flow velocity (V) and the cross-sectional area (A). These can be expressed and calculated in equation 4 [62].

$$Q = VA \tag{4}$$

Many factors can affect the flow the rate. The main parameters which affect the flow rate are the liquids viscosity, the liquids density and the friction of the liquid in contact with the tubing. In addition to these parameters, liquids can have different flow types. The three main types are uniform laminar flow, non-uniform laminar flow, and turbulent flow. These are depicted graphically in Figure 2-7. Air flow is regulated in a rotameter and is measured by the volume of air the flows through a device per unit time and is generally measured by Ls^{-1} [63].

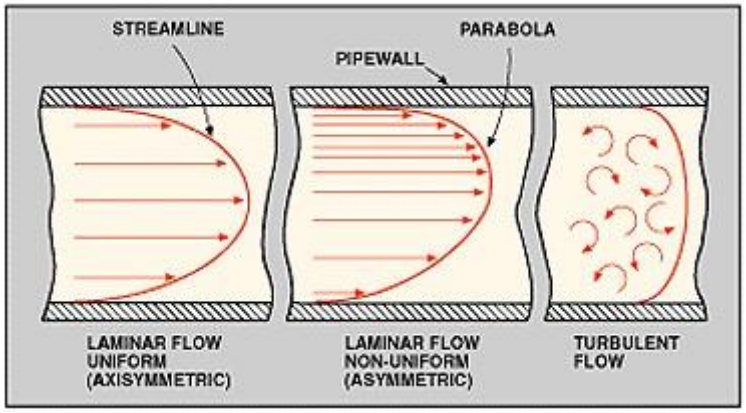

Figure 2-7. The most common types of flow experience in flow rate measurements. Laminar flow (uniform and non-uniform) and turbulent flow [63].

2.4.4.2. Residence Time

Residence time (T) is amount of time that a particle or molecule spends in a given system and is representative of how long it takes for the concentration to change. The general equation for residence time is equal to the system capacity to hold a substance (V) over the flow rate of the substance through the given system (q) and is shown in equation 6 [64].

$$T = V/q \quad (6)$$

Residence time is measured as a particle enters a given system and stops being measured when it leaves the same system. The residence time varies with the flow rate (or flow rates if more than one is present) and the size of the vessel. If the flow rates are increased, the residence time decreases, due to less time spent in the vessel. Alternatively, if the size of the vessel is increased, the residence time increases, due to the substance taking longer to pass through an increased area (assuming constant flow rate) [64].

2.4.5. Recycle Methods

Recycle methods are a useful tool within chemical process. The can be used to split product mixtures, purify products, remove impurities and increase the overall yield of the reaction and therefore minimise the waste produced. A recycle method in general includes the siphoning of material, which is then recombined with the starting material to recycle itself. It

is generally composed of multiple streams- the inlet stream which feeds the solution into a reaction vessel, the outlet stream which transports the product of the system and a recycle stream. The recycle stream feeds the unreacted reactants back to a recombination point, which combines the recycled material with new material to pass through the reaction process again. Before the recycle stream is siphoned, the product/recycle mixture passes through a splitting point, which allows the recycle stream to be siphoned off. The recombination point can provide irregular compositions as a combination of both streams can yield different ratios at different times [65-67]. Figures 2-8 and 2-9 show a flow chart of two general recycle setups, showing general siphoning of material and the use of a splitter to provide a recycle stream. The process is viable for when low yields are produced in a reaction, and rather than wasting the excess reagents they are fed back through the recycle stream and re-processed multiple times until the waste is minimised and the yield is optimised [68].

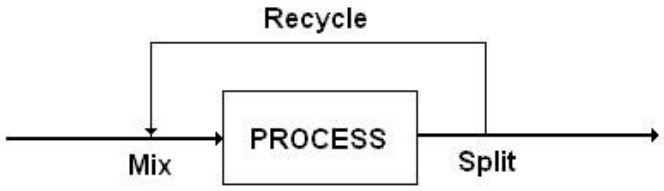

Figure 2-8. General reaction flow chart for a recycle process [68].

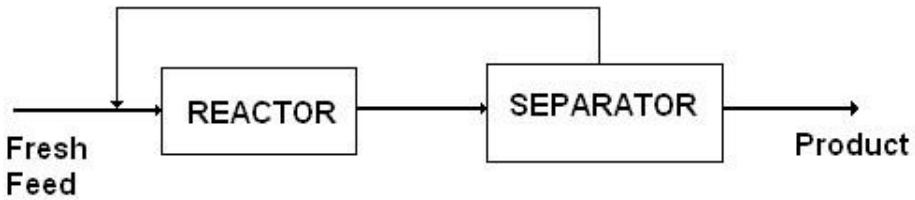

Figure 2-9. Reaction flowchart for a recycle process, using a separator to siphon off the recycle stream [68].

The basic process can encounter problems with regards to composition, especially with unwanted material in the recycle stream, that could cause build-ups and render the recycle stream unusable. The composition of the recycle stream can be tuned by a second

separator which purges the unwanted material out of the recycle stream. This would give a multi stream setup of a purge stream, product stream, process stream and a recycle stream. This is show in Figure 2-10. The opposite process to a recycle is a bypass stream. Instead of feeding the unreacted material back into the starting stream, a bypass stream feeds the starting material in the opposite direction, bypassing the reaction into the product mixture. This is generally used to obtain a precise control of the output stream. This is shown in Figure 2-11 [68-69].

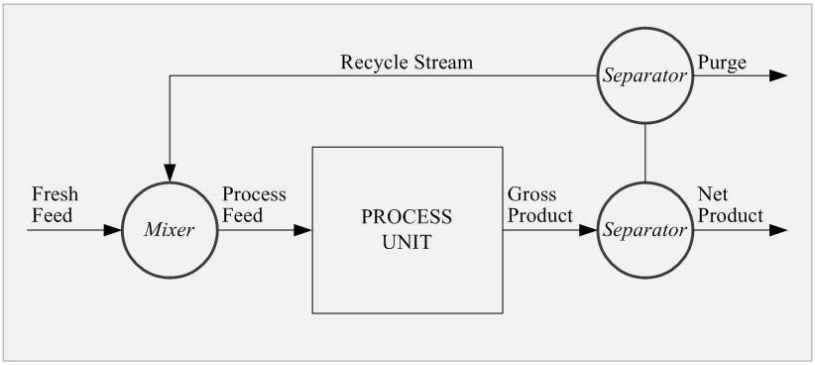

Figure 2-10. Reaction flowchart for a recycle process with the addition of a purge stream [69].

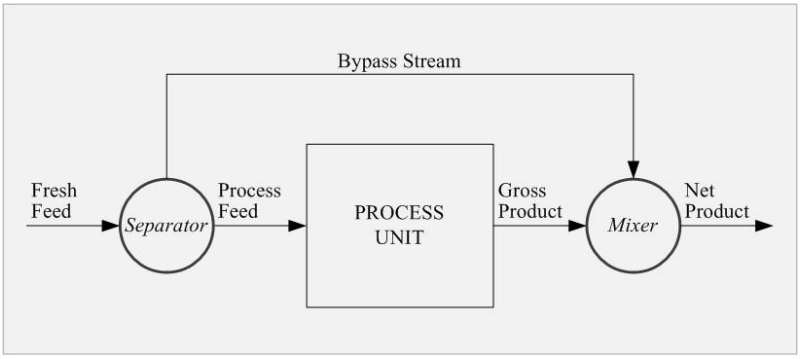

Figure 2-11. Reaction flowchart for a bypass process [69].

CHAPTER 3- MATERIALS AND METHODS

3.1. Introduction

This chapter is all about the methodology of the project. Firstly, it details the materials and the equipment used throughout the project. It then details all the methods used and finally the chapter presents some schematics of the experimental setup.

3.2. Materials and equipment used

3.2.1. Materials

The materials used for the project were used to form the initial starting product. The product formation was produced by the equipment. The materials used were Egg White Protein (EWP) (bulk powder- Sigma Aldrich), distilled water and 2 M HCl (Sigma Aldrich). Virkon was also used as a disinfectant and Decon (5 %) was the surfactant of choice for cleaning the Mastersizer2000.

3.2.2. Equipment

To obtain the desired concentration of protein solution, a Mettler PM30-K balance was used to weigh out both the EWP and the distilled water. The mixing of the solution was done using a Bell Stir Multi Stir 4 stirrer plate. To pH balance the solution, a Mettler Toledo FE20/FEP20 probe was used. The centrifuge use throughout the project was a Beckmann Coulter JS-21 with a JA-10 rotor. In the AFE production a Watson Marlow (32 rpm max) peristaltic pump was used to pump the solution. Hagen Maxima and Capex air pumps were used to pump air through a Platon air rotameter into the Sonics Vibracell Model CV334 ultrasonic probe (13 mm tip) with a VCX750 base unit (Power- 750 W, Frequency- 20 kHz, Volts- 230 VAC). To heat the solution a Tempette MWB-12L water bath (with pump) was used, as was a heat exchanger (unknown make). To analyse the AFEs, a Mastersizer2000 was used for particle size distribution and an Olympus BX50 microscope with a Motic imaging camera or a Leica

Qwin black and white imaging camera was used for imaging the AFE samples (dependant on which camera was setup in the lab at the time of analysis). For the dry weight analysis, the samples were weighed on a Mettler PC 4400 balance. A Pall Separations Microza USP-143 module was used for the cross-flow filtration steps. The secondary pump for the Cross Flow filtration steps used was a Masterflex Model 7518-00.

Figure 3-1. Picture of the Sonication probe and flow through cell (left image) and the base unit for the sonication probe (right image).

3.3. Experimental Methods

3.3.1. Air Filled Emulsion Production

A solution of 5 %w/v of Egg White Protein (EWP) was made up using EWP (75 g) and distilled water (1500 g, 83.3 mol). The solution was mixed using a magnetic stirrer plate until all the protein had dissolved (~2 hours). This concentration is based off the research by *Tchuenbou-Magaia et al*.[2], where 5 %w/v is found to produce the highest yield. Upon completion of the mixing, the solution was reduced to pH 3.8 using HCl (2M-Sigma Aldrich). The resulting pH balanced solution was then centrifuged (4 °C, 1 hour, 10000 rpm, 17000 G, brake 6, Beckmann JS-21 Centrifuge, JA-10 rotor) to remove any insoluble proteins left in the solution. The centrifuged solutions were then mixed back together in a large flask and heated to 50 °C

in a water bath. The warm solution was then passed through a high-intensity ultrasonic probe joined to a flow-through cell containing an air inlet, solution inlet and product outlet, for an hour to produce an Air Filled Emulsion (AFE) solution. The EWP protein was passed through using a peristaltic pump at 7 ml/min compared to the air which was passed at approximately 14 ml/min. The air at 14 ml/min was fed into the bottom of the flow through cell and another air flow was fed into the top of the sonicator to keep it cool. The flow rate for just needs to be a constant air flow (no flow rate calculations needed). This gave a resonance time of roughly 3 minutes. The AFE came out as foam and then settled into solution form.

The residual solutions (EWP and AFE) were allowed to cool in the cold room before analysis.

3.3.2. Air Filled Emulsion Analysis

3.3.2.1 Microscope Imaging Analysis

The first analysis was by microscope imaging to identify the particle sizes and to see how many air cells had been produced, as well as seeing if there were any extra protein aggregates in the surrounding matrix. The images also show emulsion instabilities such as flocculation. A microscope was used on the dark field setting and images were taken via a Motic Imaging camera or a Leica Qwin black and white Camera (dependent upon which was set up at the current time in the department). The slides were prepared by taking 1 drop of AFE and placing on a microscope slide and covering with a cover slip. Unless stated otherwise, the images were taken at 40X zoom.

3.3.2.2. Particle Size Analysis

The second analysis conducted was by a Static Light Scattering analyser (Mastersizer) and the software program used was Mastersizer 2000. The stirrer speed was set to 1505 rpm. The apparatus was cleaned before use using 5 % surfactant (Decon) and distilled water. The background particle intensity and blue light intensity was scanned.

Droplets of AFE were pipetted until >1.0 % laser obscurity was achieved (the acceptable

range is 1-10 but the closer to 1 %, the better). The Mastersizer was then run multiple times to giver an average value. To gain a consistent value, this process was repeated for each sample and then analysed. The Mastersizer was washed with distilled water between each analysis.

3.3.3. Experimental Variable Parameters

Reheating- During the initial testing, a test was done to see if the effect of reheating affected the quality of AFE. The procedure was carried out as stated in 1), but the EWP solution was cooled down for 24 hours. Following this, the solution was removed from the fridge and heated back up to 50 °C, and then sonicated again. This procedure was repeated until no solution remained and the samples were analysed, as stated in 2).

Varying Amplitudes- For the initial testing and later experiments, the parameters of the sonication step were changed to allow sonication at varying amplitudes. At the sonication step, the amplitude was chosen to be 30, 60 or 100 %. Each solution was sonicated at a single amplitude only. When different amplitudes were needed, a different solution was used.

Heating- Two different types of heat source were used to perform the various methods. These were a water bath and a heat exchanger. The temperature was set to heat the solution to 50 °C. The temperature was set to 50 °C as according to *Tchuenbou-Magaia et al,* asit is the optimum temperature [2,6]. Reverting to section 2.2.2.1., for thermodynamic temperature dependence unfolding of the protein, a high temperature is needed due to the dependence of ΔG and ΔH. Figure 2-3 in this section shows that at 50 °C, that the protein is in an unfolded state [43,44].

pH- A solution of pH of 3.8 was found to be the optimum pH by *Techuenbou-Magaia et al [2,6].* In section 2.2.2.1., pH unfolding of the protein is caused by ionisation of the side groups. Proteins have the potential to have hidden histidine residues, which ionise and unfold the protein at pH 3.8 [43]. However, due to the products needing to satisfy food grade

requirements, the solution cannot adopt a pH lower than this as it would be a) too acidic for formulations, rendering the product useless and b) too low to pass regulation for human consumption.

3.3.4. Critchley-Green Recycling Methods

3.3.4.1. Testing the Amount of Protein Left in Solution

This stage provided the necessary calculations for the recycle steps. To perform the recycles, the amount of protein left in the solution needed to be calculated by dry weight analysis. This led to calculating how much protein was needed to be added to the solution to recycle. To calculate this, the product solution was centrifuged (4 °C, 30 minutes, 10000 rpm, 17000 G brake 6, Beckmann JA-10 Centrifuge, JA-21 rotor). The solution was then filtered through a standard Buchner funnel and filter paper to collect the supernatant. A watch glass was weighed using an analytical balance. 10ml of the supernatant solution was then added to the watch glass and the weight was recorded again. The watch glass containing the solution was placed in a 50 °C oven until constant mass was achieved. The dried watch glass was then weighed again. The calculations were performed to determine the amount of protein required for the recycle step (equations shown in results and discussion).

3.3.4.2. Solution Top-Up Method (STUM)

The first method which has been termed the ‘Solution Top-Up Method’ involved three different methods where the heating source was the changing variable- water bath heating, heat exchanger heating with a cold solution and heat exchanger heating with the solution at ambient temperature. This method involved topping up the EWP back to 5 %w/v after it had undergone sonication by the method shown in 3.3.1. The Air-Filled Emulsion sample produced was centrifuge to remove the Air-Filled Emulsion and leave the residual protein. *Green et al* are working on a filtration method for this step, but the centrifuge acts as a crude method. Once the amount of protein was tested as stated in 3.3.4.1. The solution was

topped back up with EWP so that the solution, no matter how much of it was left, was back to 5 % w/v. The solution was then pH balanced back to 3.8 and centrifuged again to remove insoluble proteins. Both the pH balancing and centrifuge are the same as performed in 3.3.1. The new EWP solution underwent sonication again at 100 % amplitude, the same as in 3.3.1. This was repeated until the there was no solution left or the post-sonication concentration reached a plateau so that the concentration after the sonication was still 5 % w/v meaning that no more EWP could be added into the system. The various AFE samples from each recycle were analysed as stated in 3.3.2. and compared against each other for trends.

3.3.4.3 Non Top-Up Methods (NoTUM)

3.3.4.3.1 Non Top-Up Centrifugal Method (NoTUCeM)

The principles of this method follow very closely to that of STUM outlined in 3.3.4.2, with the only difference being that in between the various recycle stages, the solution is not topped back up to 5 % and the depleted solution was sonicated multiple times. The solution was centrifuged after each sonication to remove the AFE so that it was protein solution and not a mixture of AFE and EWP.

3.3.4.3.2 Non Top-Up Continuous Method (NoTUCoM)

Similar to the Non Top-Up Centrifugal Method described in 3.3.4.3.1, this method focused on not topping up the solution after sonication. There are two variations to this method, one which is continuous and one which is discontinuous. Unlike the Non Top-Up Centrifugal Method, this method involved no centrifuge step, with a mixture of AFE and EWP being the recycle mixture. The process was performed as standard to the method outlined in 3.3.1. The change comes after the first sonication stage where upon the system was allowed to reset and be cleaned and then the mixture was then placed back into the starting vessel and underwent the sonication stage again. The solution was sonicated four times (determined by other results on average amount of recycles per experiment) without any other steps being

involved in the process. After four cycles of sonication, the solution was then analysed as per the method stated in 3.3.4.1.

This led onto an adaptation of the method named the Non Top-Up Continuous Method v2 (the name represents this method as opposed to its predecessor, as this is the continuous part). This version, rather than collecting and placing back in the starting vessel, enabled a feedback loop between the output tube and the starting vessel (Figure 3.4). This allows the continuous circulation of products/starting reactants. The experiment proceeds as above, but instead of stopping and restarting the system and transferring the solution between vessels, it is a one pot reaction, so no resetting is needed until the end of the process. The reacting/product solution was sonicated for a total of four hours (one sonication step in a discontinuous recycle method lasts on average for 60 ± 5 minutes) and equates to four cycles through the sonicator so is coherent with the original Non Top-Up Continuous Method. After four hours, the process is stopped and the solution is centrifuged and analysed as per the method stated in 3.3.4.1.

3.3.4.3.3. Cross Flow Filtration Method (CFF)

There were two experiments associated with using the cross-flow filtration module. The first was done as a two stage process- Formation of the AFE, followed by the Cross Flow Filtration. A solution was prepared as stated in section 3.3.1. Following this the AFE solution was centrifuged (4 °C, 30 minutes, 1000 rpm, 200 G, brake 6, Beckmann JA-10 Centrifuge, JA-21 rotor) to remove the larger aggregates in solution. The cross flow filtration was set up as shown in Figure 3-5. The post-centrifuged AFE was then pumped through a peristaltic pump into the bottom of the cross flow filtration module. The filtered AFE solution exited at the top of the module and flowed back into the starting vessel. A secondary outlet was set up and was attached to a vacuum. This collected the EWP supernatant solution allowing the AFE solution circulating to become more concentrated with every pass. The process stopped when no supernatant was being released and the AFE had concentrated up so much that it was too viscous to pump. This was then analysed as stated in section 3.3.2.

The second experiment was an extension on the first method. The method for the way the module worked is the same. However, rather than being two separate processes; this experiment was a one stage process. This was performed for a single pass. The AFE formed in the sonicator was transferred to an intermediate collection vessel. From this vessel the AFE was pumped via a secondary peristaltic pump into the cross-flow filtration module where upon the EWP supernatant was removed into the product collection vessel and the concentrated AFE was transferred back into the intermediate collection vessel. From here the AFE was passed through the module until the process stopped because the AFE was too viscous. The setup in shown in the schematic in Figure 3-6 in section 3.4.

3.4. Experimental Flow Schematics

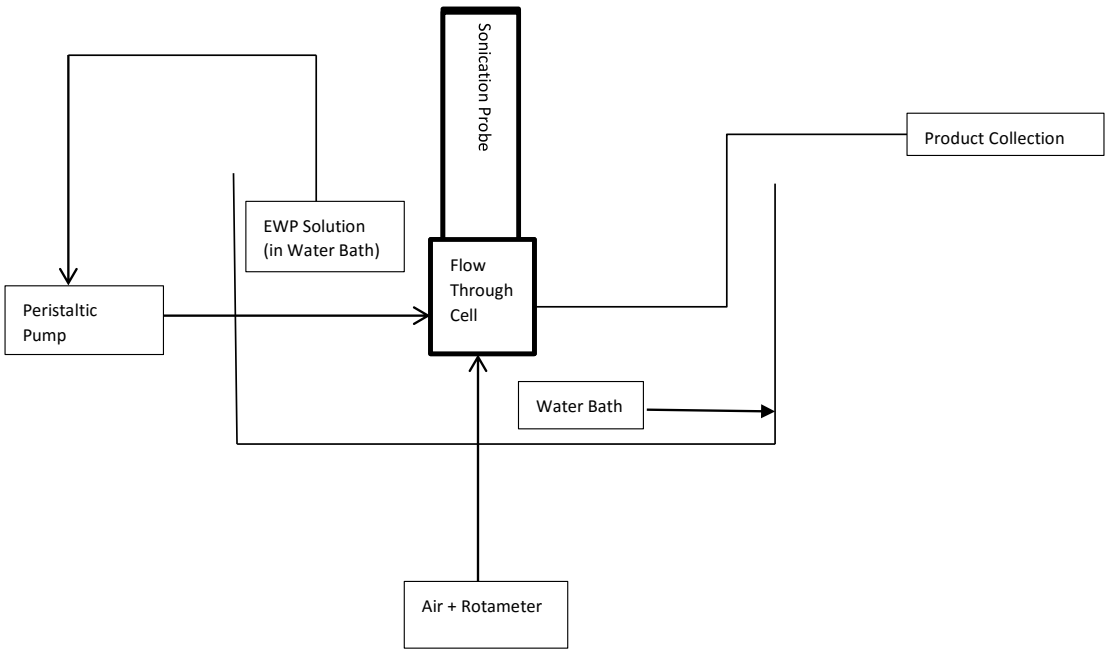

Figure 3-2. Experimental schematic for the AFE production using a water bath as the heat source.

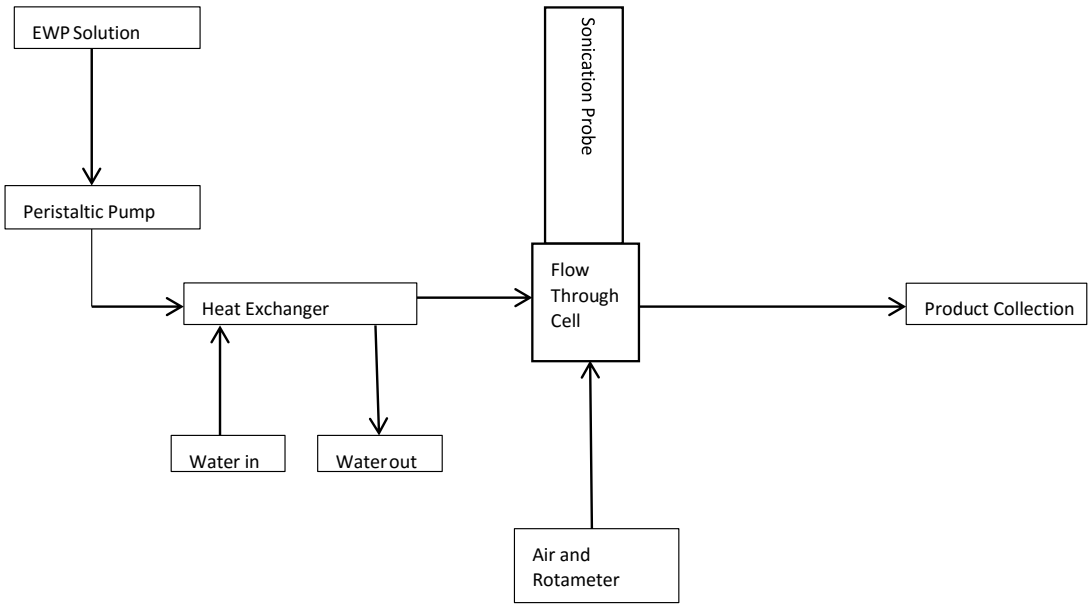

Figure 3-3. Experimental schematic for the AFE production using a heat exchanger as the heat source.

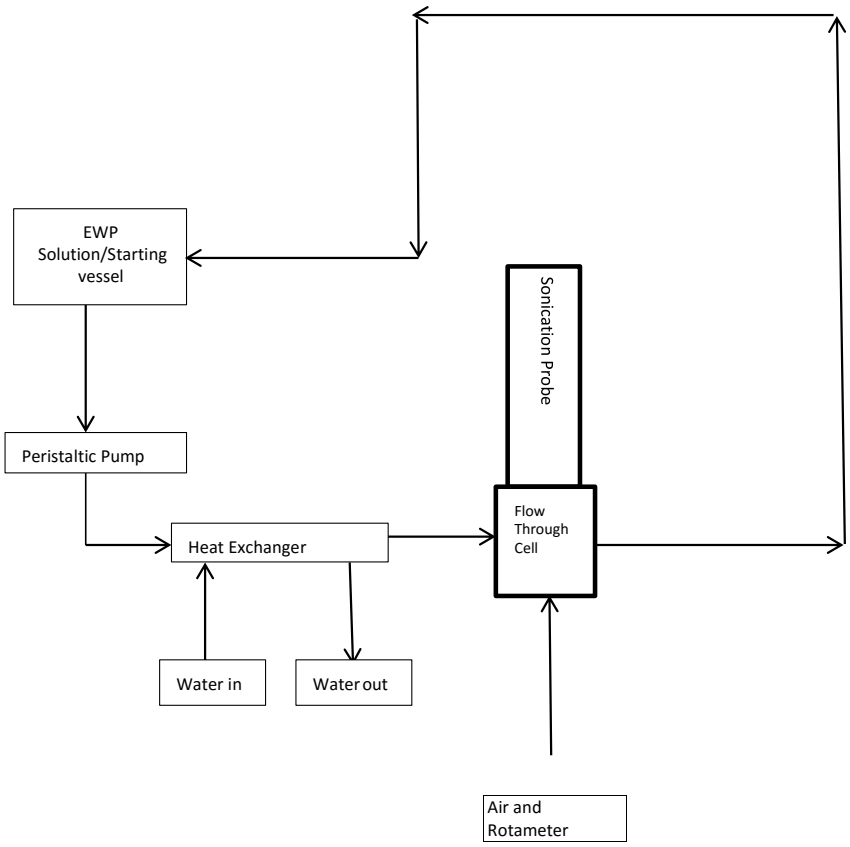

Figure 3-4. Experimental Schematic for the AFE production using the Non Top-Up Continuous Method (v2) outlined in 3.3.4.3.2.

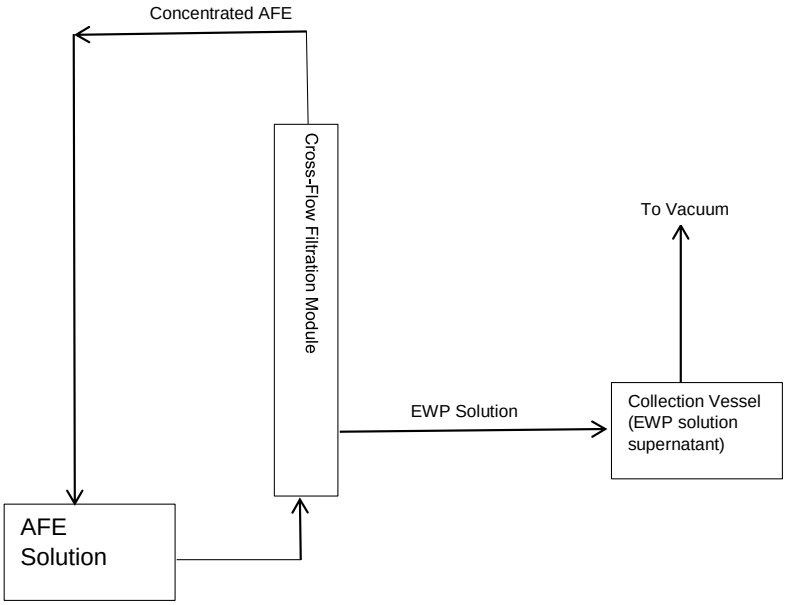

Figure 3-5. Experimental Schematic for the Cross-Flow Filtration step outlined in section 3.3.4.3.3.

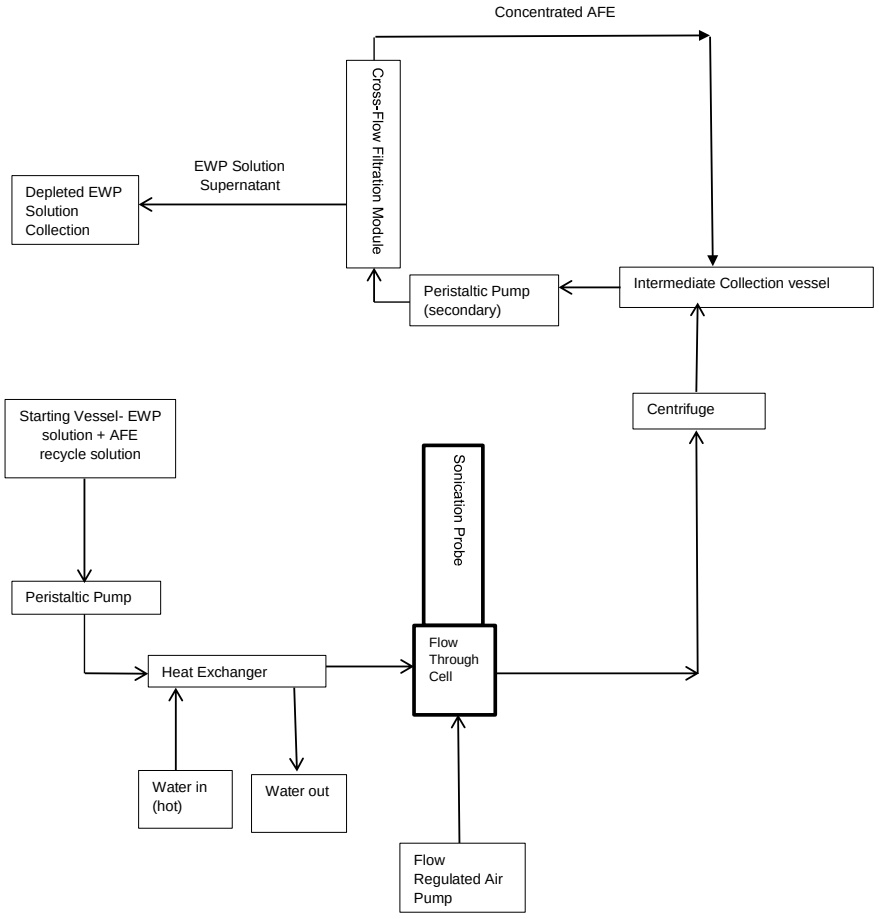

Figure 3-6. Schematic to show the 1 stage process for the Cross-Flow Filtration method outlined in section 3.3.4.3.3.

3.5 Control Experiments

The aim of the control experiments was to provide a standard result that future experiments could be tested against. Two areas were already conducted by *Green et al* and *Dos Santos et al* on mixing time and residence time, respectively. The optimum mixing time was found to be 2 hours for complete mixing and the optimal residence time was found to be 3 minutes [70,71]. Dry weight Analysis, Centrifugation, and Amplitude Vs Energy were conducted in this project.

3.5.1 Dry Weight Analysis

A control experiment was performed for dry weight analysis because it was the method of choice for testing how much protein had been used up during experiments. Because this is an important factor in the recycle process, the results needed to be accurate. To do this, the time at which constant mass was achieved needed to be calculated so that every sample dried to constant mass. This was achieved by weighing out 10 ml of protein solution onto watch glasses and heating them in the oven at 50 °C for an extended period of time. The watch glasses were weighed at various intervals to see when constant mass was achieved. The intervals chosen were 0,1,2,3,4,6,8,10,12,24,48 and 72 hours. Such a wide time frame would allow for a more accurate comparison as to when constant mass was achieved and the short time intervals at the beginning of the control allows for a differences to be shown more clearly as this is when most of liquid would be lost.

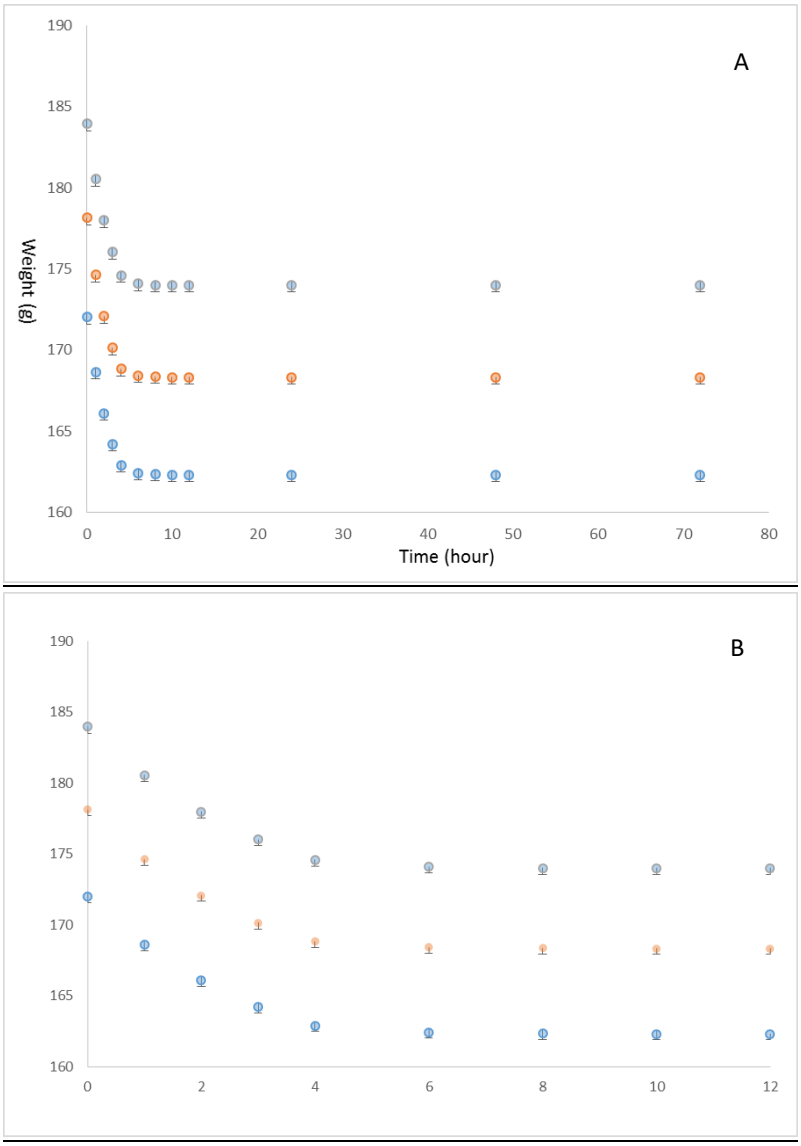

Figure 3-6. Graphs to show the drying time during the control experiment. A is the full time recorded and B shows the first 12 hours.

Table 3-1 (Appendix) and *Figure 3-6* show that the EWP solutions achieve constant mass at 10 hours and is coherent throughout all the tested experiments. Graph B shows the first 12 hours and gives a clearer picture as to when the samples achieve constant mass. Graph A shows all the data found, but due to the time differences used, it is skewed to the left; hence B is a much clearer representation. Because of these findings, any sample that underwent a dry weight analysis was left for a minimum of 10 hours, until constant mass was achieved.

3.5.2 Centrifuge

This control experiment was performed to determine the mixing time for the centrifuge process. The centrifuge step is an important process and is used quite frequently to either remove insoluble protein molecules, or to remove air cells from an AFE sample so that dry weight analysis can be performed on the supernatant. The aim was to find the time in which all particles that require removal, are removed, without falling back into the solution upon agitation in the transferring process from the centrifuge to other vessels. The solutions were made up to the standard 5 % concentration, then they were centrifuged and analysed at different times- these were 0,20,40 and 60 minutes. Because the best way to tell if all unwanted particulates were removed is by observation analysis with the naked eye, there are no quantitative results for this experiment. The results are therefore shown as images and differences can be seen between the different centrifuge times.

Figure 3-7. A series of images showing the progression of the centrifuge step. A= 0 minutes, B= 20 minutes, C=40 minutes, C1=40 minutes after slight agitation to the vessel, D=60 minutes, D1= 60 minutes after vigorous agitation to the vessel.

From the images in *Figure 3-7,* it is clear from the opaqueness of the solution that there were insoluble proteins in the solution, which are the protein particulates to be removed (A). After 20 minutes of continuous centrifugation (B), the supernatant starts to become clearer and insoluble protein residue starts to collect on the side of the centrifuge vessel. Upon first inspection of the vessel after 40 minutes (C), it appears that the supernatant is clear and free of insoluble protein particulates. This is true, however under the slightest amount of agitation (e.g. the movement of the vessel from the centrifuge to another vessel), small amounts of protein detach themselves from the surface of the vessel and back into the supernatant (C1).

After 60 minutes (D), the solution looks exactly the same as (C), however, if the vessel is exposed to vigorous agitation/mechanical energy, the insoluble protein particles stay attached to the side of the vessel. So even though after 40 minutes, all the protein has been removed from the solution, any centrifuge steps that are performed throughout the experiments will be centrifuged for 60 minutes so that none of the insoluble proteins return to the supernatant, and the solution is fully solubilised.

Table 3-2. The amount of sediment left after the centrifugation of EWP.

Tube	Tube Weight (g)	Tube + Solution (g)	Tube + Sediment (g)	Sediment weight (g)	EWP lost (%)
1	86.08	347.71	94.18	8.10	0.108
2	81.66	342.43	87.44	5.78	0.077
3	86.14	344.43	88.64	2.50	0.033
4	83.64	345.16	88.07	4.43	0.059
5	86.86	342.20	89.17	2.31	0.031
6	83.84	342.54	89.26	5.42	0.072
Total					0.381

In addition to determining when the solution has fully centrifuged, a numerical analysis of the amount of sediment left was performed. The data is show in *Table 3-2.* The process involved taking the weight of the centrifuge tubes, the weight when containing solution, and the weight of the (wet) sediment left over after the supernatant had been removed. The sediment weight was calculated by taking the tube + sediment weight and subtracting the tube weight. The sediment weight was then divided by 75 as this was the mass of the protein added to the solution to give a percentage loss. The overall amount lost was 0.38 % meaning that when a sonication occurs, the concentration of the protein solution will be 4.62 as opposed to 5 %.

3.5.3. Amplitude vs Energy

The aim of testing the amplitude against the energy output was to see from an industrial point of view, which solutions (EWP or AFE) cost the most energy, as some of the recycle methods incorporate both EWP and AFE sonication steps. The base unit for the sonication

probe records the amount of energy in Joules in a certain time period. Each amplitude was tested as an experimental run through for 5 minutes at a time with the system being stopped and restarted in between each amplitude change. The output reading was then converted into more useful units of energy.

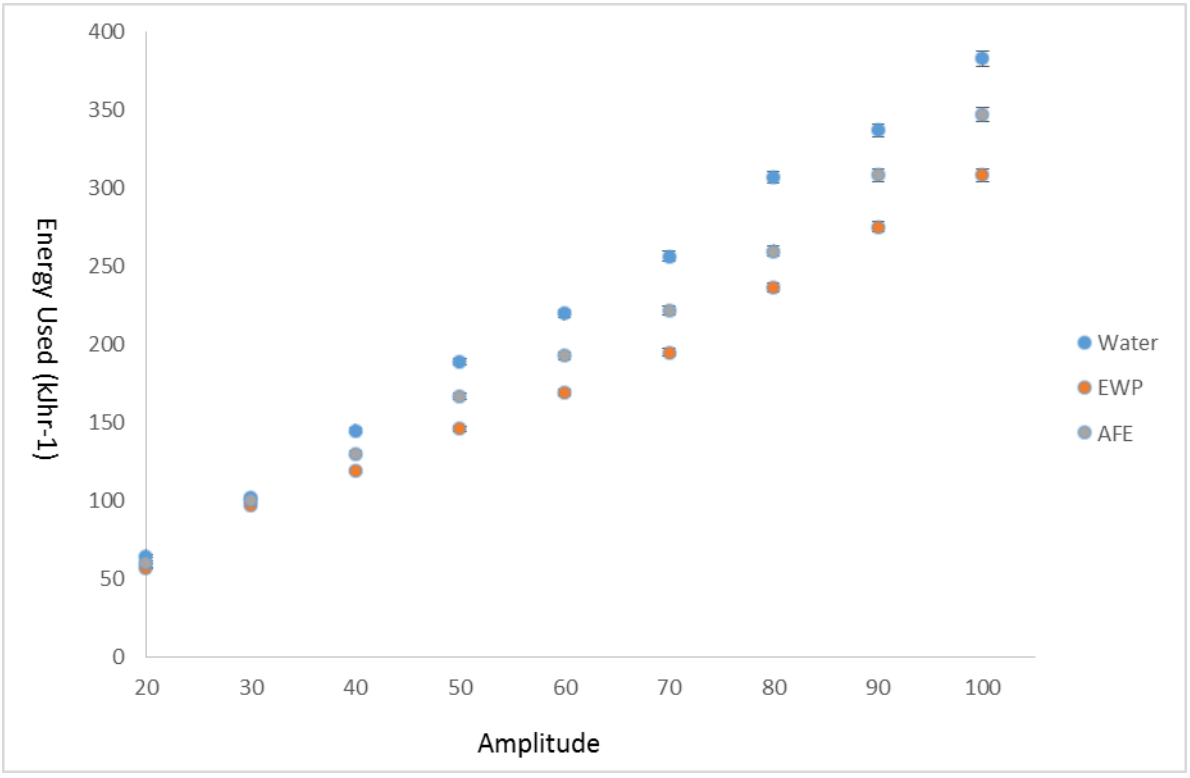

Figure 3-8. A graph showing the Energy Usage (kJhr $^{-1}$) at varying amplitudes for water, EWP and AFE.

Tables 3-3, 3-4, 3-5 (appendix) and *Figure 3-8* show that for water, EWP and AFE that when the amplitude is increased, the energy use from the sonication probe increases (which is, what is to be expected) and shows a linear relationship. Water used up the largest energy followed by AFE then EWP. The reason for this is because pure water doesn't react; it will enter and leave the flow-through cell quickly, causing the sonication probe to not be covered by as much liquid, causing an increase in energy. AFE cost more energy to react as the air cells are much larger and unreactive compared to proteins, meaning that more energy will be absorbed by the air cells but will still remain intact. The Tables show that the exact same amount of energy is used for EWP solution sonicated at 100 % and an AFE solution sonicated at 90 % amplitude. An important discovery was that at amplitudes below

40%, AFE was not produced visibly in the bulk. Air cells are formed at this amplitude but not in significant quantities that it is visible with the naked eye.

CHAPTER 4- PREVIOUS AND INITIAL STUDIES (BATCH MODE WITH NO RECYCLES)

This Chapter is associated with looking at batch mode production of AFE without performing any recycles, opposed to Chapter 5 which looks at batch process with recycles.

4.1. Previous Studies

Studies into some of the parameters and variables, associated with the methods in this project were studied prior to the start of the project. The method for using a 5 % EWP solution, as well the experimental setup was deduced by *Tchuenbou-Magaia et al (2011)*[2]. The ideal flow rates for both the air and liquid were deduced alongside the ideal residence time for AFE production by *Dos Santos et al (2014)* [71]. *Green et al* (2014) [70] tested the premise of recycling methods to see if it could theoretically be possible to produce a higher yield by reducing waste and maximising the output, which led to the formation of the project.

4.2. Parallel Studies

The research undertaken in this project ran in parallel with an EngD project [70]. Where this project focused on the scale up and process optimisation of AFE production, *Green's* EngD project focused more on the formulation approaches of AFE into low fat foods. Both projects were run in conjunction with Rich Products and ultimately focused on the same goal of incorporating AFE into an industrial setting. Some of the AFEs produced in this project were used in the formulation approaches. Both projects run parallel to each other because both projects are vital for the success of using AFE in low-fat food applications for industry.

4.3. Initial Project Studies

4.3.1 Introduction

The aim of undertaking some initial tests was to: a) get used to, and understand the experimental processes, b) test which basic parameters affect the production and c) give an indication of what areas should be studied in more detail throughout the project. The initial testing investigated the effects of reheating, amplitude and initial insights into whether recycling would be a plausible option.

4.3.2. Reheating

The aim of this test was to see if heating, followed by cooling, followed by a re-heat has an effect on the amount of air cells and protein aggregates produced. Half of the sample was produced into AFE but the whole solution was heated up. The other half of the solution was cooled in the fridge. Once the solution was cooled, it was then reheated and sonicated to see what effect multiple heating had on the sample.

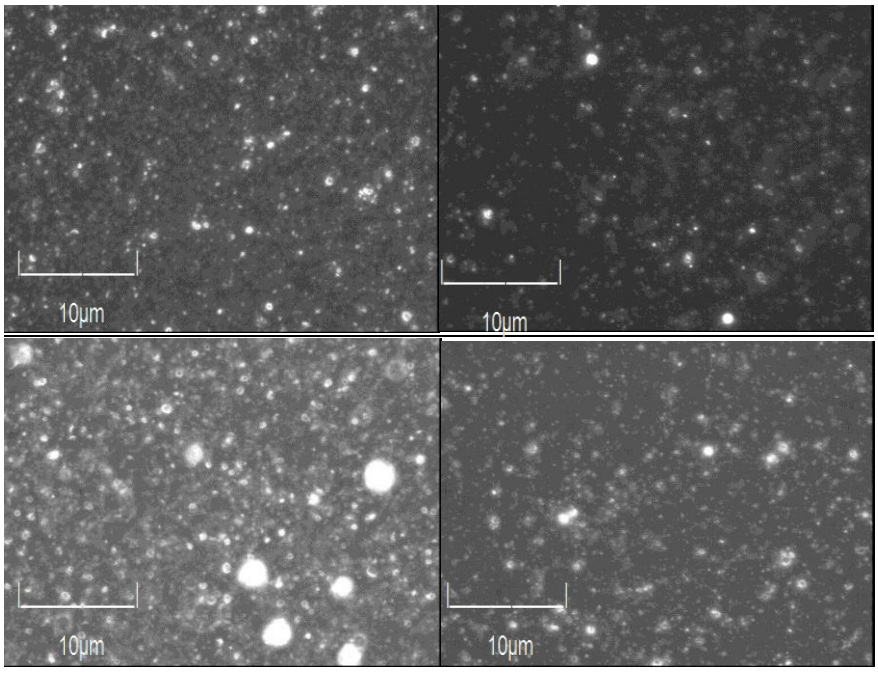

Figure 4-1. – Microscope images of the initial AFE samples produced during initial testing stage. Top Left and Top Right= Before Reheating, Bottom Left and Bottom Right= After Reheating.

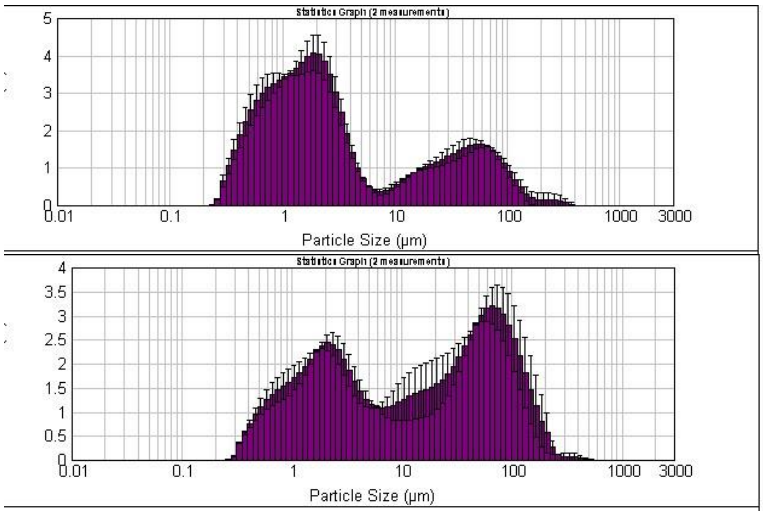

Figure 4-2. Particle size distribution analysis of the initial AFE sample produced during initial testing. Top Distribution= Before Reheating, Bottom Distribution= After Reheating.

Figures 4-1 and 4-2 physically shows the sample, and the particles size distribution, respectively. The original sample contained a small amount of protein aggregates due to being heated within a water bath for a long period of time but contained a large volume of air cells. This is evident from both of the Mastersizer distributions, where there is a large peak around one micron and a small peak around 100 microns; and from the images, where there are air cells present in the solution but some background protein is apparent in the solution. The distribution curve for the reheated solution varies dramatically from that of the first solution. The air cell concentration is down due to the peak around one micron being reduced, and at the same time, the peak around 100 microns is significantly increased showing the presence of protein aggregates. This is further reinforced by the microscope images which reveal the larger protein bodies in the sample. The heating unfolded the proteins ready for reaction; but due to the absence of air, once cooled the proteins start to reform, the likelihood of oligomerisation of multiple proteins increases, hence why there is a larger amount of aggregates in the reheated solution. On top of this, because the solution is reheated, it is exposed to multiple sets of excessive heating, meaning that irreversible denaturation is more likely to occur compared to reversible unfolding.

4.3.3 Testing Various Amplitudes

4.3.3.1 Qualitative Data

The reason for testing the sonication amplitude was to determine whether the amplitude of the sonication probe had an effect on the quality and amount of air filled emulsion produced (and the amount of protein in the surrounding medium), as it would form the basis for a major parameter to be tested on the solution recycles. A control experiment in section 3.5.3. looking at amplitude vs energy showed that when the amplitude is increased, the energy input is increased. The aim was to see if this directly correlates with not only energy input but also AFE production.

The amplitude testing was performed by making up a solution and splitting it into separate containers at the sonication stage, which were then run at varying sonication amplitudes. The solutions were heated in a water bath.

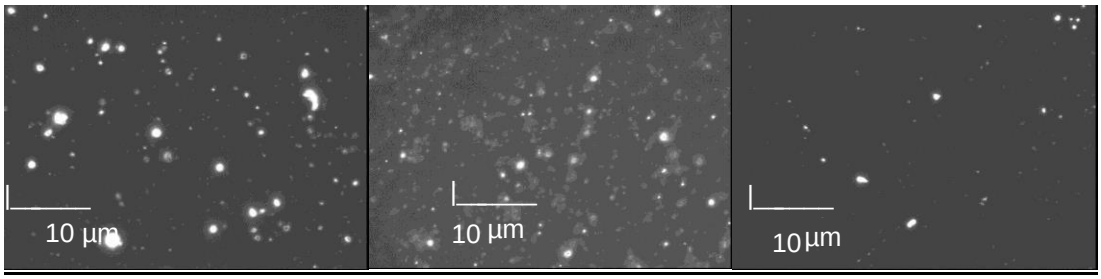

Figure 4-3. Microscope images of the AFE produced during the initial testing stage after undergoing varying amplitudes. Left=100% Amplitude, Middle= 60% Amplitude, Right= 30% Amplitude. Taken with a Leica Qwin black and white imaging camera.

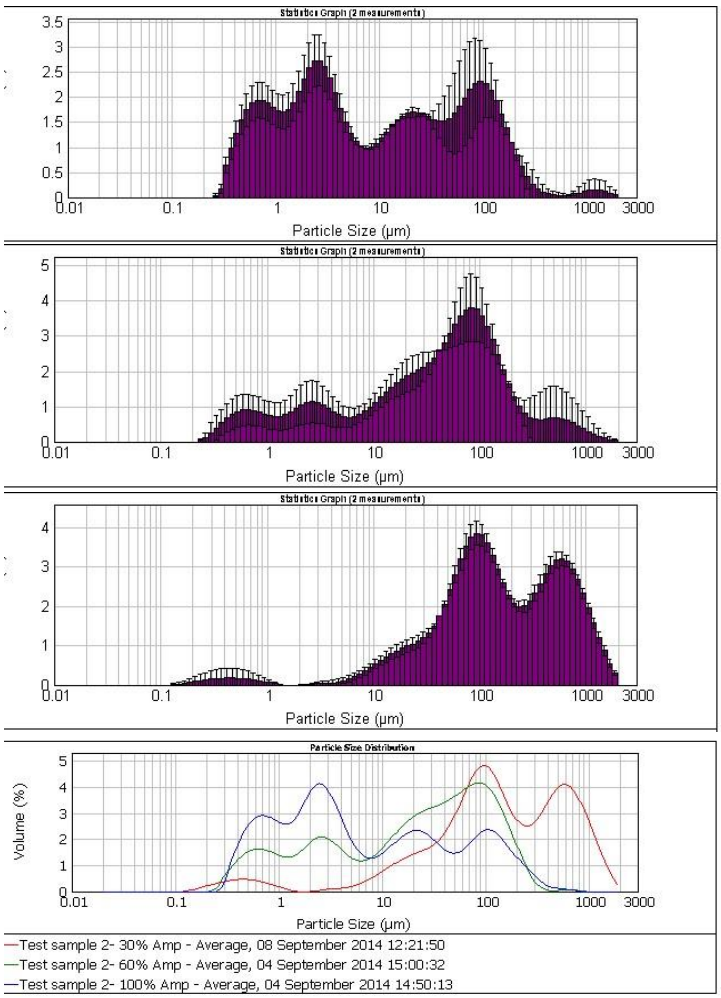

Figure 4-4. Particle size distribution analysis of the AFE produced during the initial testing stage at varying amplitudes. Top Distribution= 100% Amplitude, Second Distribution= 60% Amplitude, Third Distribution= 30% Amplitude, Bottom Distribution= Comparison of Distribution Curves.

Figures 4-3 and 4-4 show the images and particle size distribution for the samples at varying amplitudes. What is immediately apparent, is that the energy input correlates directly to the AFE production. As mentioned, when the amplitude in increased, the energy input into the system is greater, causing a larger concentration of superoxide radicals to be produced within the EWP solution. This allows more protein to be bound to the radicals resulting in a higher yield of AFE and a lower concentration of protein aggregates. The 100 % amplitude sample is not the best 'quality obtained'. However, this isn't an issue as it to be used as a comparison against each other, and the change from starting amplitude. All samples originate from the same stock solution so if one sample isn't as monodisperse as it could be, then it will be relative throughout all the samples. Looking at the samples, 100 % amplitude produces the best quality solution with highest yield of air cells and the lowest amount of

protein aggregates. This is apparent from both the images and the Mastersizer data. At 60 %, the concentration of air cells is reduced compared to the 100 % sample, and there is also a larger presence of protein aggregation. This is due to the decreased concentration of reactive radical species in solution causing more unfolded proteins to denature and aggregate. At 30 % amplitude it is very apparent that there is not very much AFE production occurring due to a low concentration of reactive species. During the control experiment in section 3.5.3., it was found that AFE in the bulk (able to see with the naked eye) did not occur until 40 % amplitude. So the production of air cells was not apparent until a microscope image was taken. The Mastersizer data shows a large presence of protein aggregates, showing that a large amount of protein has unfolded and because there is no species to react with under a large amount of heating, they have formed irreversibly aggregated. This is not as clear with the images; however, the light had to be reduced to actually see the presence of air cells and therefore the ability to see the protein aggregates was lost, but the Mastersizer provides conclusive evidence of this. At 100 microns, there is evidence of protein aggregation, so to have a large peak around over 1000 microns shows very aggregated protein networks at low amplitudes, showing that low amplitudes are counterproductive to producing a useable emulsion for formulation approaches.

The main finding is that when the amplitude is increased, it increases the energy input into the system. This causes a higher concentration of reactive superoxide radical species from the air input, which provides a higher binding surface for the protein. This gives a higher concentration of air cells and a lower concentration of protein aggregates.

4.3.3.2 Quantitative Data- Showing the Possibilities of Recycling

Based on the data found from taking the various amplitudes, a calculation to see the effect that the amplitude had on the protein used and the amount of protein needed to recycle was used.

This was to give an indication of what it is going on the system and to provide a basic grounding as to whether the recycle may be possible. The raw results are presented in Table 4-1 (Appendix).

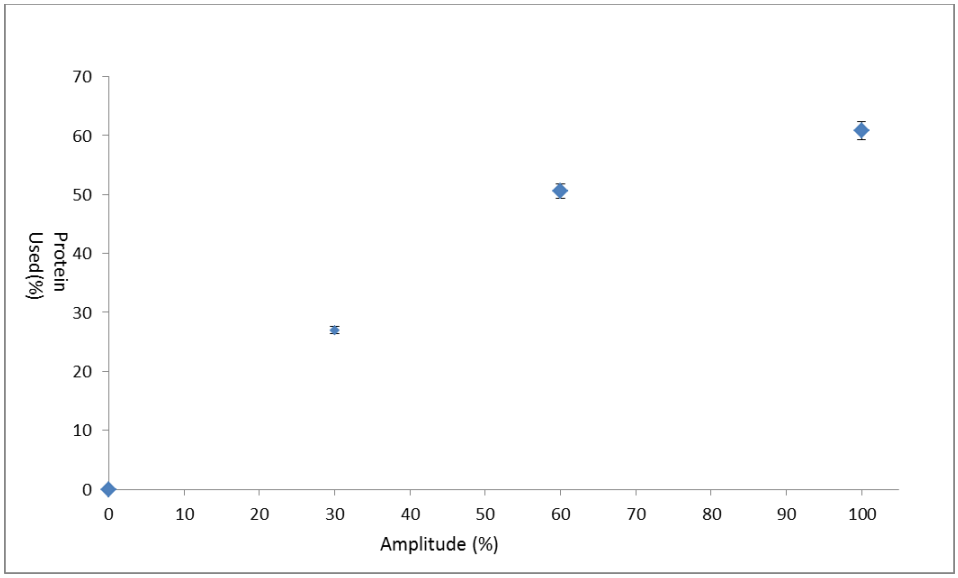

Figure 4-5. The protein used in the initial testing at varying amplitudes

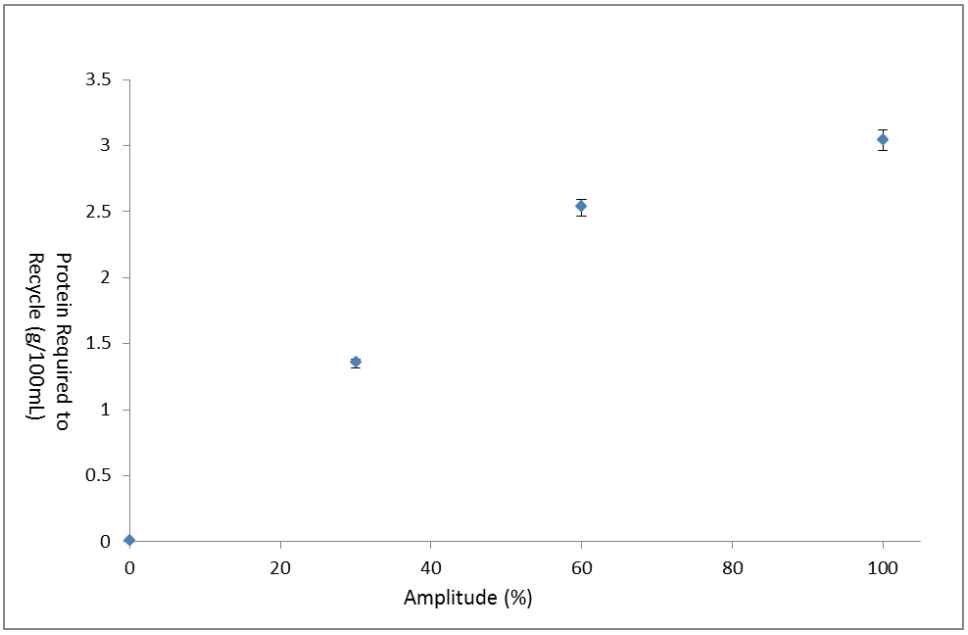

Figure 4-6. The amount of protein required to perform a recycle for the AFE produced during the initial testing.

Table 4-1 (Appendix) and Figures 4-5 and 4-6 show the protein usage at varying amplitudes and the amount of protein to be added to re-concentrate the waste solution back to 5 %. As expected, the protein usage increases with increased amplitude due to increased reactive sites. This also shows a proportional relationship to the amount of protein to be added to re-

concentrate the solution i.e. the higher the amplitude, the higher the protein to be added per recycle due to the solution having an increased depletion on protein. This shows that the recycling process is feasible and is able to be controlled via re-concentration and various analyses. It also shows that the process should produce a high yield of AFE when recycled, especially when used at high amplitudes.

4.4.4 Conclusion

These experiments were done under batch mode with no association to recycles. The aim was to determine how much protein would be required to recycle at varying amplitudes as well as giving an indication to the sample quality that could be produced at various amplitudes. The study gave an indication of what to expect when performing a recycle in terms of protein usage and the amount of protein required to re-concentrate. The experiments found that by increasing the amplitude, the amount of protein used in the reaction increases, allowing for more protein to be added for re-concentration. It also showed that when the amplitude is increased, in addition to the actual amount of protein usage increasing; the amount of air cells in the sample increases and the amount of protein aggregation decreases, due to a higher amount of superoxide reactive sites.

The initial tests have concluded however, that the reheating process is counterproductive to air cell formation. The constant heating followed by a cool down period with no reactive species to bind to, caused a large amount of the unfolded proteins to irreversibly denature and oligomerise with each other. This results in a lower air cell production and a higher protein aggregation, rendering the sample useless for formulation approaches. This also shows that excessive and constant heating could have a problematic impact on AFE production. This could be the case for the recycle process where proteins are not used up in a pass and are therefore exposed to multiple steps of constant heating and rapid cooling.

CHAPTER 5- THE CRITCHLEY-GREEN RECYCLE METHODS (BATCH AND CONTINUOUS PROCESSES WITH RECYCLES)

5.1 Introduction

This chapter is concerned with the analysis of the Critchley-Green Solution Top-Up Method as detailed in 3.3.4.2. This work follows on, but differs, from the work in Chapter 4, which looked at batch mode without recycles. Instead this chapter looks at batch (and continuous) processes where recycles are performed. This section provides an insight into the recycling methods with respect to how they work, whilst providing a quantitative and qualitative analysis into the various recycles and to what extent they can be utilised on the small (bench scale). Coupling the analysis together, the section concludes with the likelihood of the scalability from the bench scale to the pilot scale.

5.2 The Solution Top-Up Method (STUM) - Water Bath Heating (WBH)

5.2.1 Quantitative analysis

The calculations on the data analysed in this section were calculated using the following formula:

Masses:

Glass lens: g

Lens + 10 ml solution: g Dry

Mass (after heating): g

Calculation:

Mass of water= mass of solution - mass left

Mass of water= start weight - current mass

Mass left= mass of protein

Mass left= mass of solution – mass of water (-mass of lens)

Concentration= mass of protein / mass of water

Mass of protein required = mass of water x 0.05

Protein needed to be added (x) = mass of protein required – mass of protein (per 10ml)

Therefore, for 100ml of solution, x g X10 of protein is need to recycle

% Protein Used= Protein needed to recycle per 100ml/5 + x, where x= ratio per 100ml of protein added per each recycle.

The recycles were all performed with a pH of 3.8 ± 0.1, which is the pH range that proteins start to unfold but it is still in an acceptable range that it can be formulated into food products. After performing the amplitude control experiments, it was decided that the experiments would be performed at 100 % amplitude to maximise the output, in an environment where power usage was not a contributing factor. The flow rates for the air and liquid produced a residence time of 3 min. This is the ideal residence time as documented by *Santos et al* [71].

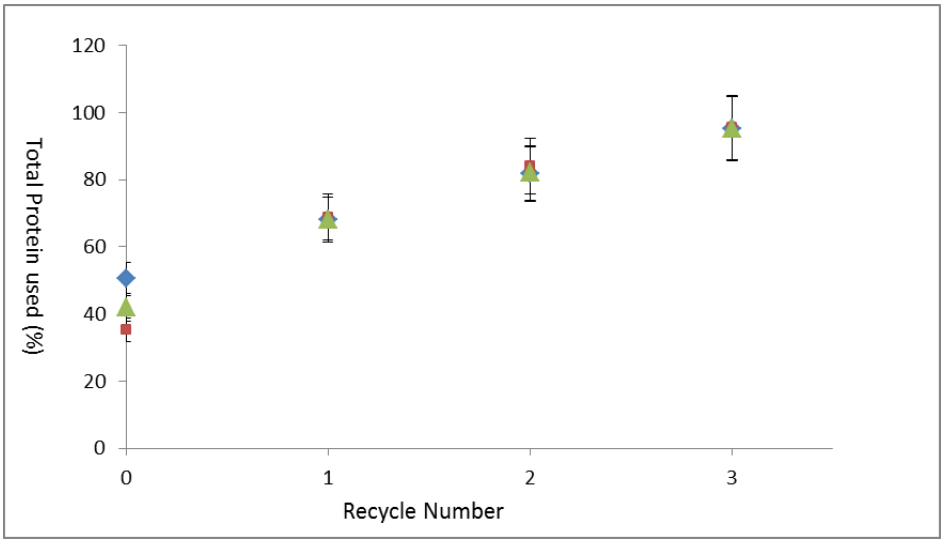

Figure 5-1. The total protein used for the STUM with water bath heating (WBH).

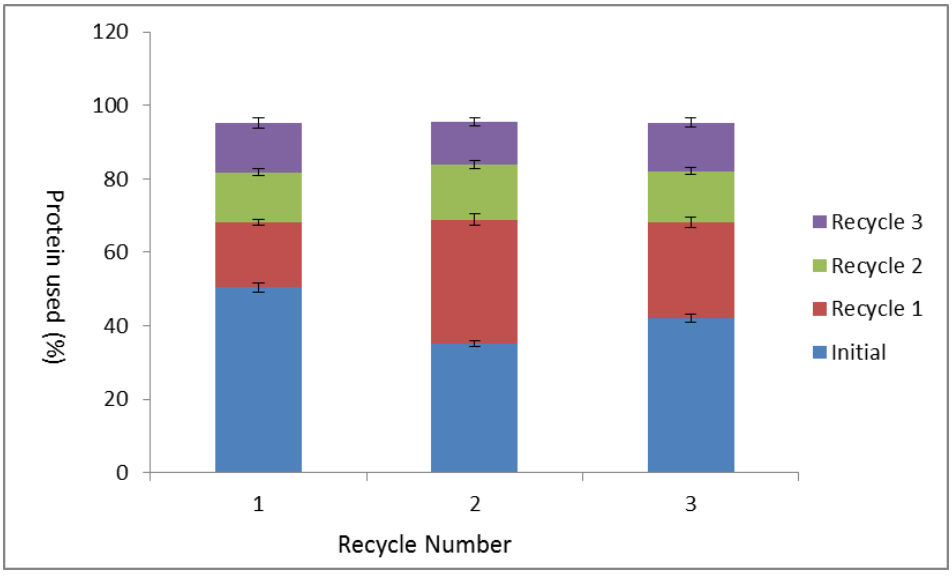

Figure 5-2. The protein used per each recycle for the STUM with water bath heating (WBH).

Tables 5-1, 5-2 (Appendix) and Figures 5-1 and 5-2 show the protein usage as a function of each individual recycle as well as the total amount used. The yield on protein usage is high and all the experiments performed showed a yield of >95 %. This is an exceptionally high yield compared to previous studies which have achieved yields of up to 50 %. What is clear from the data is that even though the amount produced on the initial sonication varies by 18.4 %, by one recycle; all three values are within 0.8 % of each other. This shows that the recycle mechanism is effective for optimisation. Because the recycle is based off re-concentration of the parent solution, it allows for variance in the amount of protein to add as well as how much solution will be left after each pass, meaning that the discrepancies from

the initial pass will even out as there will be more EWP solution to sonicate on the next pass. The protein used is also a function of not only the original protein, but also the protein added and used after each pass and is representative of the percentage used up and not the amount in grams. This means that if more protein is used up and more protein is needed to re-concentrate the solution, then the x term in the equation will be larger and will even out the percentages. The x term is important because without it, the usage would be measured against the initial mass and not take into account any extra protein added into the system, so percentages of 100 % would be possible without the x term, leading to serious anomalies in the data sets. The grams used up and added may be larger for some passes but the percentages could be similar. This is more efficient as on the larger scale the amounts used will vary drastically, so just having a usage in grams would become irrelevant as it would not be scalable. It should also be noted that protein usage does not necessarily mean a 1:1 ratio with air cell production as aggregation and denaturation of the proteins can occur. Particle size data from the Mastersizer provides more information on how much air cell formation and how much aggregation has occurred as they both appear in very different ranges where the air cells have a defined size range of submicron to 10 microns (ideally submicron- 1 micron for functional food applications). Microscope images also give an indication, although no actual values on the amount of air cells formed but physically shows if both air cell formation and aggregation have occurred in the samples.

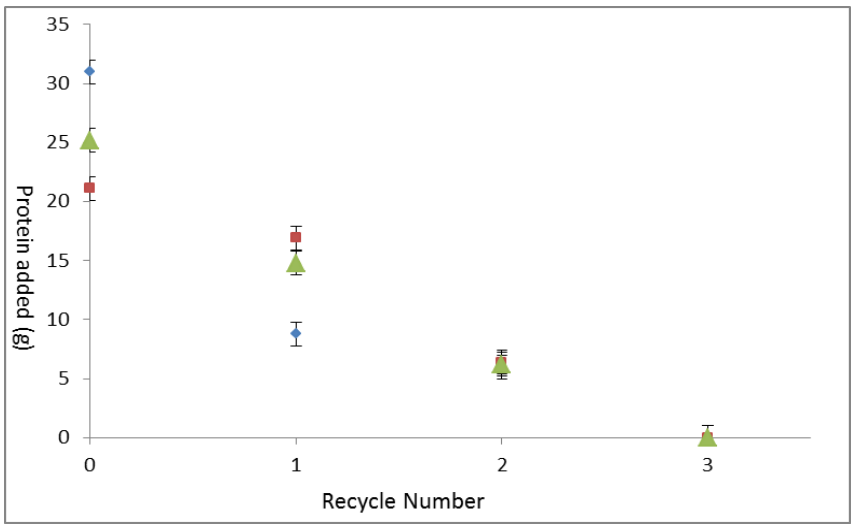

Figure 5-3. A graphical representation of the amount of protein added per each recycle for the STUM with WBH.

Table 5-3 (Appendix) and Figure 5-3 show the amount of protein added per recycle. As shown, there is an outlier on recycle number one. This is due to the reasons mentioned in the previous paragraph, where so much material was used up during the first pass, the amount of EWP solution was lower, and as protein added is a product per 100 ml of solution, the amount added is less. But as previously stated, the values correct themselves and by the end of the experiment, the amount added over the whole experiment was very similar with a maximum difference of 1.8 g, which is negligible when there has been over 100 g in total added and equates to an error of 1.4-1.5 % in terms of solid protein, and an error of 0.11 % in terms of the mass of the whole solution. Other than the one outlier, the various experiments fit a trend very well. The general trend is that the protein added decreases as the amount of recycles increases, which is to be expected. The value at recycle three is zero as this is when the experiment was stopped and the yield had achieved high amounts. The extra yield that could be produced is not efficient in terms of time and energy consumption to be a viable procedure, especially when the aim is to take the process to a larger scale. This allows the data to be usable for larger scale operations without unnecessary recycles which won't add much input compared to the cost to industry. Theoretical values were recorded for if the procedure was to continue, but as no more protein was added in the actual experiment, the value of zero is a more accurate representation of the experiment itself as opposed to theoretical values.

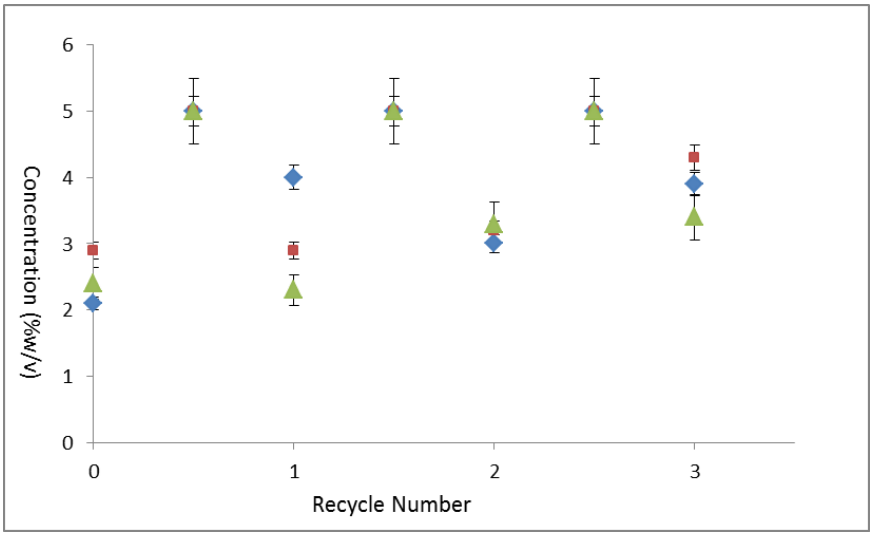

Figure 5-4. A graphical representation of concentrations of the waste protein solution after each pass and the intermediate concentrations after re-concentrating the protein solution, for the STUM with WBH.

Table 5-4 (Appendix) and Figure 5-4 shows the concentrations of the various waste protein solution throughout the experiments. The results are sporadic, but this is to be expected due to the difference in protein usage mentioned previously. A small difference in the protein usage can have a much larger impact on the concentration of the solution. The sporadic values do not have too much of an impact as the recycle is performed based of the amount to add which relates directly to the concentration; which previously mentioned before balances itself out over the course of multiple recycles. This is another reason why the recycle method is effective as it allows more controlled flexibility compared to performing a single pass. The intermediate concentrations were included at the ½ recycle points on the graph and although there is not technically ½ of a recycle it shows that the solution is re-concentrated between recycles. The main point to take away from Table 5-4 and Figure 5-4 is the observation of the concentration decrease and re-concentration and that a general rule of thumb, the more recycles performed, the closer to 5 % the new solution will be. This is due to the later stages not producing as much protein usage therefore the concentrations are expected to be higher.

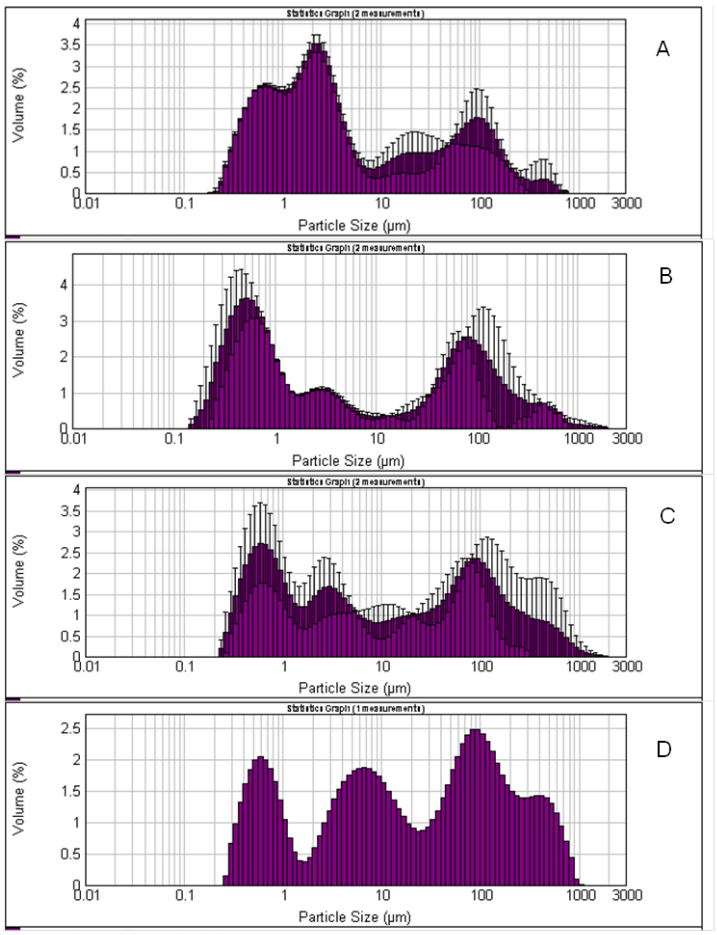

Figure 5-5. A series of Mastersizer distribution graphs showing the particle size during the STUM heat exchanger (ambient) method. A= After initial sonication, B= After first recycle, C= After second recycle, D= After third recycle.

Protein usage is not the full story with regards to AFE yields. Figure 5-5 shows the particle size analysis data obtained for the experiments. As shown, with regards to this method, the ratio of protein usage to air cell production is not 1:1. The peaks between 100-1000 microns are evident of protein aggregation, as that is a large particle size for a single protein molecule. The desired range for air cell formation is submicron to microns and it is apparent that both air cell and protein aggregate have formed throughout the series of experiments. The initial sample shows the best 'quality' of AFE out of the whole experiment, which is to be expected as the protein is all fresh. Quality is referred to the amount of air cells present in the solution and can be determined via the Mastersizer distribution and by looking at the samples under a microscope, but is subjective. For the initial sample the ratio of air cell to protein aggregation is roughly 3:1. This decreases to roughly 3:2 for the first recycle and 1:1 for the second recycle

and third recycles. This means for the protein usage value obtained, that 75 % of the value for the initial sample composed of air cells, 60 % for the values of the second recycles and 50 % of the obtained protein usage for recycles two and three. For example, taking experiment one which had protein usages of 50.5 %, 17. 6 %,13.7 %,13.4 %, the actual yield (as a rough guide) based of the rough ratio's obtained from the Mastersizer data is 38 %, 10.6 %, 6.9 % and 6.7 %, respectively. This gives an estimated yield of 62.2 % AFE from 95 % protein usage. The reason for this discrepancy between the theoretical and actual yield obtained for this method is due to the heating element of the method. Because the solution is heated for long periods of time in a water bath, the proteins are more susceptible to irreversible aggregation. This is what has occurred on the right hand side (100-1000 microns) of the distribution in the Mastersizer data and is the reason as to why there is more than a difference of 30% between the theoretical and estimated actual yields.

5.2.2 Qualitative Analysis

The quantitative analysis is the non-numerical data and physically looks at the structure under microscope with a Leica QWin black and white imaging camera. The aim of using an imaging microscope was to give an indication of how many air cells and protein aggregates are present in the sample, and to determine the 'quality' of the sample independent of numerical yield values.

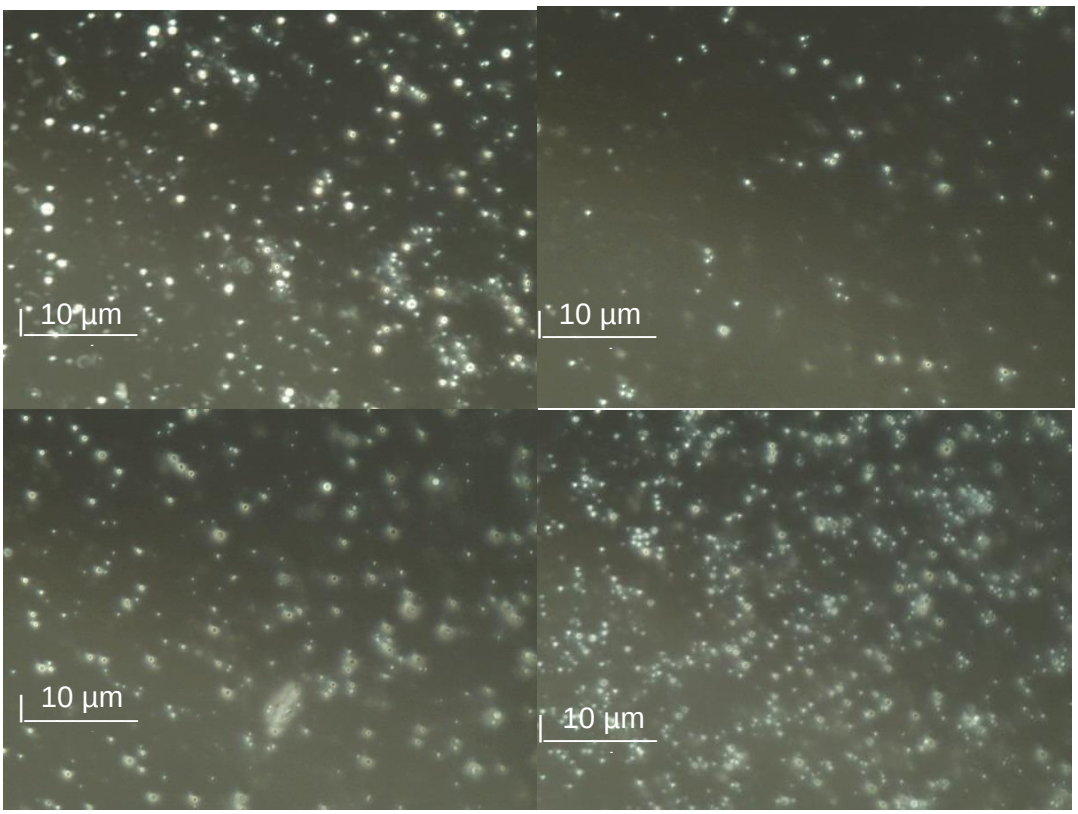

Figure 5-6. A series of images showing the Air cells in the AFE samples produced during the STUM with WBH. Top Left= Initial sample, Top Right= First Recycle, Bottom Left= Second Recycle, Bottom Right= Third Recycle. Taken with a Leica QWin black and white imaging camera.

The images in Figure 5-6 show the samples at 40X zoom. The glowing circles present in the images are representative of air cells and the cloudy/grey circles are indicative of protein aggregates, as are the amorphous molecules. From the images it is clear that the initial sample has a high concentration of air cells but also contains protein aggregates. This reinforces the reasoning as to why a there is a discrepancy between protein usage and AFE production and can be seen physically as opposed to numerically. The first recycle contains a smaller amount of air cells and once again contains protein aggregates. As the process moves towards completion, in the second and third recycles, the air cell concentration is less and the protein aggregation is more apparent. This is expected because there will be old protein in the solution that will have been heated multiple times and be more unstable and more susceptible to aggregation. The protein aggregates produced in the first two passes will still be present (due to the process being an irreversible conformation change), with the addition of any extra formed in recycles two and three, meaning that as the experiment

proceeds, the concentration of aggregates will increase. This is comparative to the numerical data and shows that what is produced numerically can be seen physically, reinforcing the reasons as to why this method produces a discrepancy in the results.

5.3. The Solution Top-Up Method (STUM) With a Heat Exchanger (HE)

5.3.1. Introduction

The aim of using the heat exchanger was to see if heating the solution en-route to the sonicator is more effective than the protein solution being sat in the water bath for an extended period of time. The flow rates were kept the same as when performing the experiments using a water bath. The Top-Up Methods with the heat exchanger has two different variations which were to do with the starting temperature of the protein solution. These were cold (~4 °C) and Ambient (room temperature). The aim of running these two different parameters was to see if the heat exchanger heated up the solution enough, so that it could be started from cold rather than room temperature, because this minimises time for the solution to warm up. On a small scale, this does not take long, but thinking in terms of scalability, a much larger solution would take a lot longer time meaning that from a business point of view, more money would be required to perform the experiments due to extra heating costs. If there is any way, however small, to drive down the costs of production, it will increase the feasibility of the scale up process.

5.3.2. Ambient Starting Temperature

5.3.2.1 Quantitative Analysis

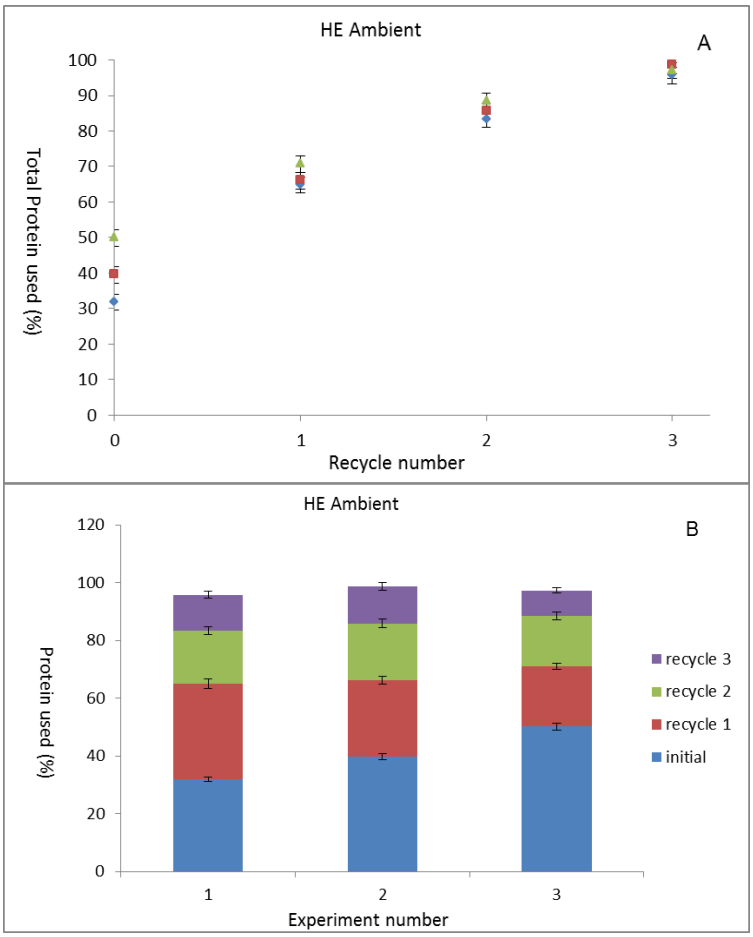

Figure5-7. The total amount of protein used (A) and the protein used per recycle (B) from ambient start.

Tables 5-5 and 5-6 (Appendix) and Figure 5-7 show the protein usage as a function of both total usage and the usage per recycle. Just like the results obtained in the previous method using the water bath as a heat source, all the experiments yielded >95% protein usage, with the highest yield obtained being 98.7 %. Again, the usage can vary drastically from one recycle to another but as stated before, the recycles balance themselves out with there being a difference of 2.9 % maximum value between the experiments after the fourth pass. This is more sporadic than with the water bath method, but the usage is slightly greater. And as previously stated, it is the AFE production from the protein usage that is key, not the protein usage in general. Because the solution is heated up during flow, it is not subjected to

high temperatures for a large period of time. This way of heating allows for the proteins to unfold and react without being exposed to too much heat and denaturing. In the water bath they could be subjected to 50 °C for up to an hour per single pass. Using the heat exchanger, this is cut down to under a minute, which is a significant difference.

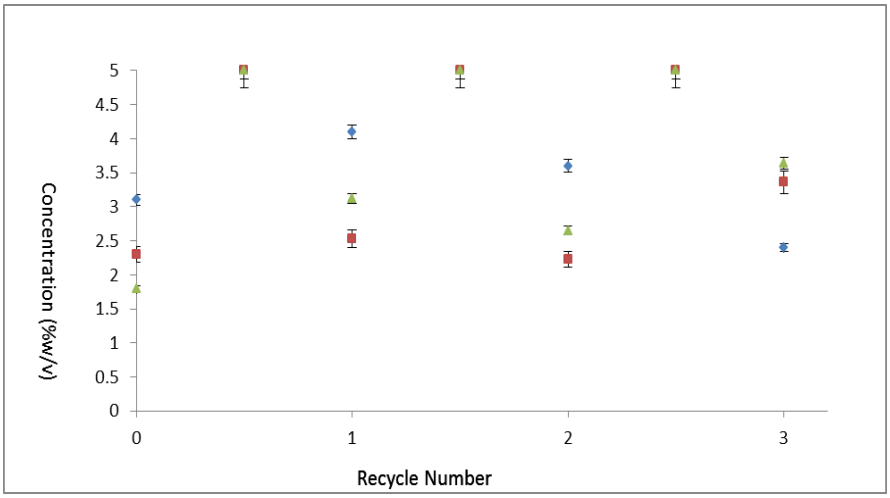

Figure 5-8. A graphical representation of concentrations of the waste protein solution after each pass and the intermediate concentrations after re-concentrating the protein solution, from ambient start.

Table 5-7 (Appendix) and Figure 5-8 show the concentrations of the waste solutions produced after each pass. The concentrations are sporadic again, but act as a function of the protein usage and relate to the values of the other contributing factors. This is a standard fit for the concentration graphs and follows a similar trend to that found for the previous method. If the concentration of a single experiment is compared against its own protein usage for the recycles and then compared against the other experiments, the concentrations correspond and fit well against each other, so the concentrations are proportional to the protein usage.

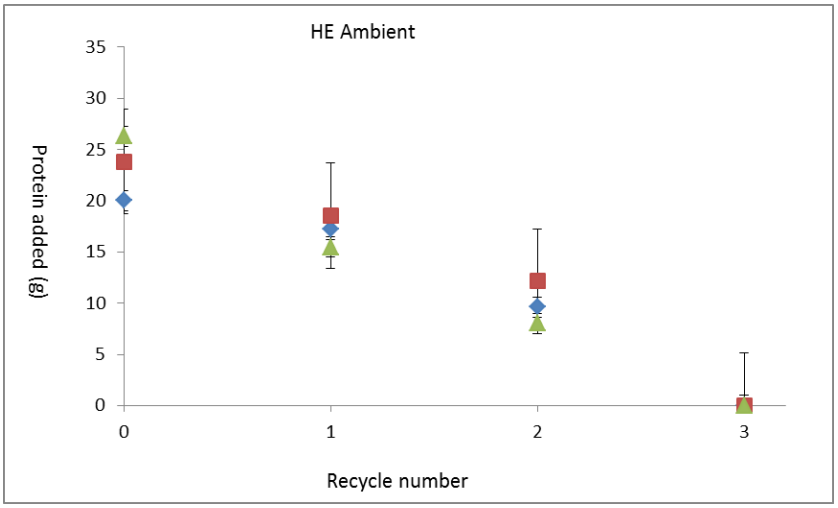

Figure 5-9. A graphical representation of the amount of protein added per each recycle from ambient start.

Table 5-8 (Appendix) and Figure 5-9 show the amount of protein added over the course of each experiment for this method. There are no outliers in the data, and the trend line for all the experiments fit a well-defined linear line. The maximum difference between the highest amount added and the lowest amount added is higher than the water bath method and equates to 7.8 g. This gives an error of 6.0-6.4 % of solid protein mass and an error of 0.48 % for the total mass of the EWP solution. Again for an accurate representation, the curve finishes with a point at zero to show that no protein was added after this point and that the experiment had reached its conclusion.

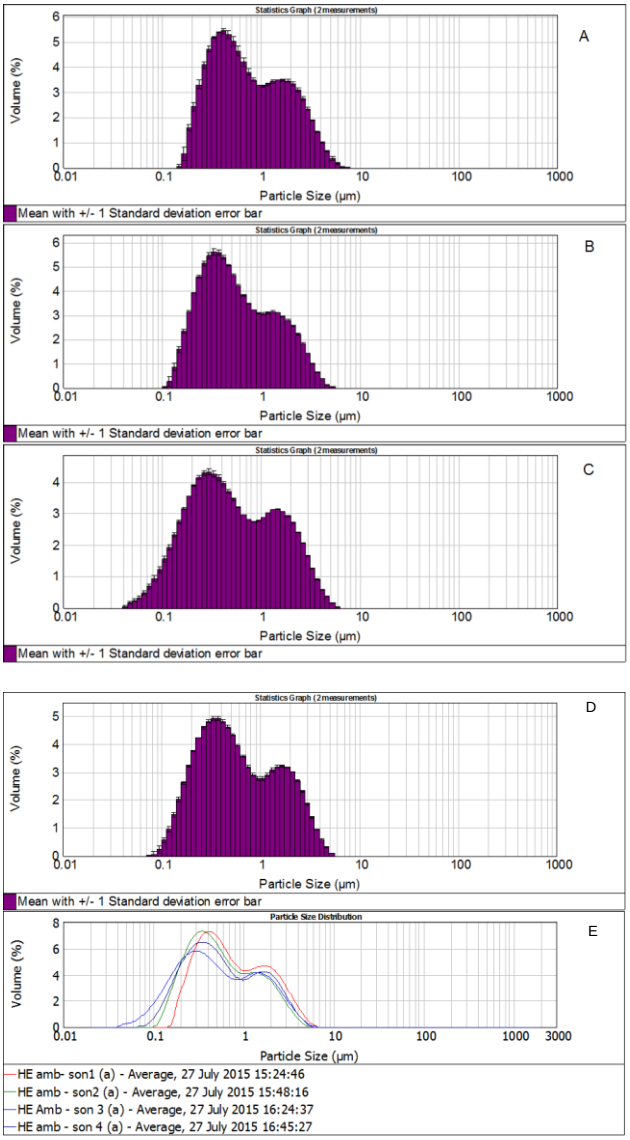

Figure 5-10. A series of Mastersizer distribution graphs showing the particle size during the STUM heat exchanger (ambient) method. A= After initial sonication, B= After first recycle, C= After second recycle, D= After third recycle, E= Comparison of all the recycles.

Figure 5-10 shows the Mastersizer data for this method which differs vastly compared to that of the water bath method. Where the water bath method was very polydisperse and contained both air cells and aggregates in varying ratios; this method produced no AFE particles over the size of 10 microns. This is the expected range for air cell formation and occurred for all recycles. This means that the protein usage is directly proportional in this case to the air cell production, and where there has been > 95% protein usage, there is also >95 % AFE yield. This is compared with the water bath method where it also achieved over >95 % protein usage, but only obtained ~62 % air cell production. This is a difference of over 30 %, showing a significant difference in both the quality of the solution produced and the

efficiency of the method. Because the solution in this method is heated up during flow, it is not subjected to high temperatures for a large period of time. This way of heating allows for the proteins to unfold and react without being exposed to excessive heat which causes denaturing and aggregation. In the water bath they could be subjected to 50 °C for up to an hour per single pass, using the heat exchanger, this is cut down to under a minute, which makes a significant amount of difference. This is true for the old proteins which may have undergone up to four passes, and will have not denatured due to the limited contact time with the heat source, as opposed to the potential of being heated for up to four hours in the previous water bath method. This shows that the excessive heating of the water bath was detrimental to the AFE production as the potential was there to produce a yield of at least 95 %. This is a much greater yield than anything obtained before the recycling mechanisms and paves a way to achieve a high yield output of AFE (not just protein usage) whilst minimising the overheads. The only disadvantage is the time it takes for the experiment to be finished.

5.3.2.2 Qualitative Analysis

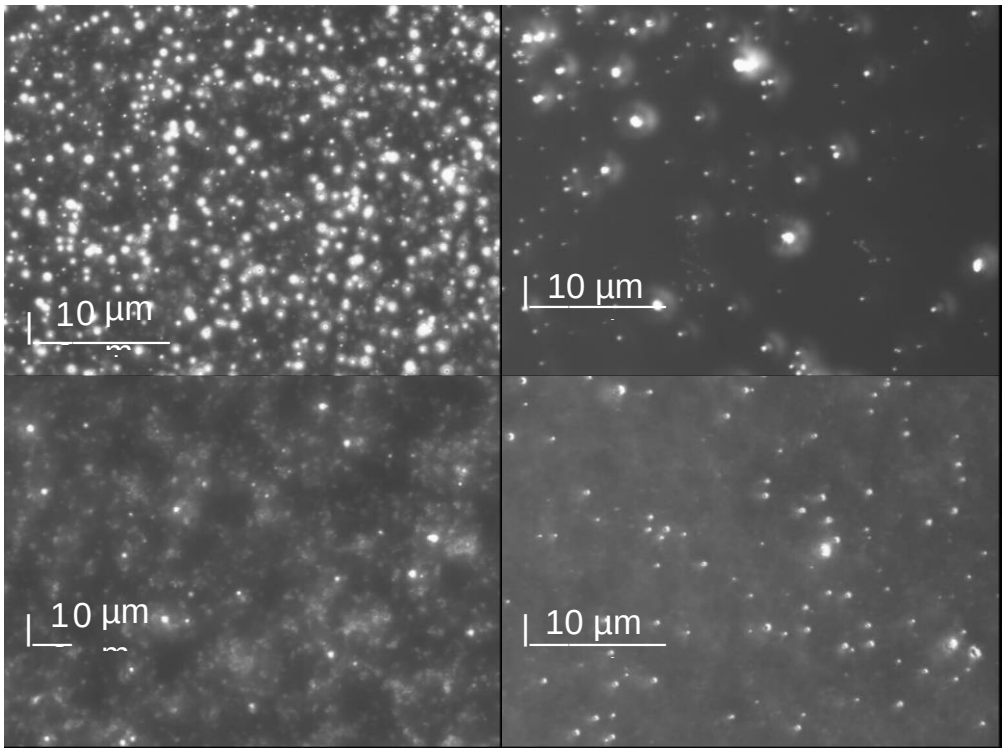

Figure 5-11. Concentration of the Air cells in the AFE samples produced during the STUM with HE at ambient start. Top Left= Initial sample, Top Right= First Recycle, Bottom Left= Second Recycle, Bottom Right= Third Recycle. Taken with a Leica Qwin black and white imaging camera.

The images taken under the microscope show a very similar story to the data obtained in the quantitative analysis. The initial sample has a high concentration of air cells with no apparent protein aggregates. Similarly, the first recycle shows no indication of protein aggregation although the air cells are in a lower concentration to the amount found in the initial sample. The second recycle shows a low air cell concentration and some protein aggregation. This could be localised aggregation as it never appeared in the Mastersizer distribution curves. In a large volume, some small local aggregation is going to have a negligible effect on the yield. The third recycle has the lowest concentration of air cells but no evidence of protein aggregation (the grey haziness was caused by cloudiness in the lens and not the sample itself), reinforcing the fact the protein aggregates observed in the image for the second recycle are most likely to be localised as they are not present in the final sample. So taking into account that the physical observation follows the numerical analysis, it has shown that the heat exchanger method from ambient temperature has been a very successful method and produce high yields, whilst limiting the protein aggregation. It is also a serious improvement on previous methods, whether they be recycling methods or otherwise.

5.3.3. Cold Starting Temperature

5.3.3.1. Quantitative Analysis

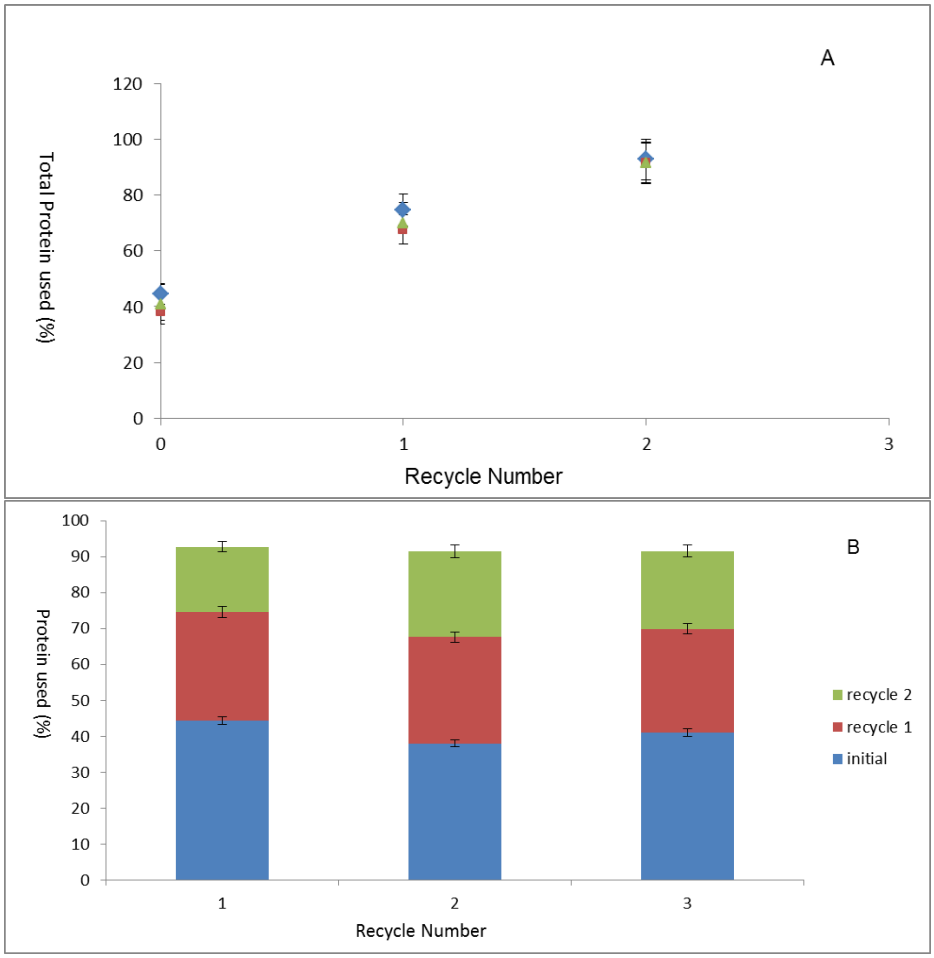

Figure 5-12. The total amount of protein used (A) and the protein used per recycle (B) from cold start.

Tables 5-9 and 5-10 (Appendix) and Figure 5-12 show the total protein usage and the protein usage per recycle for the STUM using a heat exchanger, this time from a cold starting temperature. The yields for this experiment are slightly lower than the ambient method but all the experiments achieved >90 % with the highest being 92.7 %. There are however two important factors to note with these results. The first is that there is one less recycle than its ambient counterpart. It is unknown as to why this occurred. It may be that because it started from cold so the molecules gained a larger amount of energy promoting unfolding and therefore yield. This is the only method to start form a cold temperature so there is no comparison from this temperature. Another recycle could possibly be utilised,

bringing the amount of recycles on par with the ambient method. However, when it has already achieved over 90% usage, the amount of extra time and energy would not be a viable endeavour especially when taking into account the extra costs that would be associated in an industry setting. Another important factor about this method is that the variance of protein usage on each recycle is much less than the other methods, where the usage could vary significantly, but balanced itself out. These results are all very similar in nature where the maximum difference for a single pass is 6.4 %, compared with the water bath method which could have a variance of 16 %, and the ambient method which varied by up to 18 % on some passes.

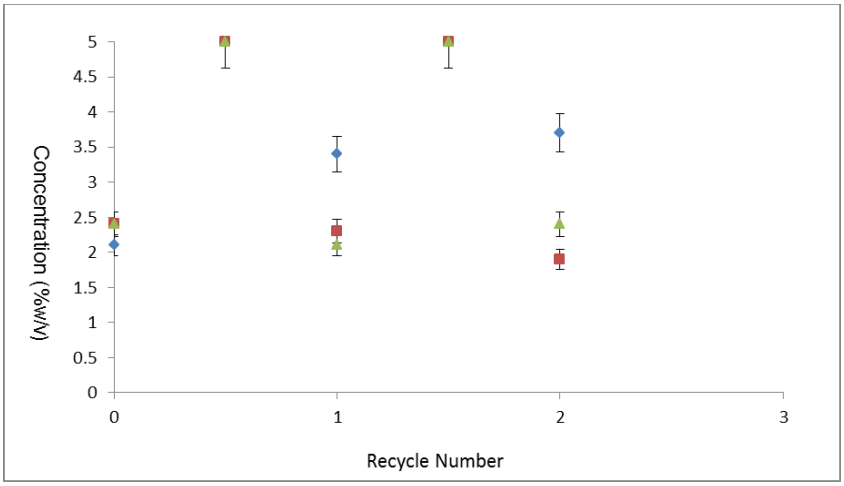

Figure 5-13. A graphical representation of concentrations of the waste protein solution after each pass and the intermediate concentrations after re-concentrating the protein solution, from cold start.

Table 5-11 (Appendix) and Figure 5-13 show the varying concentrations of the waste protein solution for the experiments performed. The same pattern is observed to that of previous methods. With the exception of one method which appears to have operated at higher concentrations, the general fit of the trend is much tighter than that seen by the other methods. Evidently the only main difference is there is less data points than the previous methods due to there being one less recycle performed.

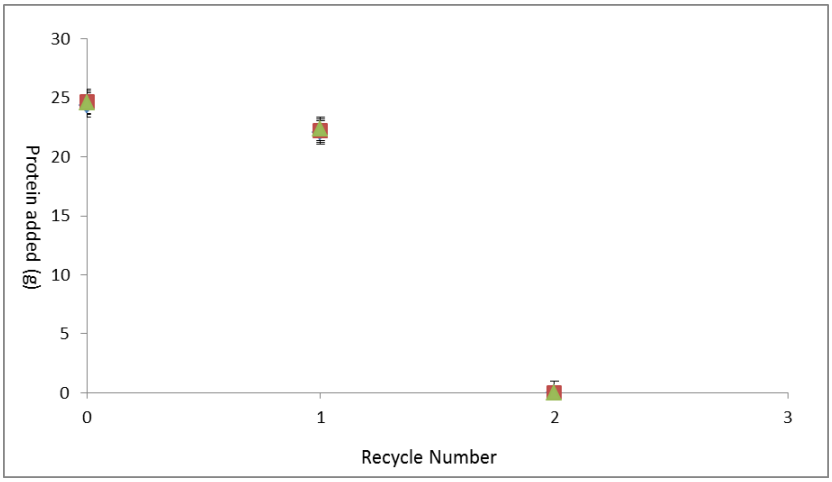

Figure 5-14. A graphical representation of the amount of protein added per each recycle from cold start.

Table 5-12 (Appendix) and Figure 5-14 show the amount of protein added for each recycle. The zero term this time is in the number two position as opposed to the three position as previously shown in other methods, which is due to the experiment only undergoing two recycles and not three. The first thing that is apparent with this data is that it is much closer together than any of the other experiments performed. This is not due to there being one less recycle as all the data is much closer together for both passes, in places where large variances have been found to occur in previous methods. The maximum difference between the highest amount added and the lowest amount added is 0.5 g. This equates to an error of 0.41 % of dry protein and equates to 0.03 % of the total mass of the solution, showing a very close set of data, especially when compared to 6-6.4 % calculated for the ambient experiment and 1.4-1.5 % for the water bath method.

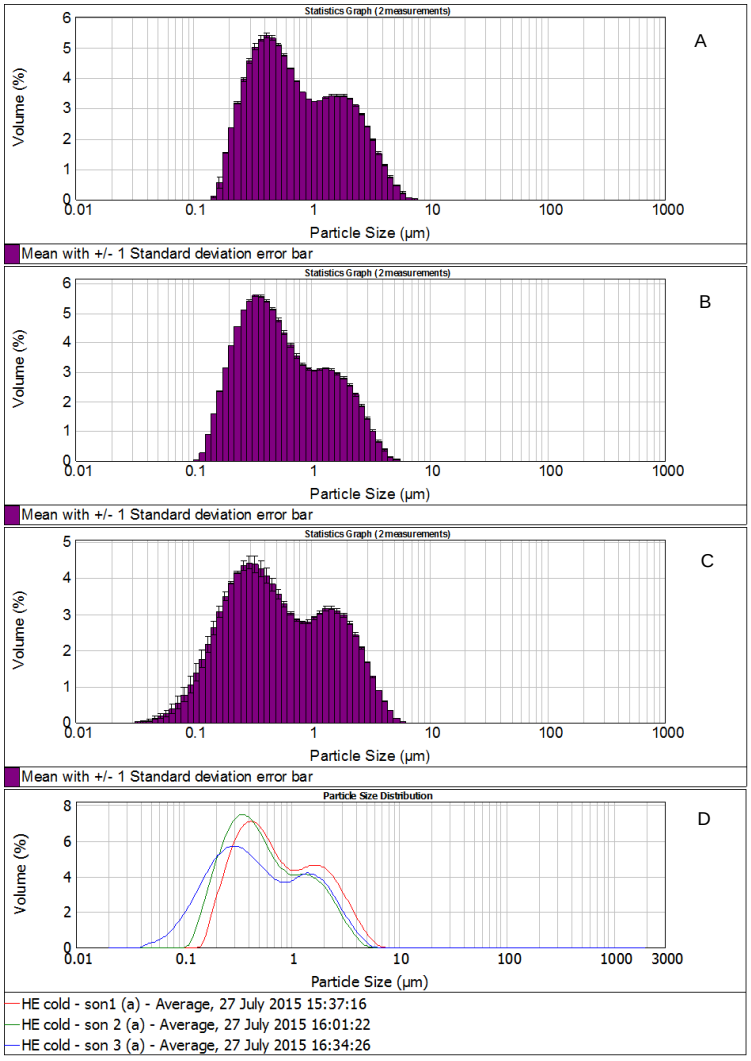

Figure 5-15. A series of Mastersizer distribution graphs showing the particle size during the STUM heat exchanger (ambient) method. A= After initial sonication, B= After first recycle, C= After second recycle, D= Comparison of all the recycles.

The particle size analysis data shown in Figure 5-15 shows a very similar trend to the ambient temperature data in Figure 5-10. All of the recycles show particles below the 10-micron region and none towards the higher end of the spectrum. This again postulates that the protein usage equates proportionally to the amount of air cells produced, so therefore the protein usage is equal the AFE yield. This means that using a heat exchanger from either ambient or cold starting temperature yields >90% AFE production. This is important because it shows that the heat exchanger exerts enough heat energy to heat up the solution efficiently without overheating and causing aggregation, independent of the starting

temperature. This could allow for solution to not be pre-heated, which would save time and money, but also preserve the native protein structure.

5.3.1.2. Qualitative Analysis

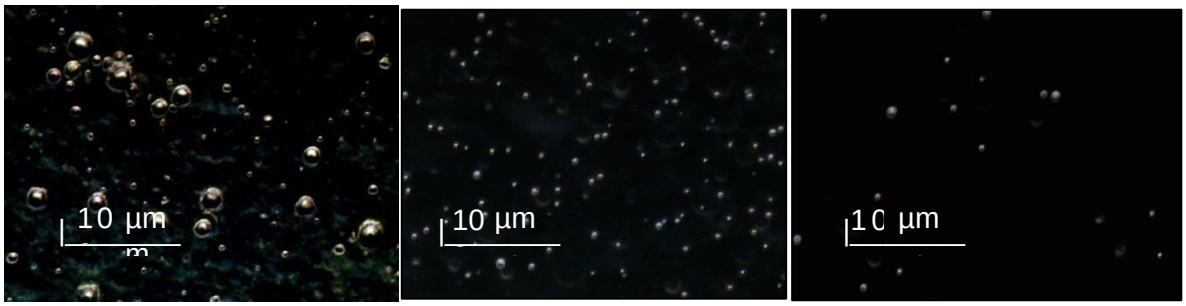

Figure 5-16. A series of images showing the air cells in the AFE samples produced during the STUM with HE at cold start. Left= Initial sample, Middle= First Recycle, Right = Second Recycle, Taken with a Motic Imaging Camera.

The images in Figure 5-16 were obtained via a Motic imaging camera and show a good correlation to the numerical data obtained. The initial sample and first recycle show a high concentration of air cells, which is to be expected giving the yields calculated. They also show negligible protein aggregates further reinforcing the numerical results, with regards to a proportional relationship between protein usage and AFE yield. The second recycle shows the presence of air cells in a lower concentration to the other two samples, which is to be expected given that the yield for this recycle was lower than its predecessors. There is also an absence of protein aggregation, showing that the sample produced is of a 'good quality'.

5.3.4. Summary of STUM Methods

The water bath method was a good starting point and showed good promise with protein usage being greater than 95 %. However, this was not the full story, as around 30 % of that was not turned into air cells, but instead formed aggregates due to excessive heating of the solution mixture. The heat exchanger methods show good promise, especially as this is the first time a heat exchanger has been used to pre-heat the protein solution prior to sonochemical irradiation. Both methods showed greater than 90 % protein usage which equated to a 1:1 ratio of air cell production with negligible protein aggregates. The ambient

method provided a yield of over 95 % with the highest achieved being 98.7 %, but performed one extra recycle compared to starting from a cold temperature. Despite one less recycle, yields of over 90 % were achieved from starting from cold, and the data in general gave a much tighter fit with less variation from the average. What these methods have shown is that the heat exchanger is a much more reliable heat source and is much more efficient in produce good yields. This leads the way for other methods to be heated by a heat exchanger as opposed to the water bath, resulting in the chance to obtain better quality samples in future methods. It also showed that the heat exchanger provides sufficient heat despite the short contact time, giving flexibility over solution starting temperatures to prevent protein destabilisation prior to reaching the reaction vessel.

5.4. Non Top-Up Recycle Methods (NoTUM)

The aim of the NoTUM was to determine the protein usage of the whole solution, without increasing the concentration back to 5 %w/v or centrifuging out the AFE. This also allows for a secondary aim, to see that if the air cells that have already been formed are stable to multiple exposures of sonication energy. There were two methods used in this category. The first method was used to sonicate the solution in stages. When the sonication had run to completion, the system was reset and the AFE was sonicated again. This was repeated multiple times. This experiment was performed by two students under my supervision. The Method was then adapted and subsequently called the NoTUCoM v2. This method produced a constant feedstock so that the system was never turned off and continually ran. After all the protein solution had been initially sonicated, without resetting the system, the solution was fed back into the starting vessel and then the output pipe (containing the product) was then fed back into the starting vessel. This produced a feedback loop, upon which the product was automatically collected back in to the starting vessel, producing a completely continuous process. It is very raw in design, but the aim was to see a feedback system could be used on the small scale and in turn give an idea to if it would be a more efficient route for recycling on the larger scale. As the recycle process takes a long time, a quicker way to

recycle on the larger scale would make the process as a whole more feasible. So taking that into account was the reason for trying this set of experiments.

5.4.1. Non Top-Up Centrifugal Method (NoTUCeM)

5.4.1.1. Introduction

The aim of this method was to see how much of the original protein could be used without the need to top-up. This could be beneficial as it would eliminate a lot of steps in the recycle process. The Air-Filled Emulsions were removed by centrifuge as per the 'Solution Top-Up Method' but the leftover solution was then re-sonicated without additional protein being added.

5.4.1.1. Quantitative Analysis

Table 5-13 and graph A on Figure 5-17 show the protein used for the NoTUCeM. The protein usage is less than the STUM methods, which is to be expected as it is old protein that is constantly being recycled, and is therefore of a lower concentration compared to the STUM counterparts. With there being less protein in the solution, the probability that the same amount of protein will come into contact with superoxide radicals is lower compared to a solution that has been re-concentrated. Therefore, there is a larger variation of protein usage with a maximum difference of 12.1 %. The protein usage is not as an important factor for this method as the aim wasn't to achieve a high yield, but to see how many passes a solution can go whilst being depleted and not re-concentrated. It was to be used as a stepping stone to outline the variables for the Non Top-Up Continuous Method (NoTUCoM), which shows more promise in term of time scales. The centrifuge was used to remove the AFE, so that the variables could be defined mainly in terms of timescales before attempting a continuous method with no removal of AFE during the experiment. Although the end results vary slightly, the trends are very tight to each other and follow the same pattern, showing reproducibility.

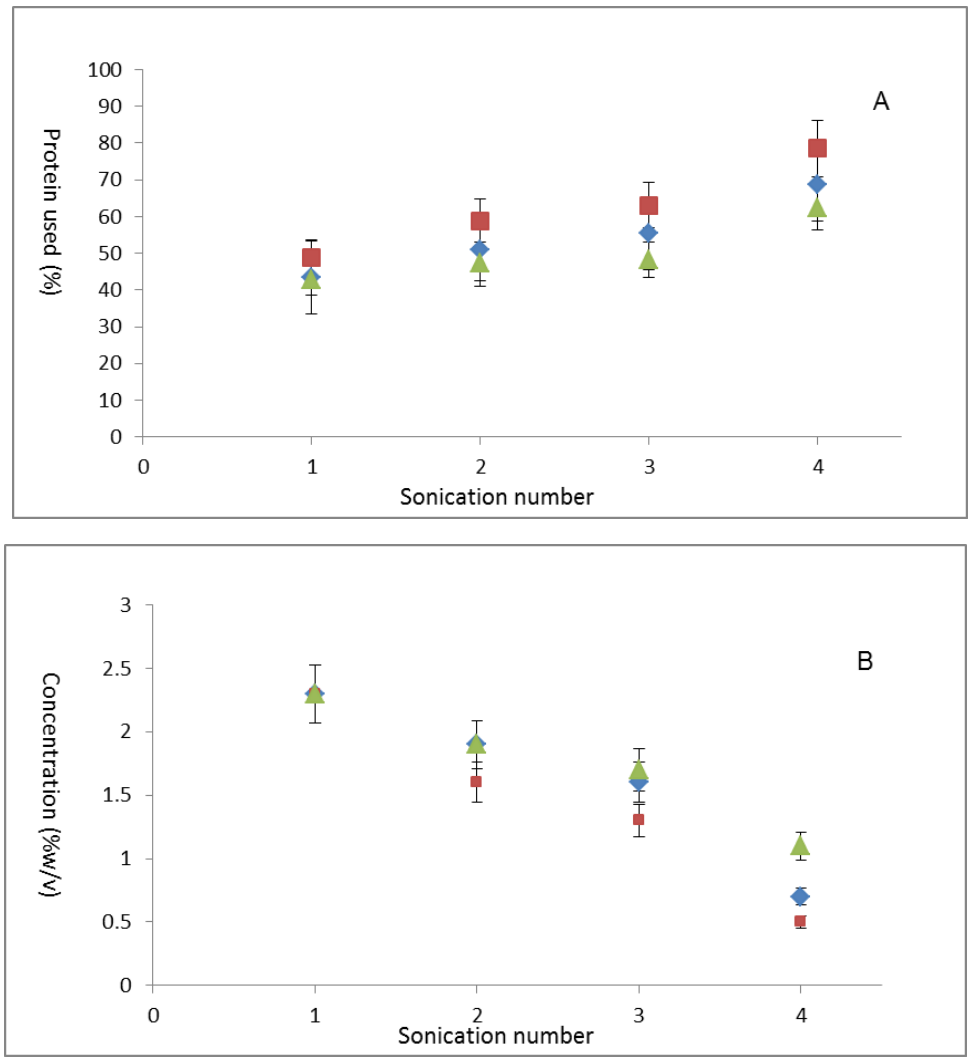

Figure 5-17. The used protein (A) and solution concentration (B) during the NoTUCeM.

Table 5-14 and Figure B from Figure 5-17 show the concentration of the waste protein solution. Unlike the STUM methods, the concentration is a continuous decrease and it is expected that the more passes the solution undergoes, the lower the solution concentration will become, as there is no replenishment of concentration. Each experiment follows a similar trend even though the values vary. The variation is due to the protein usage and there is no cause for concern as there is a constant depletion of material.

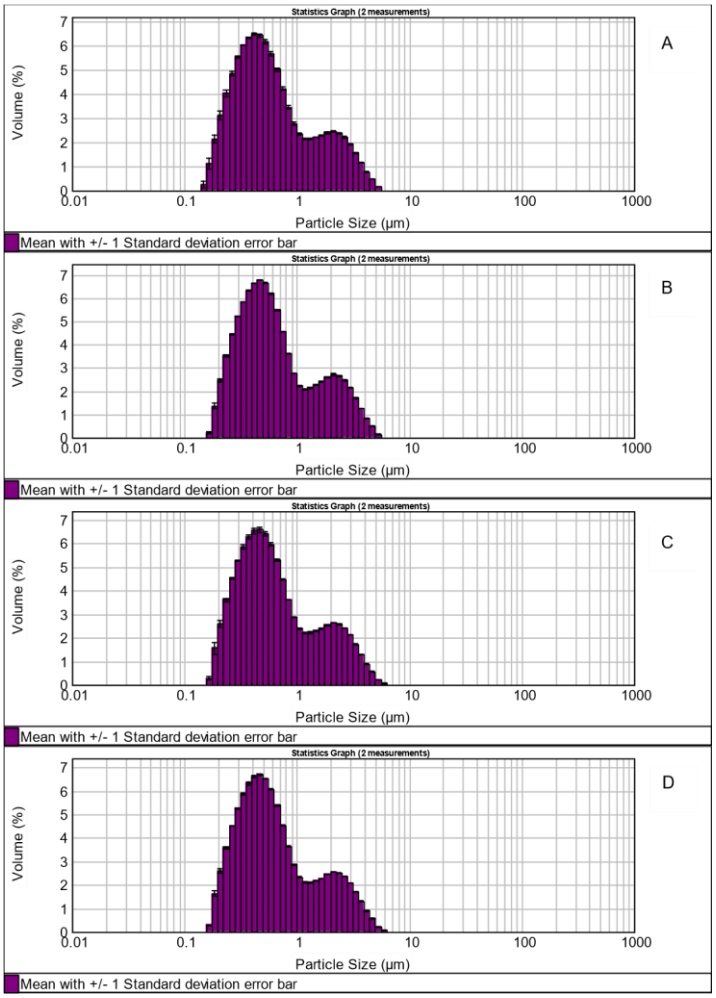

Figure 5-18. A series of Mastersizer distribution graphs showing the particle size during the NoTUCeM. A= First Sonication, B= Second Sonication, C= Third Sonication, D= Fourth Sonication.

The data shown in in Figure 5-18 shows the particle size of the samples obtained from the NoTUCeM. The data shows that the samples contain air cells with no protein aggregates (or at least negligible) and shows a similar trend to the top-up methods (with a heat exchanger). This means that the protein usage equates proportionally to the amount of AFE produced; therefore, the method has produced up to 78.5 % AFE yield without the addition of extra protein, which again is significantly more than any other yield produced prior to these set of methods. The difference between this and the top up methods is the amount of protein used by weight, therefore the amount of AFE by will vary drastically compared to the top-up methods. For example, taking the ambient method of 98.7 % where 129.60 g was added compared to this method of 78.5 % where 75 g was added. This equates to a 127.9 g protein usage compared to 58.9 g from the non-top-up method. This is a difference of 69 g compared to 20 % which is substantial, but as mentioned before, the equation balances out

the percentage of the topped up method. The values are not as important for this method as the main purpose was to determine the time to allow the continuous method to run for whilst still producing a good protein usage. This method has determined the continuous method (NoTUCoM) parameters to run for an equivalent of four recycle passes which equates to 240 ± 20 minutes.

5.4.1.2. Qualitative Analysis

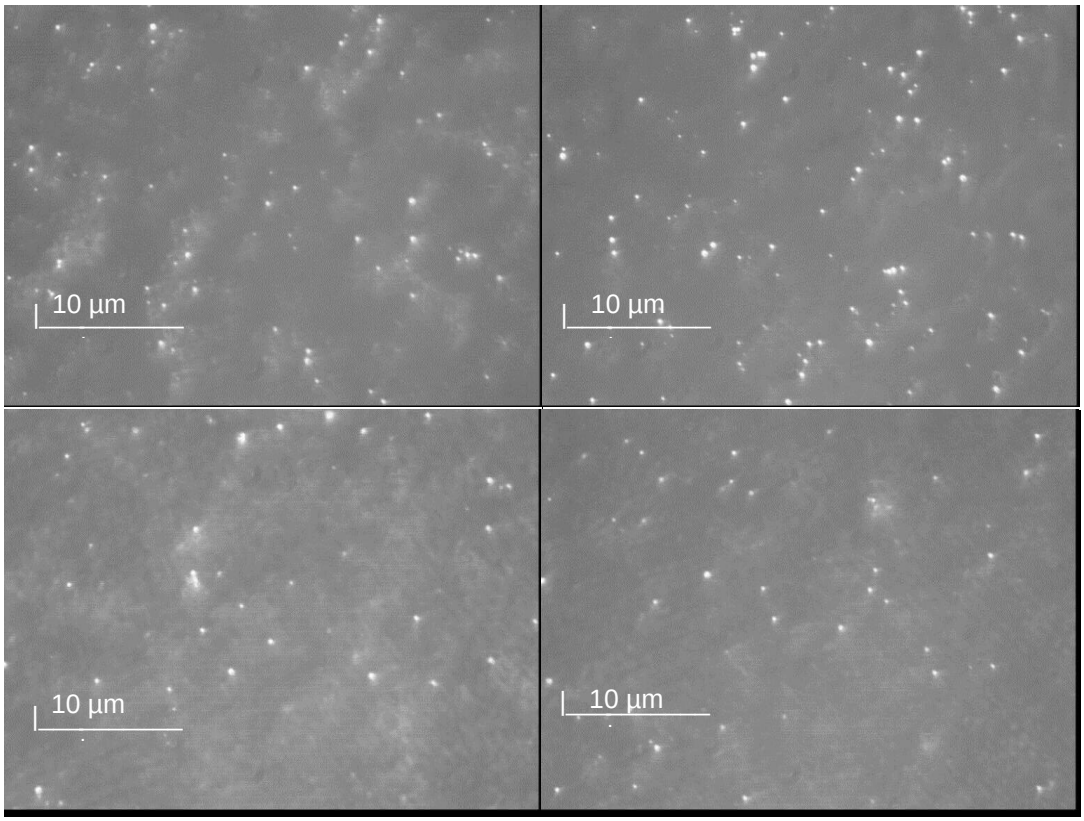

Figure 5-19. A series of images showing the air cells in the AFE samples produced during the NoTUCeM. Top Left= First Sonication, Top Right= Second Sonication, Bottom Left= Third Sonication, Bottom Right= Fourth Sonication.

The images in Figure 5-19 show the presence of air cells, but just like the Mastersizer data showed, an absence of aggregated proteins is present in the solution (the cloudiness is attributed to the focus on the lens of the microscope). What the images show, is that there is a good concentration of air cells throughout but not as many produced later on, due to the depleted solution containing a lower amount of proteins compared to the average 5 %, reacting with the superoxide radicals. This is expected to happen because in the top-up

methods, there is less solution but the concentration is still 5 %, resulting in a decent yield, whereas this method has both a depleted solution and depleted concentration.

5.4.2. Non Top-Up Continuous Method (NoTUCoM)

5.4.2.1 Introduction

The aim of this NoTUM was to determine the protein usage of the whole solution without increasing the concentration back to 5 %w/v, or centrifuging out the AFE. A secondary aim of this method was to see that if the air cells within the Air-Filled Emulsion were robust enough to withstand exposure to ultrasonic cavitations, multiple times (meaning that a continuous flow would not be a problem as the sample itself would not be damaged by the process). There were two methods used in this category. The first method was used to sonicate the solution in stages. When the sonication had run to completion, the system was reset and the AFE was sonicated again, this was repeated multiple times. The method was then adapted and subsequently called the NoTUCoM v2. This method produced a constant feedstock so that the system was never turned off and continually ran. It is very raw in design, but the aim was to see a feedback system could be used on the small scale, and in turn give an idea to if it would be a more efficient route for recycling on the larger scale. A continuous flow through would be much more beneficial for the larger scale as it would remove a lot of steps and could be set to run for a designated period of time, without interruption, allowing for timescales to be drastically cut down on the large scale.

5.4.2.1 Quantitative Analysis

Tables 5-15 and 5-16 (Appendix) show the protein usage and concentration for the original NoTUCoM and the adapted NoTUCoM v2, respectively. The protein usage for both methods is very similar, but slightly higher for the adapted method. The protein usage was considerably lower than the NoTUCeM and STUM. The reasoning behind this difference is due the recirculation of a mixture of AFE and protein solution, as opposed to pure protein solution.

Because the reaction mixture does not have the AFE removed before undertaking another pass, the ratio of EWP to AFE compared to EWP to water (in pure protein solution), reduces the concentration of EWP in the solution. This means that where there is EWP solution (even a depleted one), the only molecules interacting in the reaction vessel is protein. This is not the case when the AFE product is circulated as there is a mixture of air cells and proteins. This means that some of the superoxide radical sites could be blocked by the air cells particles, causing the protein to travel through the flow through cell without reacting. This is more likely to be the case with a high amount of air cells as their size is larger than that of a protein molecule, so will occupy up a larger volume in the flow-through cell. This means that after the initial sonication, the bulk of the air cells could inhibit the production of more air cells in subsequent passes, with little or no radical sites for the unreacted proteins to bind to. In addition to this, with comparison to the top up methods (STUM), there is no extra protein inputted into the reaction so is more likely to produce a lower yield in the reaction, due to continuous circulation of both depleted and older proteins.

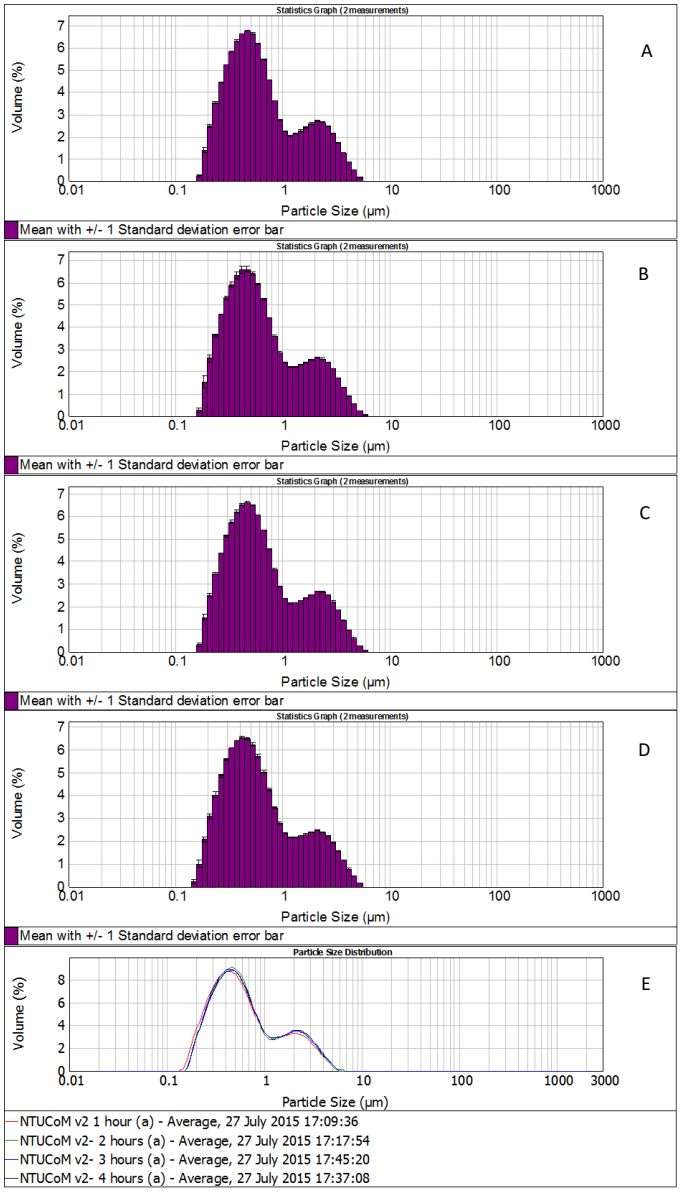

Figure 5-20. A series of Mastersizer distribution graphs showing the particle size during the NoTUCoM v2 A= After 1 hour, B= After 2 hours, C= After 3 hours, D= After 4 hours, E= Comparison of the distributions.

The particle size analysis shows the distributions after 1, 2, 3 and 4 hours of continuous circulation. The distributions do not show much variation from the sample taken after 1 hour (equates to 1 full pass), and is obvious from the comparison curves in distribution E. This shows that the air cells could be inhibiting extra protein usage by blocking the reactive radical templates, causing stagnation in both protein usage and air cell production. If this was not the case, it would be expected that there would be a greater shift of volume between the distributions when the run time is four times greater than the initial distribution. The aim of the method was not to produce the highest yield, as this would be unlikely given the change in

solution mixture ratios, and the lack of additional protein. Instead it was intended to perform the first complete continuous recycle for AFE production, which was achieved multiple times. The method also gives a significantly reduced timeframe in terms of the whole process (not just sonication stages), as it removes multiple steps that the STUM must undertake. This gives the method potential for scale up because if it can be optimised, the reduced timeframe would allow the production of AFE quicker and cheaper- both of which are major factors to consider when judging the feasibility of a process for industry. Even though the process does not produce much extra yield on the extra passes, it does give very valuable information with regards to air cell longevity. The combination of heat and ultrasonic energy is more than enough to change the conformation and structure of proteins. However, this is not the case for air cells. What this method shows is that air cells are robust enough to withstand both long periods of heat energy without breaking down, or undergoing emulsion instabilities. It also shows that they are robust and stable enough to withstand multiple exposures to ultrasonic radiation and acoustic cavitation energy without the structure breaking down or degrading. This stems from the air cells having a good balance of rigidity and flexibility which can dissipate the energy it is exposed to. This is very useful for a formulation perspective as it shows that the air cells are stable enough to withstand heat treatments and multiple industrial scale food processes, allowing them be formulated into whipped toppings without extra steps needed to be taken to preserve stability. It also shows that once in a formulated product, they will be stable enough to withstand the physiological changes associated with the formulation, e.g. rheology; and even enhance stability dependent upon the stability of the original product that the air cells are formulated into e.g. air cells enhance the stability of the emulsion in whipped toppings.

5.4.2.2 Qualitative Analysis

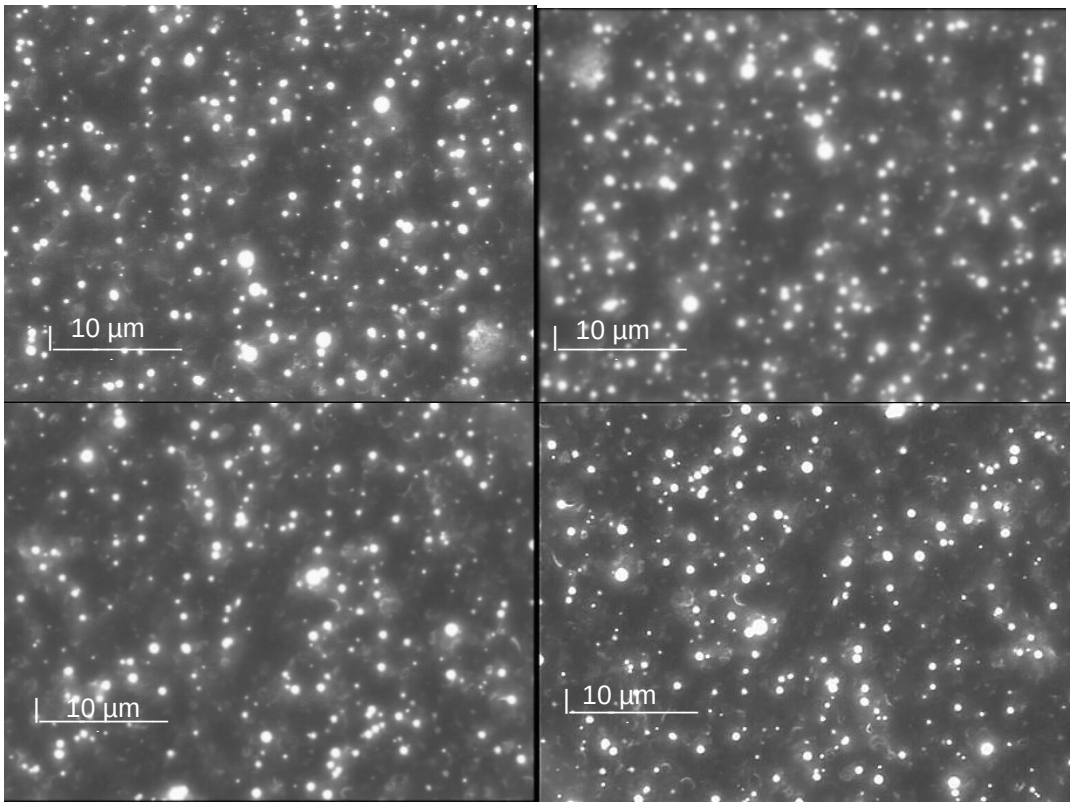

Figure 5-21. A series of images showing the air cells in the AFE samples produced during the NoTUCoM v2. Top Left= After 1 hour Top Right= After 2 hours, Bottom Left= After 3 hours, Bottom Right= After 4 hours. Taken with a Leica Qwin black and white imaging camera.

The images in Figure 5-21, show the AFE samples. The images here reinforce the fact that the consistency and concentration of air cells in the sample, does not change after the first pass. What the images do show is that there is a large concentration of air cells, sufficient enough to block the binding sites for the unreacted protein, therefore causing the volume of air cells to plateau after the first pass. What the images do show is that the structure of the air cells was undeterred after passing through the reaction vessel four times. The structures appear to be unchanged and do not show any sign of deformation or destabilisation of the outer shell. This physically shows their robustness and increased stability compared to their predecessors, which gives further evidence towards their use in formulations where their stability will enhance the end product. The images also show no evidence of flocculation, which is caused by the breakdown of long range repulsion forces, which in turn causes a net

attraction between particles. It was thought that there would be enough energy to destabilise the intermolecular interactions between particles to cause this aggregation. This however, does not appear to be the case, in part due to their durability and individual stability, but part because they are still solubilised in water. As water is a stable polar molecule, unaffected by the acoustic cavitations, it still causes interactions via hydrogen bonding, preventing the long range repulsion forces from breaking down, preventing flocculation. If the water were to be removed under these reaction conditions, then a water flux effect would occur and lateral capillary forces could cause aggregation between air cells.

5.4.3 Conclusion of NoTUM's

The NoTUM's have provided a different outlook on the production of AFE compared to the other methods previously undertaken. Instead of a focus on AFE yield via maximising the yield and minimising waste, they have shown that a depleted solution can still produce AFE in the form of the NoTUCeM, as well as showing that a fully continuous process can be performed in the NoTUCoM. The NoTUCoM also showed that the air cells are very durable, stable and can withstand multiple exposures to ultrasonic radiation energy and heat energy, without degradation or destabilisation of either the protein coat or the air filled core. The NoTUCoM has shown for the first time that a completely continuous process is possible, and could now act as a predecessor for more adapted and optimised methods, and could eventually be used on the larger scale due to having a considerably reduced time frame compared to the STUM. This could make the method more attractive from an industry point of view due to timescales and cost being major parameters when determining method feasibility, both of which are reduced by this method.

5.5 Energy output of NoTUM against STUM

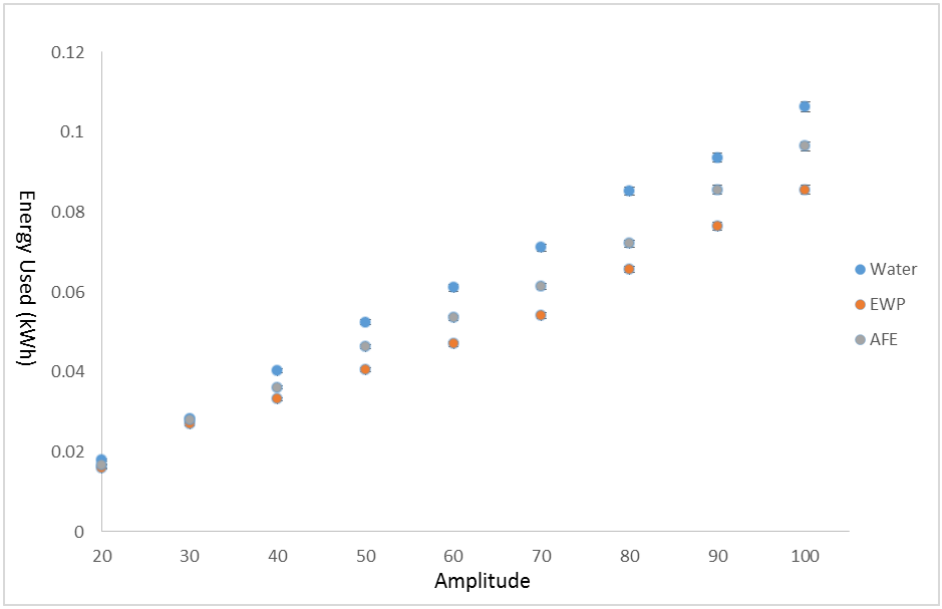

Figure 5-21. The Energy usage of water, EWP and AFE in kWh with respect to the amplitude.

From an industrial point of view, energy consumption is a major element compared laboratory scale research. The data in Figure 5-21, was plotted using the data from Tables 3-4 and 3-5 (Appendix) but re-plotted in kWh, the standard unit of energy measured by major energy companies [72]. According to the Energy Saving Trust, the average cost per 1 kWh is 14.05 pence [73]. If a STUM experiment on the bench scale involving 4 X 1 hr is performed at 100% amplitude. Then the total kWh would be 0.344 kWh compared to a NoTUM (under same time frame and amplitude) of 0.384 kWh. This equates to an increase of 11%, which is not a massive difference in terms of value for a single experiment of the laboratory scale. However, on an industrial scale where there is continuous running of larger equipment with much larger volumes, it would make a much larger difference to the total energy usage and therefore cost. It would have to be evaluated as to whether the reduced timeframe would compensate for the extra cost in energy, by saving of energy in other areas of the process.

5.6. Critchley-Green Recycling Method Conclusions

The Critchley-Green Recycling Methods provided methods based on both batch and continuous recycle processes as opposed to a single pass (Chapter 4). The methods have given valuable insights into the possibilities of recycling AFE solutions to maximise the output and minimise the waste. The water bath method was a good starting point for method development and showed a good usage of protein, but would be unusable in formulations due to the large amount of protein aggregated produced by excessive heating. A quick and effective way to heat the solution, with minimal exposure time, was found by using a heat exchanger. The heat exchanger methods showed a high protein usage which corresponded to an equally high output of AFE, with negligible protein aggregation. All methods produced over 90 % AFE yield with the highest output being 98.7 %. In terms of maximising yield and reducing the waste, these methods have proved to be the most effective. The Non Top-Up Methods did not produce as high of a yield but gave insights into other areas where yield was counteracted by efficiency in timeframes. The NoTUCeM was an intermittent method to work out the parameters for the continuous method. However, it did show that a depleted solution can still produce a good output, and was key to the success of the continuous method. The NoTUCoM was the lowest AFE producer. However, it provided a novel process for AFE production with respect to it being the first production method to be completely continuous. The method also showed that the air cells are very robust and can withstand multiple exposures to both heat and ultrasonic energy, without degradation or particle breakdown. This is useful from an industrial point of view as it has shown that AFE would be able to withstand formulation and heat treatment processes', making it useful in food applications, of which it has been engineered for.

The methods as a whole effectively addressed the challenges associated with the small scale, and more. They have also given a set of wide-ranging experiments that can be progressed and optimised for testing on larger scale systems.

CHAPTER 6- CROSS-FLOW FILTRATION (CFF) OF AFEs

6.1. Introduction

This method was a new concept to the production of AFE and aimed to not only provide an efficient method of filtration; but also to concentrate up the AFE solution, removing both water and soluble proteins and leaving just the air cells, which are ready to use in formulations. It was used as a NoTUM in the sense of that there would be no re-concentration by extra EWP solution. Instead, the solution would concentrate itself, releasing waste solution (that could undergo a recycling process), allowing the AFE to be extracted easily. Two methods were investigated. This include a two stage process, where upon a solution of AFE was made up after one sonication pass. It was then separately passed through the CFF module to release the EWP supernatant and collect the AFE, both for analysis. The second method was a one stage process and essentially combined both processes into one continuous method. There were two pumps set up bridged by an intermediate collection vessel, in which both fresh AFE produced from the sonicator and concentrated AFE were deposited into (see Figure 3-6). As this is a novel way of extracting and concentrating AFEs, these methods were tried to see if a) it was possible to extract in this manner and b) how effective it is. The one stage process could be a very useful concept for larger scale and industrial processes as it would both: minimise the time scale (reducing cost) and provide a concentrated form of AFE which is ready to use in formulations; minimising both the timescale and the need for extra complicated steps before formulation. The cross-flow filtration module used in shown in Figure 6-1.

Figure 6-1. An image of the cross-flow filtration module used during the experiments.

6.2. Two Stage Process

Table 6-1. Protein usage during the CFF two stage method and the resulting concentrations of both the concentrated AFE solution and the EWP supernatant solution.

	Protein used (%)	Concentration (%w/v)
EWP supernatant	16.5	3.9
AFE after CFF	14.0	14.0

Table 6-1 shows the difference between the two solutions produced in the CFF experiment. There is not a high amount of protein usage, however at this stage it is not an issue as the premise of the experiments was to see if it was possible to use the CFF module to concentrate the AFE solution effectively, ready for formulation, and to not obtain the highest yield as this could be optimised by the research group if the process worked. The process worked with respect to concentrating the AFE solution up to 14 % from only using 16.5 % protein usage. This shows that the AFE can be concentrated within itself and leaves plenty of scope for improving upon the yields. The solution has been roughly concentrated up

by three times from the original starting concentration and nearly four times on the resulting EWP solution concentration. In terms of AFE isolation and extraction, it is a novel method which will significantly reduce time and effort by producing AFE samples ready for formulation engineering. This is true for both small and larger industrial scales where timescales and the ability to not over complicate processes are key factors. The timescale for this was quicker than splitting up the process (including filtration and extraction). However, a small pump was used (100 $mlhr^{-1}$) so the CFF step still took a long time to reduce the solution to concentrate. In other experiments a larger pump would be key to reducing timescales even further.

A previous experiment of this kind was performed by *Green et al (unpublished data)* where upon the solution was concentrated to roughly six times the EWP solution.

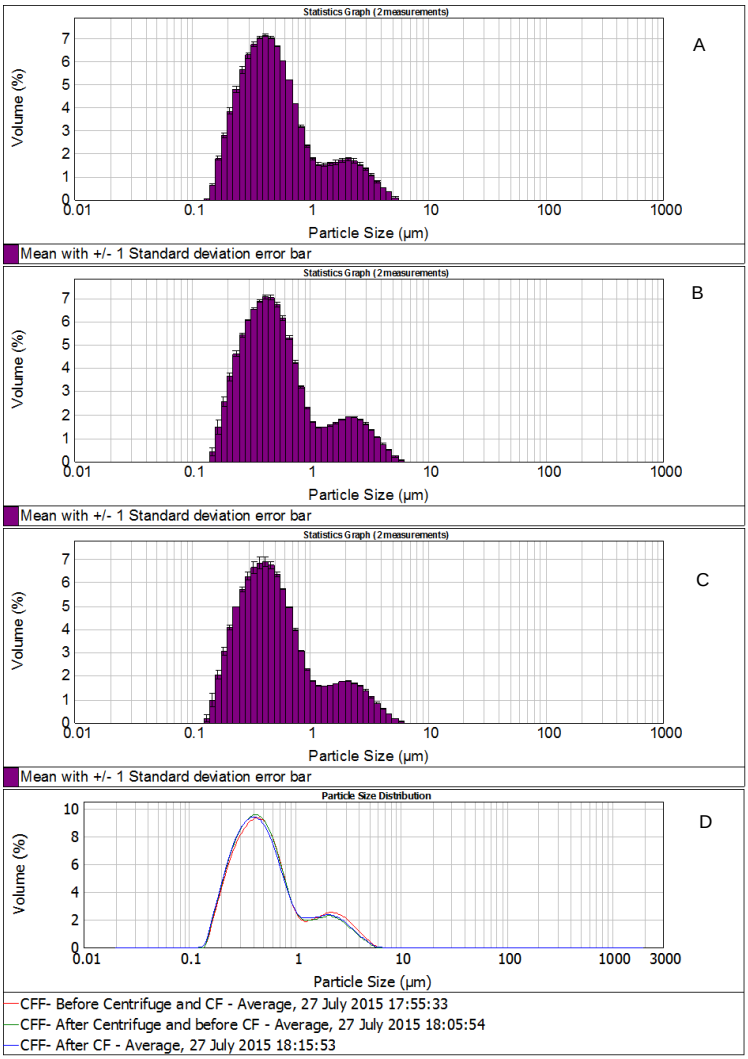

Figure 6-2. Particle size analysis of the two stage CFF experiment at varying stages. A= Before centrifuging and CFF, B= After centrifuge but before CFF, C= After CFF, D= Comparison between the various stages.

Figure 6-2 shows the particle size analysis for the one stage process and the varying stages. The analysis shows what is expected. After the CFF process has been performed, there is a reduction in particle size and a skew towards the left hand side of the graph. This is due to the larger aggregates being removed during the decanting process in the centrifuge. Also some of the larger air cells were removed from the sample as they got stuck in the tubes of the CFF module. This explains why the volume on the graph is lower after the CFF process, compared to the value from before the CFF but after the centrifuging process. This also means that the value of 14 % concentration should actually be higher as there were plenty of air cells still in the module which were too large to be removed. This may have caused a discrepancy in the values obtained, meaning the process might be more efficient than it looked at first glance. This is an issue that will have to be addressed when the process is optimised in the future, and with it should produce a very efficient method of producing concentrated AFE. This factor will also be the reason as to why not only the total volume on the curve is down, but the peak above 1 micron is less than the other distributions. On the other hand, even though there is a loss in volume, it does provide advantages with respect to increasing the monodispersity if the sample. Small air cells are required for formulation into whipped toppings and the more monodisperse a sample is that is being formulated, the less the adverse effects will be with regards to localised larger particles interacting differently in the formulation. So the loss of air cells has both its advantages and disadvantages depending on which way it is being looked at- whether it is a pure process and optimisation point of view, or whether it is being looked at from a formulation point of view for future applications.

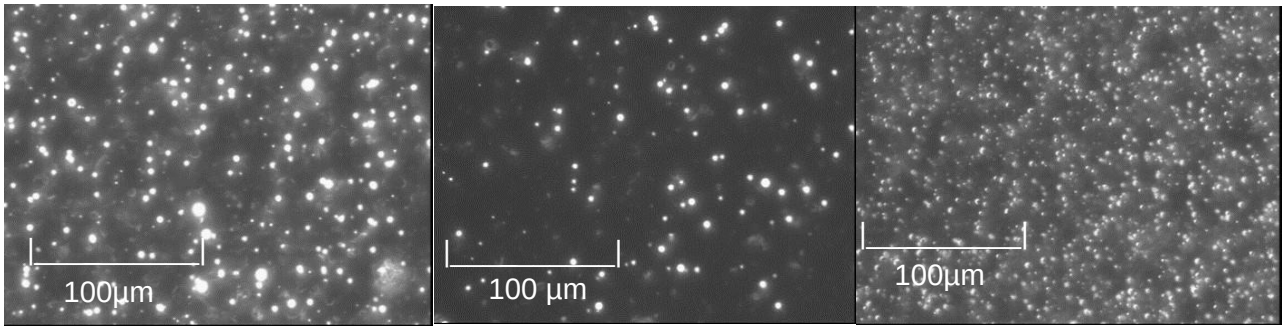

Figure 6-3. Microscope images taken with a Leica QWin imaging camera of the various stages of the 2 stage CFF experiment. Left Image= Before centrifuging and CFF, Middle Image= After centrifuge but before CFF, Right Image= After CFF.

Figure 6-3 physically shows how the CFF makes the solution change over the various processes and how it looks when concentrated. The image on the left shows the sample initially produced from the sonication stage. This contains a mix of small and large air cells. There is no apparent protein aggregation, but in case there is any that has not been noticed, the sample was centrifuged and as shown in the middle image, where the larger aggregates and air cells particles have been removed to leave the small air cells to concentrate up. The concentrated solution is shown in the right hand image. Compared to the first two images, what can be shown is that the samples contain a significantly increased amount of air cells per same area, and the air cells are all small and monodisperse compared to the other samples. This monodispersity is a combination of both the decanting process and the larger air cells getting trapped within the CFF module. It is apparent that from both a physical and numerical point of view that the two stage method worked and produced monodisperse concentrated AFE, which has opened up a novel AFE production process, compared to what has been attempted previously.

6.3. One Stage Process

The aim of the one stage process was to take the two stages and amalgamate them into one working continuous method. To achieve this, the outlet pipe from the sonicator was directly fed into an ‘intermediate’ collection vessel. From this collection vessel, a secondary pump was used to pump the solution into the CFF module. However, this time a larger pump was used compared to the one used in the previous (two stage) experiment, pumping up to 600

$mlhr^{-1}$. This faster flow rate negated the need for a vacuum as a sufficient back pressure was provided through the module to force a continuous flow of EWP solution into the EWP collection vessel. After passing through the CFF module, the concentrated solution was fed back into the intermediate collection vessel with new AFE from the sonicator and recirculated until concentrated. The EWP solution was siphoned off into a separate collection vessel in the same way as the 2 stage method. A schematic of the setup is shown in Figure 3-6. Images of the actual setup in the laboratory are shown in Figure 6-4.

Figure 6-4 Images of the cross flow filtration one stage process. Top Image= Before the experiment started, Bottom Image= During the experiment.

Table 6-2. Protein usage during the CFF one stage method and the resulting concentrations of both the concentrated AFE solution and the EWP supernatant solution.

	Protein Used (%)	Concentration (%w/v)
AFE 1	6.54	6.54
AFE 2	6.46	6.46
EWP 1	59.6	1.16
EWP2	66.2	1.07

The data in Table 6-2 shows a high protein usage, but the concentration is low compared to that found in the two stage process. The reason behind this is due to systematic problems encountered during the course of the experiment. Although the larger pump provided a much quicker time for the solution to pass through the module, it caused the larger particles to get trapped in the module much quicker. This blockage produced a build-up in pressure which caused the outlet pipe to detach from the module, causing a large amount of the AFE solution to be lost. After this problem, approximately 10 % of the original solution was left causing a huge error in the numerical values compared to the two stage method. Because this occurred, two samples were taken for dry weight analysis to check for discrepancies. It was found that the protein usage was roughly three times that of the two stage process. This indicates that the potential concentration using this correlation could be roughly 42 % (three times the concentration in the stage process). Another way of working out the potential could be by taking the concentration found at 6 % and multiplying by ten (as there was roughly 10 % of solution left after the AFE leakage) meaning that there could be a potential concentration of 40-60 % if experimented without any problems. The solution looked more concentrated in the bulk than the AFE produced in the two stage process, so there is a greater likelihood that when performed without problems, it will produce a highly concentrated sample, more than was produced in the two stage process. But as with the two stage process, it shows that the CFF process worked and this time with a continuous process from the starting solution through to a concentrated AFE solution, this time in a much reduced time frame.

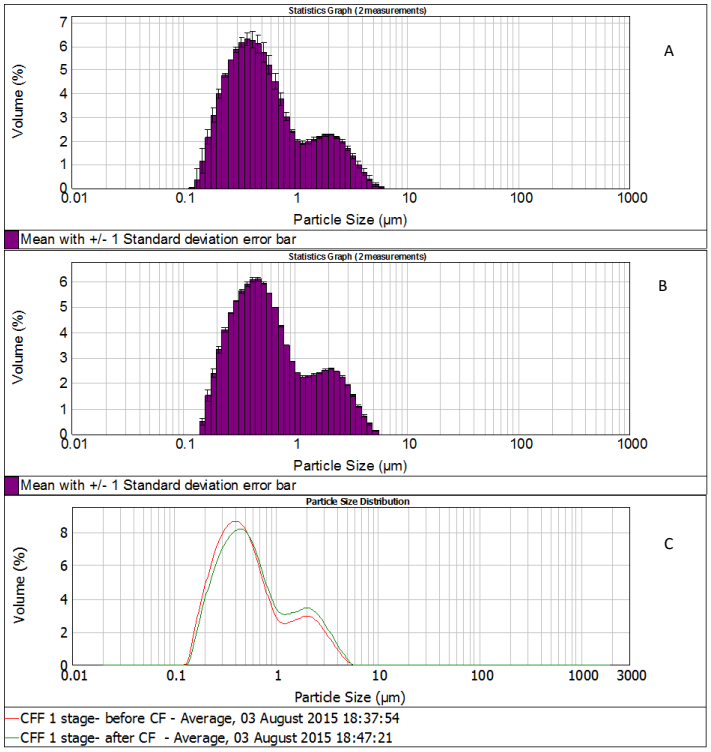

Figure 6-5. Particle size analysis of the 1 stage CFF experiment at varying stages. A= Before CFF (taken before it had time to pass through the module) B= After being concentrated through the CFF module, C= Comparison of the two samples.

The Mastersizer data in Figure 6-5 shows the particle size for the samples produced just after the sonication step (before it travelled through the CFF module), and after the solution had passed through the CFF module. Because there is no decanting step, unlike in the 2 two stage method, the larger particles and any protein aggregates will get trapped within the tubes of the CFF module. This is what can be seen on the Mastersizer graphs as the volume drops. There is no apparent protein aggregation in the sample, even without the decanting step, just small and larger air cells.

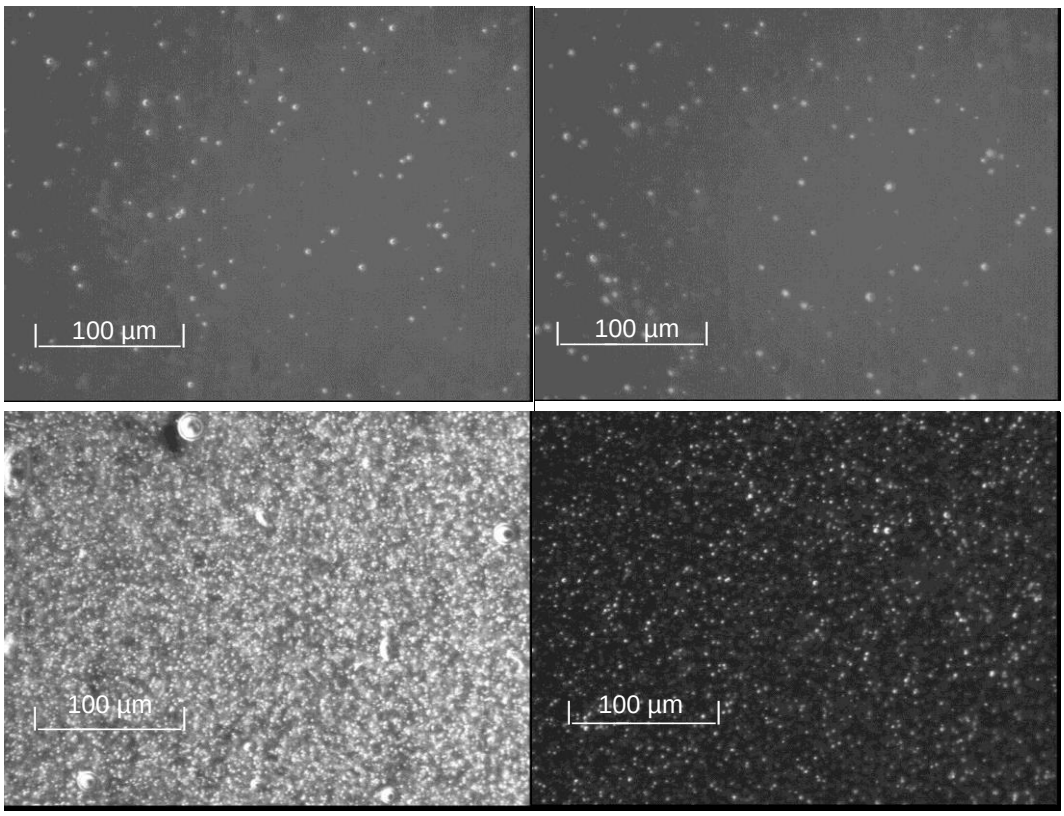

Figure 6-6. Microscope images taken with a Leica QWin imaging camera of the one stage CFF experiment. Top Left and Top Right Images= Before AFE had passed through the CFF module, Bottom Left and Bottom Right Images= After AFE had been concentrated through the CFF module.

The images in Figure 6-6 show a large increase in concentration even though the numerical values are not high. Comparing the concentration of these to the two stage method shows that if most of the solution was not lost during the experiment, then this solution would be of a much higher concentration than was recorded. The concentration of small air cells in the same area is much higher than the sample initially produced from the sonication alone and much higher from the two stage samples. There is a presence of larger air cells which would explain a larger peak in the Mastersizer spectrum. But barring a few larger air cells, the emulsions are once again monodisperse, showing that the larger particles got trapped within the modules. What the data does show is that both a two stage and a one stage process work efficiently and concentrate the solution highly compared to a normal pass. This is a big step toward AFE scale up as it provides a much quicker time frame in terms of AFE production and extraction, for formulation approaches. The process and ideas could be scaled up to a larger scale and provide a more efficient method. The cross-flow module

would need to be of a much larger scale but the premise would be kept the same and would be likely to be efficient on a larger scale due to the increased flow rate and capacity of the pumps on the pilot scale. This would provide more backpressure and a quicker concentration of the air cells through the module.

6.4. CFF Conclusion

The aim of these experiments was to provide a novel method of AFE concentration without adding protein, and not to focus on the protein usage. This method worked and was able to produce concentrated solutions of at least three times previously found. The CFF worked for both a one stage and two stage process, showing reliability and consistency in the method for future work. It was not without its own problems, where over-pressuring at high flow rates and larger timescales at slower flow rates, proved to be some of the more limiting factors. Some changes to the setup were changed to enhance efficiency. If these parameters can be optimised easily, it could produce a new and efficient way for the production of formulation-ready AFE. This could be a very useful method for larger scale applications as it would significantly reduce the timeframes compared to current methods, and could fit in with the timeframes associated with industry; and with reduced timeframe comes reduced energy usage. The initial studies into this method are promising and could pioneer a new way of AFE production in the future, especially once the process is optimised and a recycle can be performed, for both the bench and larger scale setups.

CHAPTER 7- PILOT SCALE WORK (CAMPDEN BRI)

7.1. Introduction

The aim of the work at Campden BRI was to take the production of AFE from the bench scale, to the pilot scale, and determine the scalability of the product for future developments/projects. The work at Campden BRI was the first major attempt to produce AFE on a larger scale, so for this reason, the main aim was to collect products using different experimental parameters rather than using recycling methods. The work was aimed to be a benchmark to produce AFE and upon successful completion, to then (at a later date) incorporate the recycling methods on the pilot scale to maximise the output with minimal waste.

7.2. Methods

7.2.1. Equipment and Materials

7.2.1.1 Materials

The materials used during the Design of Experiments (D.O.E) and other experiments at Campden BRI were Egg White Protein, 2 M Hydrochloric acid and distilled water. D1 was used as the disinfectant of choice. D10 was used to clean small equipment and the reaction system was cleaned with Sodium Hydroxide and Peroxyacetic Acid. The makes are unknown as they were purchased in-house by Campden BRI.

7.2.1.2 Equipment

The protein solution was mixed in a pilot scale food mixer (Winkworth 200 L). A HTST/UHT pasteuriser [FT74XTS, Armfield] contained a pump and a steam based heat exchanger, all contained in one machine. The sonication vessel consisted of a jacketed flow through cell (heated up by a separate heat exchanger), a generator, transducer and a sonication probe (IUP1000, Hielscher, 1 kW). Air flow was regulated by a Platon rotameter and the centrifuge

used for absorbance analysis was an Avanti J-E (Beckmann Coulter, 250 ml). Other equipment included Toledo pH probes, various Mettler weighing balances, piping and a hand-held temperature probe.

7.2.2. Method for AFE Production

The method for AFE production is the same basic methodology as outlined in section 3.3.1. However, there were some differences between the bench scale and the pilot scale experiment. In some of the experiments there was an addition of ingredients (sugar and/or salt), these were added during the mixing step (Winkworth 200L). Also there was no centrifuge step before the solution was passed through the sonicator (IUP1000, Hielscher, 1 kW, 26 mm tip), as there was no centrifuge large enough to accommodate the pilot scale volumes.

The method is show more clearly in the flow chart in Figure 7-1.

A centrifuge (4 °C, 30 minutes, 10000 rpm, brake 6, Avanti J-E, Beckmann Coulter, 250 ml) was used before measuring the absorbance (450 nm) to achieve a yield, as dry weight analysis would not be accurate to the large quantities of solution. For absorbance analysis, the solution was centrifuged and the AFE particulates were discarded leaving the supernatant solution. The supernatant solution (700 µL) was diluted into distilled water (10 ml). The solution was then poured in to a translucent cuvette and analysed in the

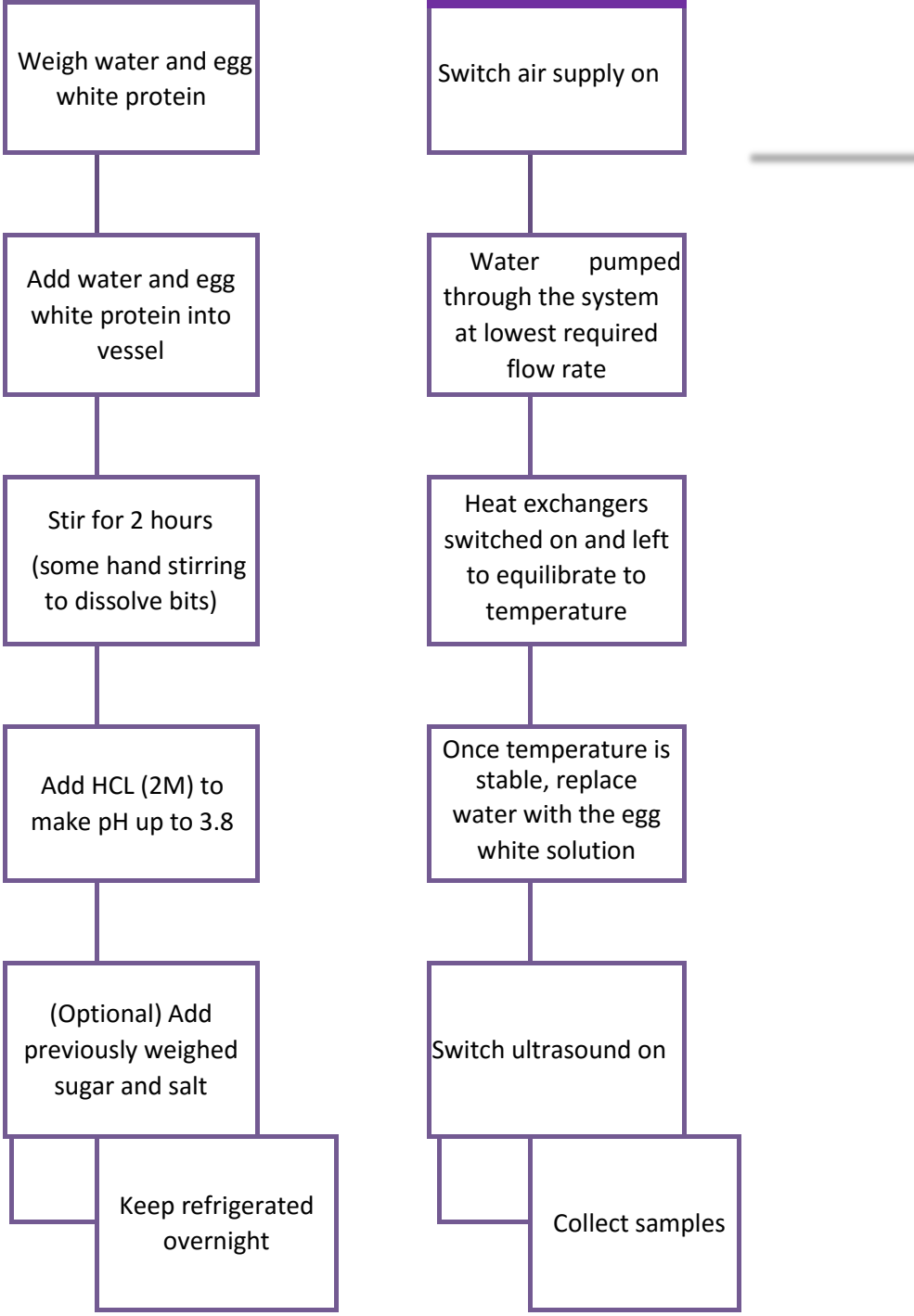

Figure 6-2 . Flow Chart produced by Jermann et al for the experimental procedure at Campden BRI. Left hand column= method for making EWP solution Right hand column= Method for Ultrasonic processing [80]

spectrophotometer at 40 nm. A blank solution consisting of 5 % EWP solution was also centrifuged under the same conditions and diluted with water in the same ratio. The blank was scanned first followed by the other sample.

7.2.3. Design of Experiments

The design of experiments was designed to utilise various parameters that can affect the production of the air filled emulsion. The parameter changes and experimental order were determined by the statistician a Campden BRI, where the three parameters tested were

amplitude (5 intervals- 20, 26, 60, 94, 100 %), residence time (changes in flow rates) and addition of ingredients (5 intervals of sugar-0, 1.125, 7.5, 13.87, 15 % and salt- 0, 0.0037, 0.025, 0.04625, 0.05 %), which were determined by the statistician at Campden BRI. The design of experiments is show in Table 7-1.

Table 7-1 Design of experiments undertook at Campden BRI.

Run	Day	am/pm	Sugar (g)	Salt (g)	Temp (°C)	Amplitude (%)	Residence Time (min)
1	1	am	0	0	55	20	1
2	1	am	0	0	45	100	1
3	1	am	0	0	45	20	1
4	1	am	0	0	45	20	6.5
5	1	am	0	0	55	100	1
6	1	am	0	0	55	20	6.5
7	1	am	0	0	45	100	6.5
8	1	am	0	0	55	100	6.5
9	1	pm	15	0.05	45	100	1
10	1	pm	15	0.05	55	20	6.5
11	1	pm	15	0.05	55	20	1
12	1	pm	15	0.05	55	100	1
13	1	pm	15	0.05	45	100	6.5
14	1	pm	15	0.05	45	20	6.5
15	1	pm	15	0.05	55	100	6.5
16	1	pm	15	0.05	45	20	1
17	2	am	1.125	0.025	50	60	3.75
18	2	am	1.125	0.025	50	60	3.75
19	2	am	1.125	0.025	50	60	3.75
20	2	am	7.5	0.025	45.75	60	3.75
21	2	pm	7.5	0.025	50	60	3.75
22	2	pm	7.5	0.025	54.25	60	3.75
23	2	pm	7.5	0.025	50	60	3.75
24	2	pm	7.5	0.025	50	26	3.75
25	2	pm	7.5	0.025	50	94	3.75
26	2	pm	7.5	0.025	50	60	6.0875
27	2	pm	7.5	0.025	50	60	3.75
28	2	pm	7.5	0.025	50	60	1.4125
29	3	am	7.5	0.025	50	26	3.75
30	3	am	7.5	0.025	50	94	3.75
31	3	am	7.5	0.025	45.75	60	3.75
32	3	am	7.5	0.025	50	60	3.75
33	3	am	7.5	0.025	50	60	3.75
34	3	am	7.5	0.025	50	60	1.4125

35	3	am	7.5	0.025	50	60	6.0875
36	3	am	7.5	0.025	50	60	3.75
37	3	pm	7.5	0.025	54.25	60	3.75
38	3	pm	13.87	0.025	50	60	3.75
39	3	pm	13.87	0.025	50	60	3.75
40	4	am	0	0.05	55	100	6.5
41	4	am	0	0.05	45	100	6.5
42	4	am	0	0.05	55	20	6.5
43	4	am	0	0.05	55	100	1
44	4	am	0	0.05	45	100	1
45	4	am	0	0.05	45	20	6.5
46	4	am	0	0.05	55	20	1
47	4	am	0	0.05	45	20	1
48	4	pm	15	0	55	100	6.5
49	4	pm	15	0	55	20	6.5
50	4	pm	15	0	45	100	6.5
51	4	pm	15	0	45	100	1
52	4	pm	15	0	45	20	1
53	4	pm	15	0	45	20	6.5
54	4	pm	15	0	55	20	1
55	4	pm	15	0	55	100	1
56	5	am	7.5	0.0037	50	60	3.75
57	5	am	7.5	0.0037	50	60	3.75
58	5	am	7.5	0.0037	50	60	3.75
59	5	am	7.5	0.025	45.75	60	3.75
60	5	pm	7.5	0.025	50	60	3.75
61	5	pm	7.5	0.025	54.25	60	3.75
62	5	pm	7.5	0.025	50	60	3.75
63	5	pm	7.5	0.025	50	26	3.75
64	5	pm	7.5	0.025	50	94	3.75
65	5	pm	7.5	0.025	50	60	3.75
66	5	pm	7.5	0.025	50	60	3.75
67	5	pm	7.5	0.025	50	60	3.75
68	6	am	7.5	0.025	45.75	60	3.75
69	6	am	7.5	0.025	50	94	3.75
70	6	am	7.5	0.025	50	60	3.75
71	6	am	7.5	0.025	54.25	60	3.75
72	6	am	7.5	0.025	50	60	6.0875
73	6	am	7.5	0.025	50	60	3.75
74	6	am	7.5	0.025	50	60	1.4125
75	6	am	7.5	0.025	50	26	3.75
76	6	pm	7.5	0.025	50	60	3.75
77	6	pm	7.5	0.04625	50	60	3.75

As well as the actual experimental parameters, the composition of the starting EWP solutions was calculated by *Jermann et al* prior to performing the D.O.E. The figures for the starting material compositions are show in Table 7-2.

Table 7-2. A series of tables to the show the ingredient ratio of all the stating protein solutions.

Day 1 (am)

Ingredients	Percentage (%)	Actual weight (kg)
Water	93.3	54.805
EWP	5	2.925
HCl(2M)	1.7	1.73
Sugar	0	0
Salt	0	0
Total	100%	58.5

Day 1 (pm)

Ingredients	Percentage (%)	Actual weight (Kg)
Water	78.25	45.77625
EWP	5	2.925
HCl(2M)	1.7	1.2
Sugar	15	8.775
Salt	0.05	0.02925
Total	100%	58.5

Day 2 (am)

Ingredients	Percentage (%)	Actual weight (kg)
Water	92.15	35.9385
EWP	5	1.95
HCl(2M)	1.7	0.663
Sugar	1.125	0.43875
Salt	0.025	0.00975
Total	100%	39

Day 2 (pm)/3(am)

Ingredients	Percentage (%)	Actual weight (kg)
Water	85.775	206.288875
EWP	5	12.025
HCl(2M)	1.7	3.74
Sugar	7.5	18.0375
Salt	0.025	0.060125
Total	100%	240.5

Day 3 (pm)

Ingredients	Percentage (%)	Actual weight (kg)
Water	79.405	30.96795
EWP	5	1.95
HCl(2M)	1.7	0.6635
Sugar	13.87	5.4093
Salt	0.025	0.00975
Total	100%	39

In *Table 7-1,* it shows that the D.O.E was scheduled for 6 days' work. However, in *Table 7-2* it shows only three days' worth of solution. This is due to the problems associated in 7.3.1.

7.3. Problems and Solutions

7.3.1 Problems

There were many problems associated with the visit to perform the D.O.E. at Campden BRI. The week was scheduled to perform the first four days' worth of experiments, however, only three days' worth of experiments actually occurred, with the majority of these either been disbanded or the 'products' discarded. For the sample which did not fall into this category, the results by eye we're not promising. Rather than looking like a white/milky solution, the product came out looking exactly like the starting product and it looked like nothing had happened at all. This occurred throughout all the experiments for that week. As Previously mentioned, some were discarded. This is because, the solution came out looking black and looked like (and smelled like) it had burnt. The runs which were scheduled for that session after the solution had coming out looking black, were the ones which were disbanded. The process may be scaled up effectively, however, on this visit it appeared to not work due to the systematic/experimental setup. Areas where problems occurred are detailed below:

Firstly, one of the main problems was due to browning and burning of the solution. The most plausible reason for this occurrence was due to the choice of heat exchanger on the pilot scale setup. Even though the net heat for the heat exchanger was set between 45-55 °C, the heat exchanger was steam jacketed, meaning that steam at 100 °C was used to heat the piping. This could have caused localised heating in parts of the piping which would have soared the temperature above 45-55 °C. Because the solution was mainly composed of protein, this extra temperature would easily denature proteins, rendering them unusable and could have been a major contributing factor as to why the experiments never produced any AFE. Also, because sugar was present within most of the solutions, the localised higher temperatures was hot enough to caramelise the sugar, which would explain the burning colour and smell produced during the experiments.

The flow-through cell in the lab held 50 ml and the one at Campden BRI held 500 ml. With the tip in the lab being 13 mm, the tip at Campden BRI was not 10x the size of the one in the lab. This threw off the surface area of the tip to volume ratio of the flow-through cell quite dramatically. This caused the dead zone for cavitations to be significantly increased, which caused fewer interactions between the cavitations and protein, therefore resulting in a lower production of AFE.

Thirdly, another major problem could have been with the utilisation of the ultrasonic probe. The sonication probe in the lab penetrates the flow through cell quite deep, so that solution was in the vicinity of tip from the moment it entered the flow-through cell until it left. However, the sonicator at Campden BRI was quite short, so this did not happen. This meant that a lot of solution did not come into near contact with the sonication probe because of the size of the flow-through cell. This also brings in another problem with solution possibly sitting and cooking in the flow through cell without reacting (this may have formed the black solutions).

The fourth major issue lied with the air inlet. The air inlet in the lab went directly into the flow-through cell which meant that when the proteins are unfolding, the air was there to quickly react with the protein forming AFE. However, with the flow through design at Campden BRI, this was not possible, so the air is introduced into the tube before the solution reached the flow-through cell. If the solution inside the flow-through cell was just ‘sitting’ there then because the air is less dense, it will have travelled in and out of the flow though cell without reacting. This is also possible even if it is not sitting there because of the density difference; and the affinity to travel quicker through the pipes; and because the flow though cell was much larger, it could easily escape without reacting, which may be why it looked like protein solution was coming out as the ‘product’. Also, the air inlet to the pipe was not secure and was fastened on by tape, it was unclear as to whether any air was leaking, but if it was then that would have a bearing on the flow rate and could have an impact on the product formation.

The problems listed above are what are believed to be the main concerns and are the most likely to have the biggest impact on whether the process will work or not. However, there could be other contributing factors as to why the process did not work like it should do: The first of these is in regard to the mixing efficiency of the protein solution. The mixing stage at Campden BRI was by far less effective than in the lab. The main difference apart from the volume of solution to be mixed, is that in the lab the stirrer bar mixing was quick and from the centre out and forms a 'whirlpool'. Whereas the larger mixer was much slower, so the protein did not dissolve as easily, as it was subjected to bulk flow mixing. Another potential problematic area was with regard to the centrifuge step (or lack of). Because on the pilot scale, there was no centrifuge capable of holding the required amount of solution, then the process was automatically going to be less efficient compared to the laboratory. Even when best efforts were tried to get the sediment from the bottom into the system (some protein settled out naturally), the solution looked cloudy and opaque compared to the centrifuged solutions in the lab, which are translucent in nature. Another potential issue is with regard to ingredient composition during the D.O.E., particularly with respect to the HCl. In the laboratory, the amount of HCl is not taken into account with regard to the w/v% as it was not a large amount. The solution was made up to 5 % and then the acid is added. However, at Campden BRI, the statistician added in the HCl as part of the overall % composition, meaning that there could be less than 5% EWP actually present. This however, should still produce AFE (and not a protein solution), so it should not have a large bearing on the issues, but could be part of a series of issues that need addressing.

7.3.2. Solutions

Following on from the problems associated with the D.O.E, another visit was scheduled to find the main root of the problem highlighted in section 7.3.1. This time the aim was to test different parameters that could be affecting the production to find out how to either a) optimise the process and/or b) fix the major problems.

The air flow was tested to see if this had an impact on the process, as the change in volume ratio of the flow could have meant a different residence time/ different ratio of air and liquid flow might be needed. The amplitude, temperature and liquid flow rate were kept constant so that the only variable was the air flow. The liquid flow was kept constant so that on each test, the ratio varied in a controlled environment. The test is shown in Table 7-3.

Table 7-3. The parameters tested to determine if air flow played a major factor in the problems of the Pilot Scale.

Product flow rate	9.80 L/hour (0.16 L/min)
Residence time	3.83 mins
Solution temperature	49.1 to 50.7 ° C
Sugar and salt content	0 %
Amplitude	60 %
Air flow rates	0.1 L/min 0.2 L/min 0.3 L/min 0.45 L/min 0.75 L/min

The aim to solve all of the associated problems was to change the position of the output pipe so that it was in line with the sonication tip, as with the lab scale. This aimed to remove the excess volume (of the flow through cell), creating a better volume ratio as the solution did not flow above the outlet pipe. It also meant that the solution did not have to travel so far to exit the vessel, and it would mean that the penetration depth of the probe was not as important, as the solution would reach the probe before the outlet pipe.

A statistical analysis was also performed by the statistician at Campden BRI to determine if a different combination of all the variables could produce a specific and required output. Aside from the variables, the data used was that of the energy usage throughout the experiment and the measured absorbance of the supernatant solutions. However, the absorbance measured an energy used are independent of each other and therefore makes it hard to give a direct comparison between the two.

In addition to what has already been performed, two major solutions could come to fruition by changing the shape of the ultrasonic probe. A longer probe would not only allow greater

penetration into the solution, but also magnify the intensity of the ultrasonic waves, causing a larger amount of cavitations in the sample for the air and protein to bind to. In addition to the probe, the flow through cell needs to be of a smaller volume. The distance between the probe and cell wall is key to producing cavitation-sample interactions. A smaller flow-through cell would decrease the number of dead zones in the sample and therefore promote cavitation-sample interactions, resulting in a greater yield of AFE.

7.4. Results

7.4.1 Optimisation Analysis

7.4.1.1 Air Flow

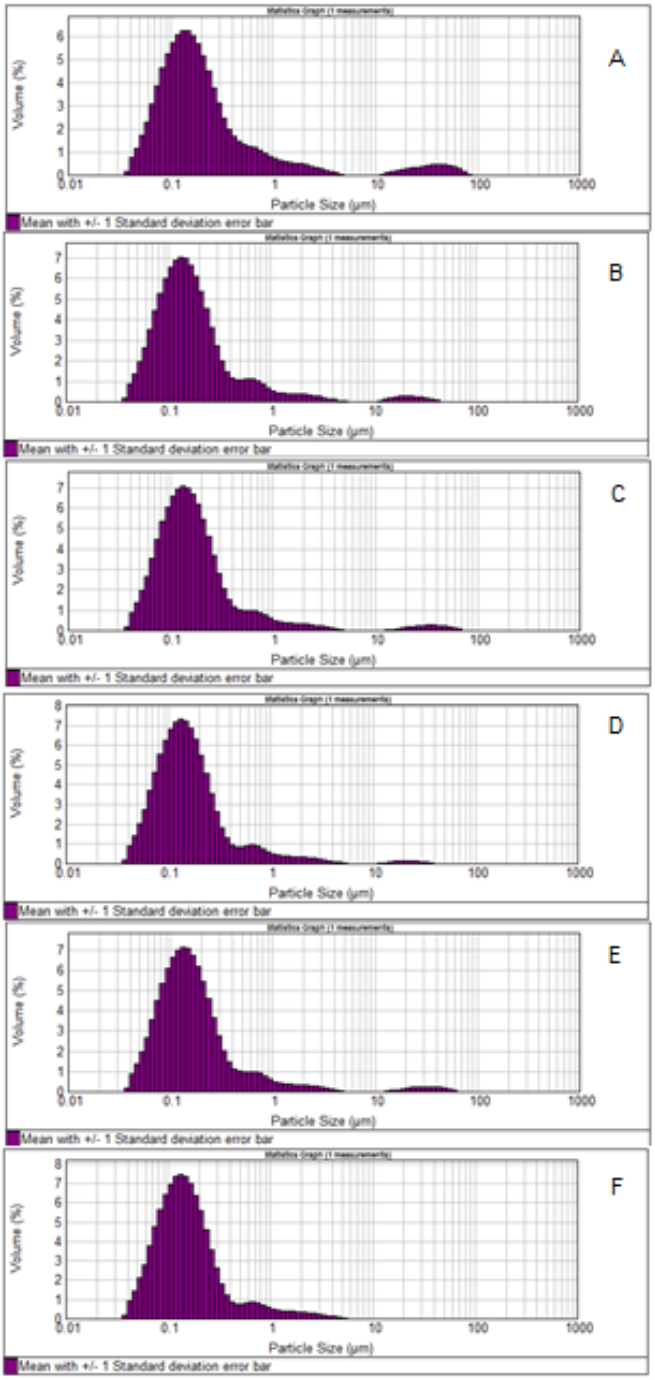

Figure 7-4. A series of MasterSizer graphs to show the particle distribution of the results from varying the air flow at Campden BRI during optimisation experiments. A= A standard experiment where the other variables are not controlled. Air flow rate varied experiments: - B= 0.1 Lmin^{-1}, C= 0.2 Lmin^{-1}, D= 0.3 Lmin^{-1}, E= 0.45 Lmin^{-1}, F= 0.75 Lmin^{-1}.

Images A-F in *Figure 7-4* show the particle size analysis for the production of AFE at Campden BRI under varying flow rates. The air flow rate was changed under controlled conditions (only changing one variable), to test the air flow had any effects on the system. From the images, it is clear that all of the flow rates that good monodisperse samples were produced, due to the large peaks around 0.1 microns. There is a small peak at 100 microns which is attributed to aggregates in the solution. This however. is less prominent in the higher air flow samples. The peak is small and is negligible in terms of volume. The size at 100 microns is attributed to either a small protein aggregate of air cell aggregate, as it is too small to be a large protein aggregate, as they occur up and around the 1000 micron range. This is a minor issue as the small aggregates will be able to be centrifuged at a low g-force, whilst still retaining the small air cells in solution. So in conclusion, it appears that the flow rate has a minor effect on the production under controlled conditions, as the amount of aggregates in solution decreased, however, it appears that there is negligible effect on the amount of air cells produced within the desired range of 0.1-1 micron range.

7.4.1.2 Outlet Pipe

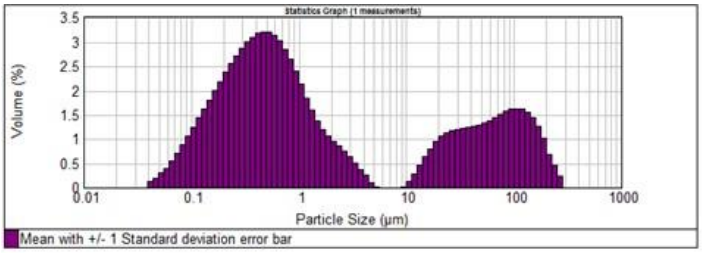

Figure 7-5. Particle size analysis (MasterSizer) graph to show the particle size distribution when the output pipe was lowered to be in line with the sonicator.

Looking at the particle size analysis in Figure 7-5, it would appear that changing the level of the outlet pipe had a counterproductive effect on the production of air cells and the reduction of aggregates. It was believed that the outlet pipe was a major issue, as the level was too high compared to the bench scale. From the analysis, it appears that the amount of air cells decreased and the amount of protein aggregates increased compared to the samples in Figure 7-4. However, I believe more rigorous tests need to be performed on this parameter as only one sample was taken, not long after the outlet pipe had been changed over.

Because of other issues associated (mentioned in section 7.3.1.) there is a possibility that a large amount of protein solution could have been sat within the flow through jacket for an extended period of time. This would skew the results as the protein would have a higher tendency to form irreversible denaturation and aggregation as opposed to just unfolding, having been exposed to a long period of heating. This is believed to be the case because the samples were not long obtained after those shown in Figure 7-4, so the main cause of the difference must be due to the protein which has been stuck at the bottom of the flow through jacket, finally being able to remove itself from the flow through cell, hence it will have undergone more heating and therefore more susceptible to aggregation. It is believed that more work should be undertaken on this parameter in the future, because with the same setup around the sonication vessel, a greater reliability between the bench and the pilot scale could be produced.

7.4.2. Statistical Analysis

Deviations occurred within the statistical analysis due to the fluctuation of controlled variables that the statistics could not predict. The main cause being the fluctuation in temperature of the heat exchanger, due to being heated by steam. Because of this, the range was between 42.8 and 54.3 °C rather than between the intended 45-55°C range. These variations unbalanced the correlations and therefore led to the sequential sum of squares being used to calculate the p–values for each co-efficient.

The variables which were measured and are changeable, are the absorbance and energy usage measurements. The variables ranged from -0.0155 to 0.3069 for absorbance and 53.5 to 239.50 W for energy usage (The small negative values are attributable to measurement noise and had negligible influence on the statistical analysis). To both of these variables a full quadratic surface response model was fitted consisting of linear terms for each variable; a quadratic term for each variable and a 2-way interaction terms for each pair of variables.

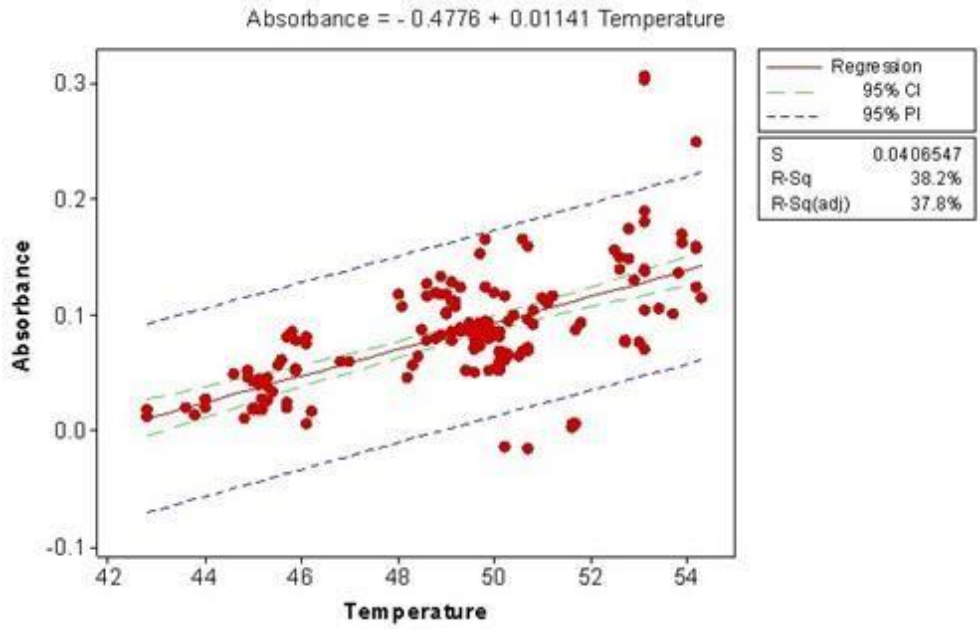

Figure 7-6. A graph showing the Absorbance Vs Temperature with data obtained from the statistical model. Produced by Jermann et al [74].

There is evidence ($p<0.001$) that the quadratic response model used may not be the best model and other models may present a better fit. This is due to the data deviating from the line of best fit with values (MS=0.000962) which are larger than the error that can be explained by repeatability (MS=0.00017). The deviation of the data and the model is attributed to the lack of fit (24 %). The response surface fits quite well (R-Sq=76 %) but the dataset is not large enough to explore alternative statistical models.

From the statistical absorbance results obtained, it can be determined that the temperature has the biggest effect on the absorbance with 38 % sum of the sequential squares. The remaining 38 % (to make it up to 76 % plus 24 % lack of fit) were due to linear terms of the amplitude and the salt, the square terms and the interactions between terms. Looking at it from a statistical point of view, the evidence suggests that there is an effect with sugar, principally in the square term and with the interaction of temperature. The effect of residence time is determined by its interaction with the effect of temperature.

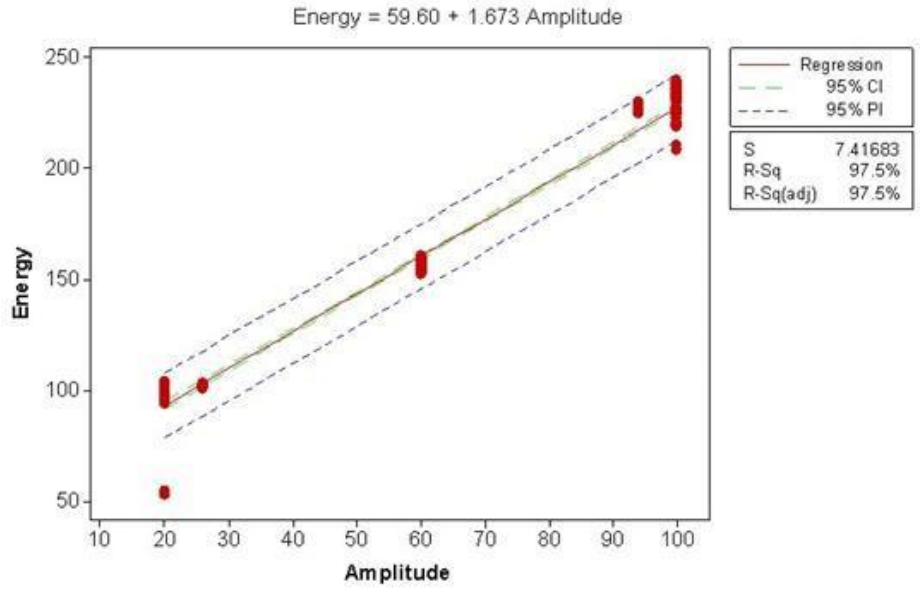

Figure 7-7. A graph showing the Amplitude Vs Energy with data obtained from the statistical model. Produced by Jermann et al [74].

Unlike absorbance, the energy usage depends on less parameters, as it is a function process rather than recipe and structure. Therefore, the model was only fitted for temperature, amplitude and residence time but not for ingredients (salt and sugar). From the statistical analysis there is strong evidence that the effect of amplitude ($p<0.001$), temperature ($p<0.001$) and weaker evidence of residence time ($p=0.014$). The fit in the model summary is 98 %, most of which is accounted for by amplitude (97.5%). The effect of temperature and residence time share the extra 0.5 %, so they have a much smaller effect. A linear relationship to amplitude fits 97.5 % of the energy usage. This shows that the amplitude is directly correlated to the energy usage. This was proved in small scale tests in section 3.5.3., so reinforces this relationship. And it shows that ultrasonic probes, independent of size show a linear relationship to energy usage both statistically and experimentally, allowing for more controlled experiments to be undertaken.

7.4.3. Performing a Recycle on the Pilot Scale

A recycle was performed for the first time on the pilot scale at Campden BRI. Due to the lack of centrifuge and timescales associated with the industrial setup, the recycle method of choice was the Non Top-Up Continuous Method (NTUCoM) v2. This allowed a constant

cycle of reactants/products. As this was the first attempt, rather than a four-hour cycle consisting of a large reactant volume to flow thorough cell ratio, a smaller amount was used. The amount was enough so that all of the system was filled with either reactant or product, and then this volume was circulated for an hour. It was calculated that one pass through the whole system took 15 minutes, so this was equivalent to four passes, same as on the laboratory scale. Samples were taken at 10, 20, 40 and 60 minute intervals. This gave a rough equivalent to 0, 1, 2 and 3 recycles, respectively.

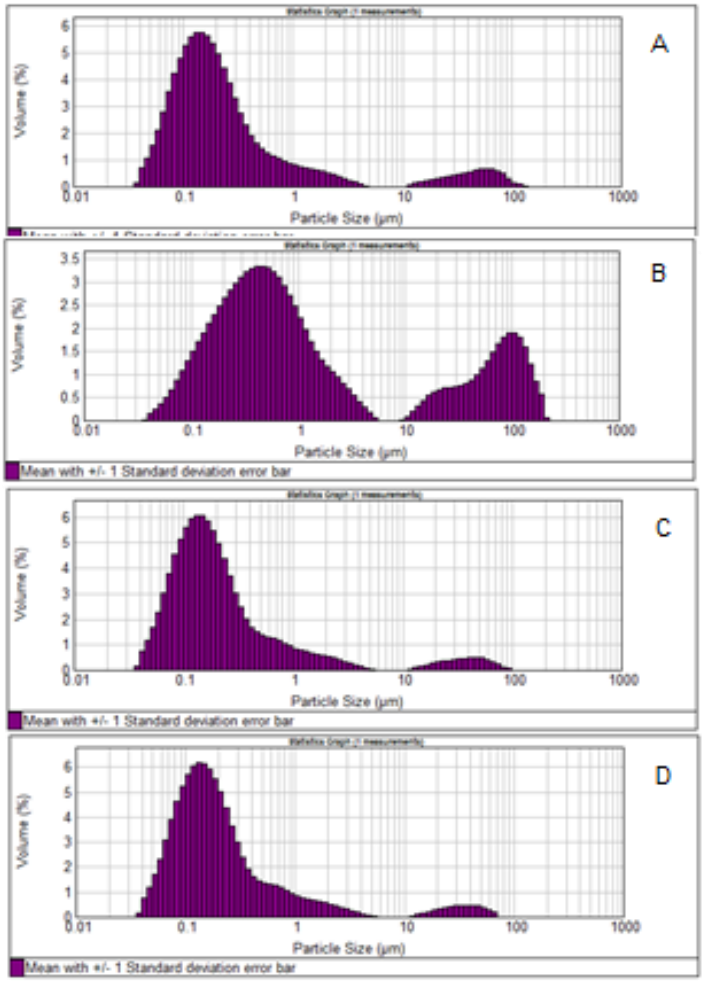

Figure 7-8. Particle size analysis (MasterSizer) graph to show the particle size distribution when a continuous recycle was performed at Campden BRI. A= 0 recycles (10 minutes), B= 1 recycle (20 minutes), C= 2 recycles (40 minutes), D= 3 recycles (60 minutes).

Images A-D in *Figure 7-8* show the particle size analysis for the recycle. Aside from image B, which is believed to be an anomalous result, the particle size is very similar throughout the process, where there is a large peak in the desirable range around 0.1 microns and a small peak around the 100 micron range, where aggregates would be expected. The lack of

aggregates is a promising factor as it was expected to be higher because the solution is not centrifuged. Much care was taken to make sure that the protein sediment did not enter the system. However, allowing for human error, it would be expected that some would be deposited into the system, so it is a promising result that there is no evidence of this occurring and obscuring the particle size analysis as a general trend. However, B is an anomalous result and does not fit the pattern, like the rest of the images. It could be attributed to this, or because the sample taken for analysis is so small, it could have just had a large amount of protein/AFE aggregates in a localised amount of solution.

The peak at 0.1 microns increases with time and recycles, showing that as the process progresses, the amount of AFE is increased and the amount of aggregates decreases. This shows that the recycle process was a success and provides a starting point for more experiments of its kind and better optimisation into the larger scale production.

7.5. Conclusion

Conclusions drawn-up from the scale up process work at Campden BRI would render the process as a success; but also a success that still needs a lot of work and optimisation. A recycle was performed and the ability to produce samples at varying parameters was also successful. However, these are successes in the fact that there was production for the first time on a larger scale rather than it being confined to just the bench setup. The samples produced were not as concentrated as those on the bench scale and did not produce the same quality of emulsion. The D.O.E. encountered problems, some of which have been resolved to date but the D.O.E was performed too early and more optimisation of the various parameters should have been utilised prior to the D.O.E. There is still a large amount of work to be undertaken in terms of optimising the process and bringing the production amount up to what can be produced on the small scale and beyond. But it has shown good early signs that this could be a viable option for industry once the parameters for a larger scale have been identified and optimised, as a lot of the parameters used on the smaller scale were not applicable to the larger scale.

Chapter 8- Conclusion and Future Work

8.1. Conclusion

The aims of the project were to maximise the output of AFE whilst minimising the waste from the parent EWP solution, and to take AFE production up to the pilot scale (or prepare sufficient parameters and methodologies to take the production to a larger scale). This was achieved in a number of ways.

The Critchley-Green Recycle Methods showcased a variation of methods, each of which focused on different parameters of AFE production, giving a good understanding of the whole picture and not just the yield obtained. The water bath method was a good starting point for method development and showed a protein usage, but would be unusable in formulations due to the large amount of protein aggregation caused by excessive heating. The optimal way to heat the solution with minimum exposure time to excess heat energy was found by using a heat exchanger. The heat exchanger methods showed a high protein usage which corresponded to an equally high output of AFE, with negligible protein aggregation. All methods produced over 90 % AFE yield with the highest output being 98.7 %. The ambient heat exchanger method was found to be the most efficient in terms of yield with all yields obtaining >95 % yield. However, the same process from a cold starting temperature produced less recycles, so is more efficient in terms of time scales compared to its ambient counterpart. In terms of maximising yield and reducing the waste, these methods on the whole have proved to be the most effective.

The Non Top-Up Methods did not produce as high of a yield, but gave insights into other areas where yield was counteracted by efficiency in timeframes. The NoTUCeM was an intermittent method to work out the parameters for the continuous method; however, it did show that a depleted solution can still produce a good output and was key to the success of the continuous method. The NoTUCoM was the lowest AFE producer. However, it provided

a novel process for AFE production with respect to being the first production method to be completely continuous. The Method also showed that the air cells are very robust and can withstand multiple exposures to both heat and ultrasonic energy, without degradation or particle breakdown. This is useful from an industrial point of view as it has shown that AFE would able to withstand formulation and heat treatment processes', making it useful in food applications, of which it has been engineered for. It was the ability of being able to produce a continuous method that allowed for the adaptation using the cross-flow filtration module and provided a much reduced time scale compared to top-up methods, showing feasibility for larger scale processes where timeframes are an important factor as well as output.

The scale up work at Campden BRI was not designed to be as effective as the laboratory scale processes. The aim was to achieve AFE formation on a larger scale. With respect to this, the work was a success, even if it was in low amounts. It showed that the production is transferrable to the larger scale if the process is optimised. In addition to showing that the production is scalable, a number of issues with the scale up were effectively addressed. Some of these were resolved throughout the course of the project, but some will require substantially more time and maybe even a separate project within itself. If the issues can continue to be addressed effectively, then the optimisation of the process should increase and eventually start to produce the quantities of AFE comparable to the laboratory scale test, and improve upon this to take the production further.

The final method attempted was the cross-flow filtration (CFF) methods. This method stemmed from the NoTUCoM where it was shown that a complete continuous process was feasible. Where the issue of air cell production after the first pass was the major limiting factor in the method, the aim of using the CFF module was to isolate the AFE particles and remove the unreacted EWP solution. It was unsure as to whether this would work for AFE, so the aim was not to produce a recycle, but to show that the method worked and that it could be feasible for a continuous recycle process, which could yield much higher results than that of the NoTUCoM. This was effectively done through two different methods- a two

stage process and a one stage process. The two stage process was a precursor to a fully continuous method to see if the CFF module worked within itself, with no other factors for AFE processing. The one stage process combined these two stages into a single continuous process, emulating a more complex version of the NoTUCoM. The process caused the AFE solution to concentrate itself and produce not only a higher volume of air cells per area, but also a monodisperse sample. These results showed that the method worked effectively and was able to produce concentrated AFE solutions of at least three times of that found previously, with the potential to achieve up to a 10x concentrated solution. The CFF worked for both a one stage and two stage process, showing reliability and consistency in the method for future work. It was not without its own issues, where over pressuring at high flow rates and longer timescales at slower flow rates proved problematic. Some changes to the setup were changed to enhance efficiency and it was found that introducing backpressure into the CFF module negated the need for a vacuum pump to remove the EWP supernatant from the solution bulk. If the parameters can be optimised, it has the potential to produce a new and efficient way for the production of formulation ready AFE, as the AFE would not need as many homogenisation steps due to the monodispersity and concentration of the emulsion. This could be a very useful method for larger scale applications as it would significantly reduce the timeframes compared to current methods and could fit in with the timeframes associated with industry. The initial studies into this method are very promising and could pioneer a new way of AFE production in the future, especially once where the process is optimised and recycles have been tested using this process. This is synonymous for both the bench and larger scale setups.

Overall, the method effectively answered the questions asked of the project and went beyond the scope into novel processes never attempted before for AFE production. The aim was to take it to a larger scale in any form. This happened in the form of various methods but more work is needed on both the laboratory and pilot scale to take the process up to an industrial scale. But the foundations have been laid to take the research beyond the scope of this project and there are potentially many avenues to explore with regards to laboratory

scale work (detailed in section 8.2) as well as optimising the processes already in place to take the production to the industrial scale.

8.2 Future Work

In terms of future research, it is an open book. This is the first time recycling methods have been used for AFEs and has opened a wide variety of potential research. Specific research that could be undertaken in the future is looking partial recycles, where upon you take a certain percentage of product, and recycle, as opposed to the full batch of solution. This could lead to modelling of what is the 'perfect recycle' in terms of concentrations amount and whether a full batch needs to be recycled, or only a portion of it. Also, looking at the recycles as a function of different amplitudes is an area which could provide a lot of useful information. Amplitude and energy output has been tested for a single pass, but it would give data on whether recycling more times at a lower amplitude for longer is more effective than recycling at a higher amplitude for a shorter amount of time. It would also give a comparison for energy output which would be more useful in determining which to choose for industrial purposes where the cost of energy is taken into account. In addition to this, recycles could be performed with the addition of salt and sugar ingredients to see how much affect they have on the AFE production on the laboratory scale.

The cross flow-filtration method was tried to determine if a single pass could work and produce results. Following on from the results obtained, a recycle could be performed in the same way as the one stage process using the same methodology, but instead of collecting the EWP supernatant, it could be transferred back into the starting vessel. It could also be adapted with the addition of a spin centrifuge, so that it is a purely continuous process, saving time, and reducing the amount of foam produced. From the spin centrifuge it would have to go into the intermediate collection vessel, ready to be passed through the secondary peristaltic pump. Another potential addition to the setup could be for the solution from the intermediate collection vessel to travel through a secondary heat exchanger with cold water running through it to cool the solution down, so that it did not a) damage the cross-flow

filtration module and b) diffuse through the membrane more than it should do, due to having higher solubility and energy compared to a cold state. It would then travel from the heat exchanger into the cross-flow filtration module which would deposit the concentrated/filtered AFE solution into the original starting vessel ready for another pass (like in the one stage method). As a single pass was able to be performed with good efficiency, a recycle should be able to be produced, and the addition of the extra apparatus would enhance the efficiency of the process (but should be able to be produced without the additional equipment). Due to the size of the lab and equipment available, the larger setup would not be possible, but a schematic is shown in *Figure 8-1* on what the setup would look like. In addition to using performing a non-top-up recycle, like the one stage process, a STUM could potentially also be performed using the CFF module and be a purely continuous process. This would be the first completely continuous process for a STUM method. Because the outlet streams can be monitored, the supernatant and the AFE solution concentrations can be worked out by dry weight analysis. Instead of adding more solid protein into the mix and centrifuging, a protein solution containing the same percentage of protein, as used up in the reaction, could be made up and used to top up the existing supernatant solution e.g. if the dry weight analysis of the Concentrated AFE was 10 %, then a 10 % EWP solution could be made up to add the extra protein back into the system. This would save time and energy and would produce a more viable option for industry and larger scale processes.

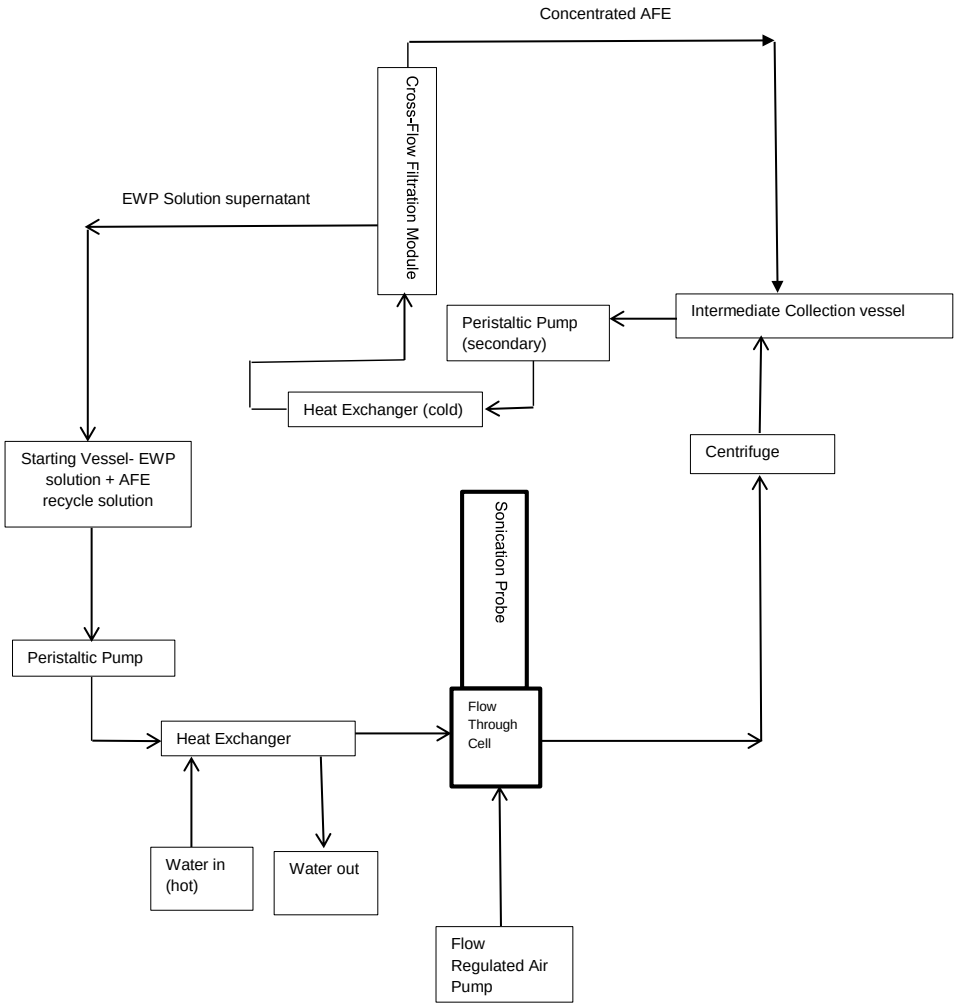

Figure 8-1. A schematic to show the potential setup of a 1 stage process combining the Non Top-Up Continuous Method and the Cross-Flow Filtration Module.

Aside from using the CFF module, a small adaptation to the setup could be implemented, mainly for the Non Top-Up continuous methods, where a secondary heat exchanger is placed between the sonication vessel and the collecting vessel. Due to the process being continuous, the AFE coming out will be hot, so if some protein is still left in solution then it could be exposed to much longer periods of heat and denature (similar principle to water bath method). A secondary heat exchanger with cold water flowing through it would cool down the AFE after production. Therefore, it would not be hot in in the collecting vessel for a prolonged period of time, minimising the protein denaturation. The idea for the setup is shown in the schematic in *Figure 8-2*.

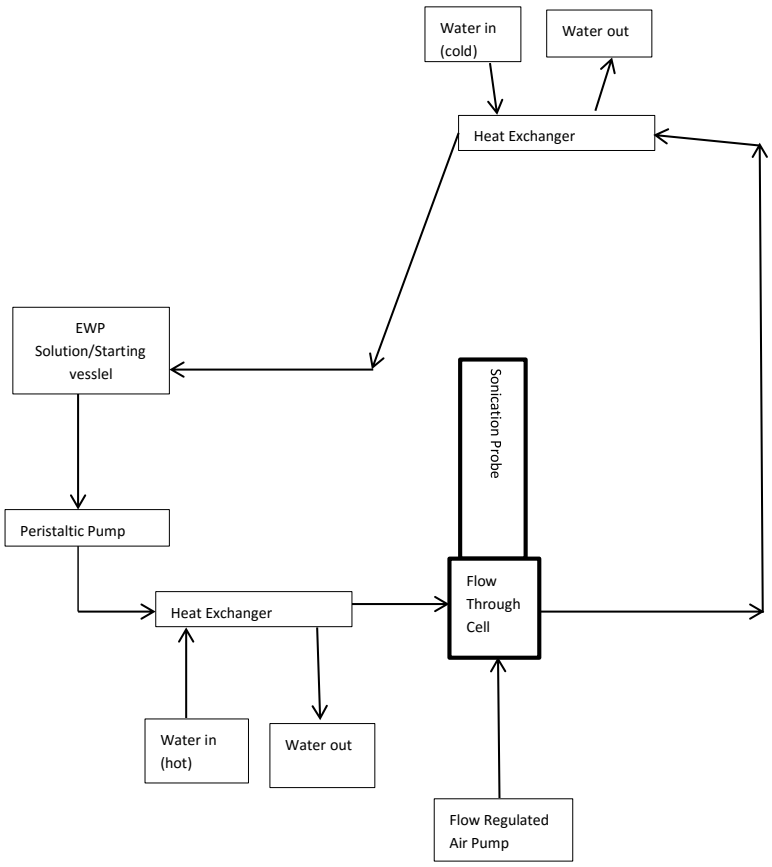

Figure 8-2. A theoretical schematic for the set up involving two heat exchangers. One hot and one cold.

Another prospect for other methods is to use more one sonicator, either in series or in parallel. In parallel, the pipe would split after heating in the heat exchanger (although it could potentially split after the pump and have two heat exchangers) and the solution would branch off into two sonicators which are not connected together, and then the resulting AFE product would collect at the same point. This could minimise the backpressure, with regards to air being minimised due to more diffusion of the air through multiple pathways. It also means that in theory that you could sonicate double the amount of solution on the laboratory scale in the same amount of time. The theoretical schematic is shown in *Figure 8-3*.

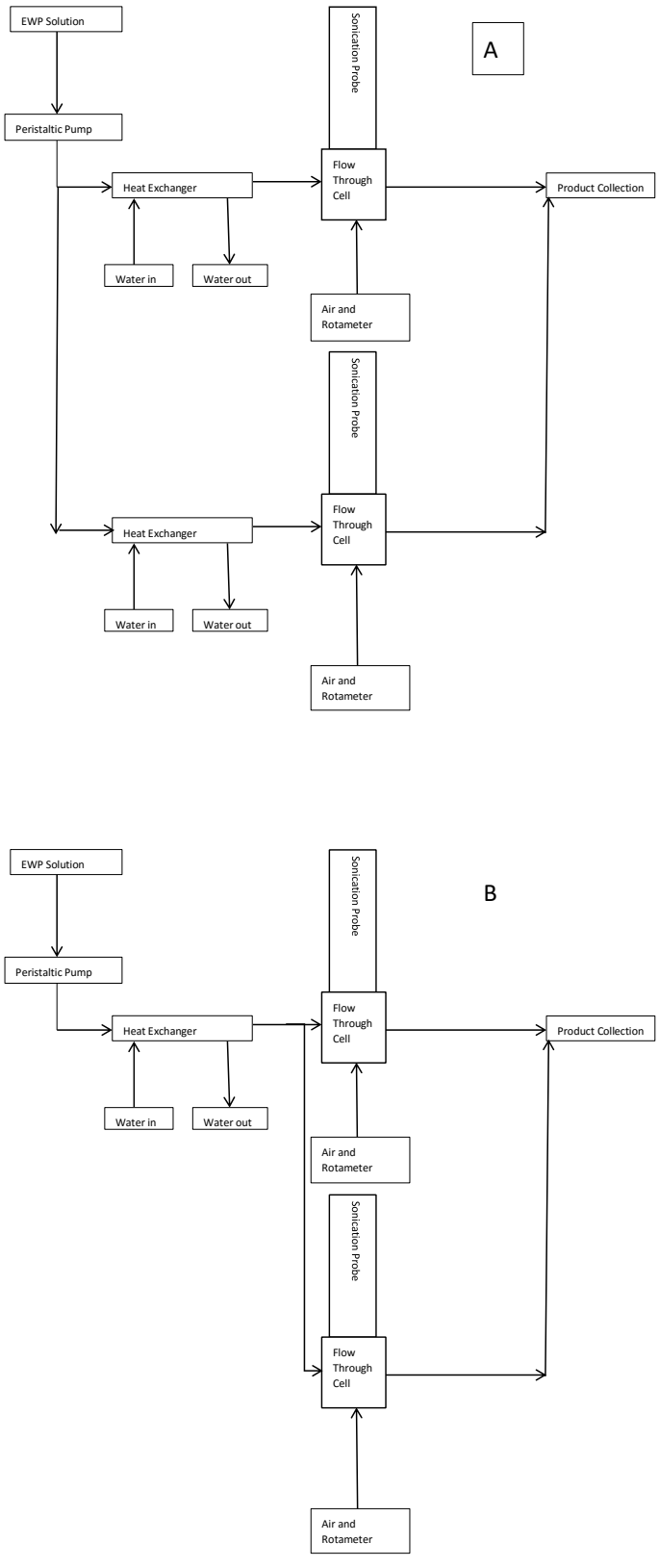

Figure 8-3. A Theoretical Schematic to show how a system with two sonicators in parallel would look. A= Two sonicators attached to two heat exchangers- split after pump. B= Two sonicators with one heat exchanger- split after heating.

In series, the setup would be essentially the same but with the addition of an extra sonication probe and air flow. Utilising two sonication probes in series could minimise the need for multiple recycles as it would essentially act as a recycle in itself. Any protein that has unreacted would pass into the second sonicator and react with the superoxide radicals there. The flow rates would have to be adjusted accordingly but with two sonicators and two air flows/radical production, it could give the proteins twice the chance of reacting (so long as the AFE produced in the first sonicator does not block the cavitational voids in the second sonicator). The theoretical schematic is shown in *Figure 8-4.*

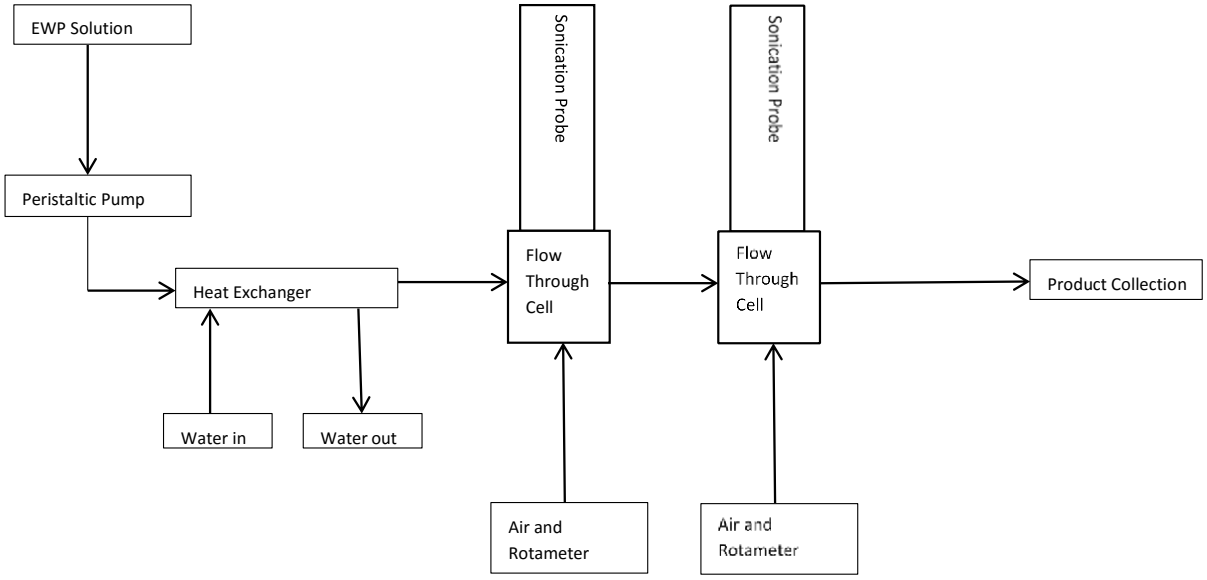

Figure 8-4. A Theoretical Schematic to show how a system with two sonicators in series would look 8-4.

So the parallel sonicators would look at minimising the internal pressures and increasing volume output, whilst the series sonicators would look at minimising the amount of recycles, which for both the Non Top-Up Continuous Method and large scale systems, it could prove quite useful as it would minimise the production timescale.

Similar to the tandem and series sonicator, the same principles could be used and applied to the heat exchanger. Multiple heat exchangers could be used for one sonication probe and give a larger surface area for heating if in parallel, and a longer period of heating if in series. However, from the results it appears that heating is sufficient, so out of these the parallel would be the more useful of the two. And as shown in Figure, if there are multiple sonication vessels in parallel, then more than one might be required if two separate reaction pathways were to be created. After the heat exchanger proving very useful as a heating source, it is very doubtful that any future work will include a water bath as the heating source.

A tangent to the main goals would be to look at the tip degradation with respect to energy usage and AFE production. As shown in section 3.5.3. The amplitude relates directly to the energy input, which in effect is the amount of energy input into the reaction, affecting yield. If the tip is old, then pitting can occur and therefore the amplitude to energy conversion is not as effective. This could have an impact on AFE production. The tip can be monitored by an interferometer at defined periods of time. This could be compared against energy output which could then be compared to AFE production and would lead to the understanding of how tip quality affects the AFE production. Modelling of the data could also be done, to see when the best time to change to a new tip is.

With regards to future work on scaling up the process, the process needs to be optimised and the problems stated in section 6.3.1., need to be addressed. If these points are addressed with regards to the setup, then the yields and production could increase especially once the optimal conditions are found (which could be different to the small scale). If this is successful, then the future would be to take everything that has been discovered on both the laboratory and pilot scale and implement it to an industrial scale production, where it will be of great use to industry.

As well as focusing on EWP, now that recycle methods have high efficiency for EWP-AFE production, other types of AFE such as BSA-AFE could be tested to see if the effect is the

same as experienced with these methods, or whether the different proteins react to the recycle methods in different ways.

And as with any research, more repeats and more analysis will give a deeper understanding into the mechanisms of the production and how best to ‘tune’ and optimise the production process.

REFERENCES

[1] Tchuenbou-Magaia F.L., Cox P.W., Tribological study of suspensions of cysteine-rich protein stabilized microbubbles and subsequent triphasic a/o/w emulsions, J. Textural Studies, 2011, **42,** 185.

[2] Tchuenbou-Magaia F.L., Hydrophobins and Air Filled Emulsions, PhD thesis, The University of Birmingham, 2011.

[3] Tchuenbou-Magaia F.L., Norton I.T., Cox P.W., Microbubbles with protein coats for healthy food: Air filled emulsions, Food Hydrocolloid, 2009, **23**, 1877-1885.

[4] K.S. Suslick, Y.D. Idenko, M.M. Fang, T. Hyeon, K.J. Kolbeck, W.B. McNamara III, M.M. Mdleleni and M. Wong., Acoustic Cavitation and Its Chemical Consequences R. Soc. Lond., 1999, **357**, 335–353.

[5] K.S. Suslick, M.W. Grinstaff, K.J. Kolbeck, M. Wong., Ultrasonics Sonochemistry., 1994, **1**, S65-S68.

[6] Tchuenbou-Magaia F.L, Al-Rifai N., Ishak N. E. M, Norton I. T., Cox P. W., Suspensions of air cells with cysteine-rich protein coats: Air-filled emulsions, J. Celluar Plastics 2011 **47(3)** 217-232.

[7] Green A., Littlejohn K. A., Hooley P., Cox P.W., Current Opinion in Colloid and Interface Science, 2013, **18**, 292-301.

[8] Norton I.T., Cox P.W., Tchuenbou-Magaia F.L., 2011 Low Fat Food Containing Gas Bubbles, US Patent Application 20110287150.

[9] Zuniga R.N.,Aguilera J.M., Aerated food gels: fabrication and potential applications, Food Sci Technol 2008, **19** 176–187.

[10] Wildmoser H., Scheiwiller J., Windhab EJ., Impact of disperse microstructure on rheology and quality aspect of ice cream, Lebensm Wiss Technol 2004, **37,** 881–891.

[11] Lau C.K., Dickinson E., Instability and structural change in an aerated system containing egg albumen and invert sugar, Food Hydrocolloids ,2005, **19,** 111–121.

[12] Grinstaff M.W., Suslick K.S., Air-filled proteinaceous microbubbles: synthesis of an echo-contrast agent, Proc. Natl. Acad. Sci. 1991, **88,** 7708–7710.

[13] Villanueva F.S., Jankowski R.J., Manaugh C., Wagner W.R., Albumin microbubble adherence to human coronary endothelium: implications for assessment of endothelial function using myocardial contrast echocardiography, J. Am. Coll. Cardiol., 1997, **30,** 689– 693.

[14] Tsutsui J., Xie F., Porter R., The use of microbubbles to target drug delivery, Cardiovasc.

Ultrasound. 2004, **2**, 2–7.

[15] Xu Q., Nakajima M., Ichikawa S., Nakamura N. and Shiina T.A., A comparative study of microbubble generation by mechanical agitation and sonication, Innovative Food Sci. Emerg.

Technol., 2008, **9** 489–494.

[16] Benjamins, J., Vingehoeds, M.H., Zoet, F.D., De Hoog, E.H.A. and Van Aken, G.A., Partial coalescence as a tool to control sensory perception of emulsions, Food Hydrocoll., 2009, **23**, 102–115.

[17] Mine, Y., Kovacs-Nolan J., New Insights in biologically active proteins and peptides derived from hen egg., J. World's Poultry Sci., 2006, **62(1)**, 87-95.

[18] Hoppe A., Examination of egg white proteins and effects of high pressure on select physical and functional properties., Master of Science Thesis, University of Nebraska, 2010. [19] http://www.fordras.com/ovalbumin/ [Accessed: 15/08/2015].

[20] Ngarize S., Herman H., Adams A., Howell N., Comparison of changes in the secondary structure of unheated, heated, and high-pressure-treated beta-lactoglobulin and

ovalbumin proteins using fourier transform raman spectroscopy and self-deconvolution., J. Agric. Food Chem., 2004, **52(21)**, 6470-7.

[21] Carrell R.W., Evans L.L.D., Stein P.E., Mobile reactive centre of serpins and the control of thrombosis., Nature, 1991, **353**, 576-578.

[22] Kilara A., Panyam D., Enhancing the functionality of food proteins by enzymatic modification., Trends Food Sci. Technol., 1996, **7**, 120-125.

[23] Smith M.B., Back J.F., Modification of ovalbumin in stored eggs detected by heat denaturation., Nature, 1962, **193,** 878–879.

[24] Lumry R., Eyring H., Conformation changes of proteins., J. Phys. Chem., 1954, **58,** 110–120.

[25] Privalov P.L., Stability of proteins: small globular proteins., Adv Protein Chem., 1979, **33**, 167-241.

[26] Privalov P.L., Stability of proteins. Proteins which do not present a single cooperative system., Adv. Protein Chem., 1982, **35**, 1-104.

[27] Privalov P.L., Thermodynamic problems of protein structure., Annu. Rev. Biophys. Chem., 1989, **18**, 47-69.

[28] Alting A.C., Hamer R.J., de Kruif C.G., Visschers R.W., Formation of disulfide bonds in acid-induced gels of preheated whey protein isolate., J Agric. Food Chem., 2000, **48(10)**,

5001-7.

[29] Weijers M., Barneveld P.A., Stuart M.A.C., Visschers R.W., Heat-induced denaturation and aggregation of ovalbumin at neutral pH described by irreversible first-order kinetics., 2003, **12(12)**, 2963-2703.

[30] Schade A.L., Caroline L., Raw hen egg white and the role of iron in growth inhibition of Shigella dysenteriae, Staphylococcus aureus, Escherichia coli and Saccharomyces cerevisiae. Science, 1944, **100**, 14–15.

[31] Baker H.M., Baker E.N., Lactoferrin and iron: Structural and dynamic aspects of binding and release. Biometals., 2004, **17**, 209–216.

[32] Abeyrathne E.D.N.S.,Lee H.Y., Ahn D.U., Egg white proteins and their potential use in food processing or as nutraceutical and pharmaceutical agents—A review., Poultry Science, 2013, **92(12)**, 3292-3299.

[33] Wu J., Acero-Lopez A., Ovotransferrin: Structure, bioactivities, and preparation., Functional Foods and Nutraceuticals, 2012, **46(2)**, 480-487.

[34] Kovacs-Nolan J.K.N., Zhang J.W., Hayakawa S., Mine Y., Immunochemical and structural analysis of pepsin-digested egg white ovomucoid., J. Agric. Food Chem., 2000, **48**, 6261–6266.

[35] Oliveira F.C., Coimbra J.S.R., Silva L.H.M., Rojas E.E.G., Silva M.C.H., Ovomucoid partitioning in aqueous two-phase system., Biochem. Eng. J, 2009,. **47**, 55–60.

[36] Omana D.A., Wang J., Wu J., 2010. Co-extraction of egg white proteins using ionexchange chromatography from ovomucin-removed egg white., J. Chromatogr. B Analyt.

Technol. Biomed. Life Sci., 2010, **878**, 1771–1776.

[37] Hiidenhovi J., Aro H.S., Kankare V., Separation of ovomucin subunits by gel filtration: Enhanced resolution of subunits by using a dual-column system., J. Agric. Food Chem., 1999, **47**, 1004–1008.

[38] Robinson D.S., Monsey J.B.,The Composition and Proposed Subunit Structure of Eggwhite β-ovomucin., Biochem. J., 1975, **147**, 55–62.

[39] Mine, Y., 2008. Egg Bioscience and Biotechnology., John Wiley & Sons Inc., Hoboken, NJ.

[40] Alderton G., Ward W.H., Fevold H.L., Isolation of lysozyme from egg white. J. Biol. Chem., 1946, **157**, 43–58.

[41] Cegielska-Radziejewska R., Leśnierowski G., Kijowski J., Properties and Application of Egg White Lysozyme and its Modified Preparations- A Review., Pol. J. Food Nutr. Sci., 2008, **58(1)**, 5-10.

[42] Wan Y., Lu J., Cui Z., Separation of Lysozyme from Chicken Egg White Using Ultrafiltration., Separ. Purif. Tech., 2006, **48**, 133–142.

[43] Walstra P., The Physical Chemistry of Foods, Marcel Dekker Inc., 2003, Chapter 7.2.1., pages 235-242.

[44] Walstra P., The Physical Chemistry of Foods, Marcel Dekker Inc., 2003, Chapter 7.2.1., page 236.

[45] Walstra P., The Physical Chemistry of Foods, Marcel Dekker Inc., 2003, Chapter 7.2.2., pages 242-249.

[46] Mason, T.J. and Lorimer, J.P., Sonochemistry: Theory, Applications and uses of Ultrasound in Chemistry, Wiley-Interscience, New York., 1989.

[47] Mason, T.J., Practical Sonochemistry: User's Guide to Applications in Chemistry and Chemical Engineering, Ellis Horwood Ltd, New York., 1992.

[48] Mason, T.J., Sonochemistry, Oxford Chemistry Primers, Oxford, UK., 2000.

[49] Santos H.M., Lodeiro C., Martínez J.L.C., Ultrasound in Chemistry: Analytical Applications, Chapter 1- The Power of Ultrasound., WILEY-VCH Verlag GmbH & Co. KGaA, Weinheim, 2009., ISBN: 978-3-527-31934-3.

[50] Suslick, K.S., Cline, R.E., Hammerton,D.A., Sonochemical hot spot, Journal of the American Chemical Society, 1986, **108**, 5641-5642.

[51] Wibetoe, G., Takuwa, D.T., Lund,W.D., Sawula, G., Coulter particle analysis used for studying the effect of sample treatment in slurry sampling electrothermal absorption spectrometry., Fresenius. Journal of Analytical Chemistry, 1999, **363**, 46-54.

[52] Capelo-Martınez J.L., Ximenez-Embun P., Madrid Y., Camara, C., Advanced Oxidation Processes for Sample Treatment in Atomic Spectrometry., Trends in Analytical Chemistry, 2004 **23**, 331.

[53] Santos, H.M. and Capelo, J.L., Trends in ultrasonic-based equipment for analytical sample treatment, Talanta, 2007, **73**, 795–802.

[54] Patricio, A., Fernandez, C., Mota, A.M., Capelo, J.L., Dynamic versus static ultrasonic sample treatment for the solid–liquid pre-concentration of mercury from human urine, Talanta, 2006, **69**, 769–775.

[55] Bandelin Electronic, GmbH & Co., www.bandelin.com [Accessed 24/08/2015]

[56] Capelo, J.L., Galesio, M.M., Felisberto, G.M. et al., Micro-focused ultrasonic solid–liquid extraction (μFUSLE) combined with HPLC and fluorescence detection for PAHs determination in sediments: optimization and linking with the analytical minimalism concept. Talanta, 2005, **66**, 1272–1280.

[57] Harrison, R.G., Todd, P., Rudge, S.R., Petrides D.P., Bioseparations Science and Engineering. Oxford University Press, 2003.

[58] Roder H., Maki, K., Cheng H., Early Events in Protein Folding Explored by Rapid Mixing Methods, Chem. Rev., 2006, **106(5)**, 1836-1861.

[59] Arthur Rosinger (June 6, 1944). "Magnetic Stirrer", US 2350534 A, United States Patent Office.

[60] Winkworth Group, http://www.mixer.co.uk/ [Accessed: 24/08/2015].

[61] Howland, John L., Cell Physiology, New York: Macmillan, 1973.

[62] Potter M., Wiggart D.C., Fluid Mechanics, Schuam's outlines, McGraw Hill (USA), 2008.

[63] http://www.omega.com/techref/flowcontrol.html [Accessed: 25/08/2015]

[64] Davis, M; Masten, S., Principles of environmental engineering and science. New York: McGraw Hill, 2004.

[65] Felder, R.M. and R.W. Rousseau, Elementary Principles of Chemical Processes, 2nd Edition, John Wiley, 1986.

[66] Felder, R.M. and R.W. Rousseau, Elementary Principles of Chemical Processes, 3rd Edition, 2005.

[67] Nagiev M.F., The Theory of Recycle Processes in Chemical Engineering, volume in International Series of Monographs on Chemical Engineering, 1964.

[68] Price R.M, http://facstaff.cbu.edu/rprice/lectures/recycle.html [Accessed: 25/08/2015].

[69] Bambase M.E., Che 31. Introduction to Chemical Engineering Calculations, Lecture 12-Recycle, Bypass, & Purge Calculations, Department of Chemical Engineering. University of the Philippines Los Baños. http://che31.weebly.com/uploads/3/7/4/3/3743741/lect12-recycle-bypass-purge.pdf [Accessed: 27/08/2015].

[70] Green A.J., Unpublished Data, EngD thesis, The University of Birmingham.

[71] Dos Santos J.B., Unpublished Data, Air Filled Emulsions Summer Student Intern Report, The University of Birmingahm, 2014.

[72] https://www.ukpower.co.uk/home_energy/tariffs-per-unit-kwh [Accessed: 22/08/2015].

[73] http://www.energysavingtrust.org.uk/content/our-calculations [Accessed: 22/08/2015].

[74] Jermann C. et al., Unpublished Data, Rich Products Teleconference Presentation, Pilot Scale Production of Air Filled Emulsions, Campden BRI, 21/7/2015.

APPENDIX

Data tables

Table 3-1. The various weights of the protein solution plus watch glass during the control experiment.

Time (hours)	Mass (g)		
	Watch Glass 1	Watch Glass 2	Watch Glass 3
	161.91	167.93	173.58
0	172.02	178.14	183.97
1	168.63	174.62	180.55
2	166.09	172.09	177.98
3	164.21	170.14	176.04
4	162.90	168.83	174.60
6	162.44	168.43	174.09
8	162.35	168.36	174.02
10	162.31	168.34	174.01
12	162.31	168.34	174.01
24	162.31	168.34	174.01
48	162.31	168.34	174.01
72	162.31	168.34	174.01

Table 3-3. The energy recorded for pure water after 5 minutes of constant sonication and a conversion to other energy representations.

	Energy used				
Amplitude	($Jmin^{-1}$)	$kJhr^{-1}$	$eVhr^{-1}$	Watts (Js^{-1})	kWh
20	1076	64.56	4.03×10^{23}	17.93	0.018
30	1693	101.56	6.34×10^{23}	28.21	0.028
40	2413	144.77	9.04×10^{23}	40.21	0.040
50	3145	188.68	1.18×10^{23}	52.41	0.052
60	3659	219.53	1.37×10^{23}	60.98	0.061
70	4267	256.01	1.60×10^{24}	71.11	0.071
80	5110	306.59	1.91×10^{24}	85.16	0.085
90	5613	336.78	2.10×10^{24}	93.55	0.094
100	6375	382.51	2.39×10^{24}	106.25	0.106

Table 3-4. The energy recorded for 5 % EWP solution after 5 minutes of constant sonication and a conversion to other energy representations.

Amplitude	Energy Used ($Jmin^{-1}$)	$kJhr^{-1}$	$eVhr^{-1}$	Watts (Js^{-1})	kWh
20	948	56.88	$3.55x10^{23}$	15.80	0.016
30	1611	96.65	$6.03 x10^{23}$	26.85	0.027
40	1988	119.26	$7.44 x10^{23}$	33.13	0.033
50	2430	145.80	$9.10 x10^{23}$	40.50	0.041
60	2816	168.94	$1.05 x10^{24}$	46.93	0.047
70	3245	194.66	$1.21 x10^{24}$	54.07	0.054
80	3938	236.30	$1.47 x10^{24}$	65.64	0.066
90	4583	274.97	$1.72 x10^{24}$	76.38	0.076
100	5133	307.97	$1.92 x10^{24}$	85.55	0.086

Table 3-5. The energy recorded for AFE solution after 5 minutes of constant sonication and a conversion to other energy representations.

Amplitude	Energy used ($Jmin^{-1}$)	$kJhr^{-1}$	$eVhr^{-1}$	Watts (Js^{-1})	kWh
20	1007	60.43	$3.77 x10^{23}$	16.79	0.017
30	1673	100.39	$6.27 x10^{23}$	27.89	0.028
40	2165	129.90	$8.11 x10^{23}$	36.08	0.036
50	2775	166.49	$1.04 x10^{24}$	46.25	0.046
60	3211	192.67	$1.20 x10^{24}$	53.52	0.054
70	3688	221.26	$1.38 x10^{24}$	61.46	0.061
80	4325	259.50	$1.62 x10^{24}$	72.08	0.072
90	5133	307.98	$1.92 x10^{24}$	85.55	0.086
100	5784	347.04	$2.17 x10^{24}$	96.40	0.096

Table 4-1. The calculation results from the data obtained from the initial amplitude testing as a guide to recycling.

Amplitude (%)	Protein Required to Recycle (g/100mL)	Protein Used (%)
0	0	0
30	1.35	26.9
60	2.53	50.6
100	3.04	60.7

Table 5-1. The amount of protein used per each recycle for the STUM heated by a water bath.

Recycle	Protein Used Per Recycle (%)		
	Experiment 1	Experiment 2	Experiment 3
0	50.5	35.2	42.1
1	17.6	33.7	26.1
2	13.7	15.1	13.9
3	13.4	11.5	13.2

Table 5-2. The total protein used for the STUM with water bath heating (WBH).

Recycle	Total Protein Used (%)		
	Experiment 1	Experiment 2	Experiment 3
0	50.5	35.2	42.1
1	68.1	68.9	68.2
2	81.8	84.0	82.1
3	95.2	95.5	95.3

Table 5-3. The amount of protein added per each recycle for the STUM with WBH.

Recycle	Protein Added (g)		
	Experiment 1	Experiment 2	Experiment 3
0	31.0	21.1	25.2
1	8.8	16.9	14.8
2	6.0	6.4	6.2
3	0	0	0

Table 5-4. The concentrations of the waste protein solution after each pass for the STUM with WBH.

Recycle	Concentration (w/v%)		
	Experiment 1	Experiment 2	Experiment 3
0	2.1	2.9	2.4
	5.0	5.0	5.0
1	4.0	2.9	2.3
	5.0	5.0	5.0
2	3.0	3.2	3.3
	5.0	5.0	5.0
3	3.9	4.3	3.4

Table 5-5. The total amount of protein used when using a heat exchanger from ambient start.

Recycle	Total Protein used (%)		
	Experiment 1**	Experiment 2	Experiment 3
0	32.0	39.7	50.1
1	65.0	66.2	70.9
2	83.4	85.8	88.5
3	95.8	98.7	97.2

. Table 5-6. The amount of protein used per recycle when using a heat exchanger from ambient start.

Recycle	Protein used per recycle (%)		
	Experiment 1**	Experiment 2	Experiment 3
0	32.0	39.7	50.1
1	33.0	26.5	20.8
2	18.4	19.6	17.6
3	12.4	12.9	8.7

Table 5-7. The concentrations of the waste protein solution after each recycle from ambient start.

Recycle	Concentration (w/v%)		
	Experiment 1**	Experiment 2	Experiment 3
0	3.1	2.3	1.8
	5.0	5.0	5.0
1	4.1	2.5	3.1
	5.0	5.0	5.0
2	3.6	2.2	2.7
	5.0	5.0	5.0
3	2.4	3.4	3.8

Table 5-8. The amount of protein added per each recycle from ambient start.

Recycle	Protein Added (g)		
	Experiment 1**	Experiment 2	Experiment 3
0	20.0	23.8	26.3
1	17.2	18.6	15.5
2	9.6	12.2	8.0
3	0	0	0

Table 5-9. The total amount of protein used when using a heat exchanger from cold start.

Recycle	Total Protein Used (%)		
	Experiment 1**	Experiment 2	Experiment 3
0	44.4	38.0	41.0
1	74.6	67.6	69.9
2	92.7	91.4	91.5

Table 5-10. The amount of protein used per recycle when using a heat exchanger from cold start

Recycle	Protein Used Per Recycle (%)		
	Experiment 1**	Experiment 2	Experiment 3
0	44.4	38.0	41.0
1	30.2	29.6	28.9
2	18.1	23.8	21.6

Table 5-11. The concentration of the waste protein solution after each recycle from cold start.

Recycle	Concentration (%w/v)		
	Experiment1**	Experiment 2	Experiment 3
0	2.1	2.4	2.4
	5.0	5.0	5.0
1	3.4	2.3	2.1
	5.0	5.0	5.0
3	3.7	1.9	2.4

Table 5-12. The amount of protein added per each recycle from cold start.

Recycle	Protein Added (g)		
	Experiment 1**	Experiment 2	Experiment 3
0	24.4	24.7	24.6
1	22.1	22.2	22.4
2	0	0	0

Table 5-13. The amount of protein used in each sonication step during the NoTUCeM.

Sonication	Protein Used (%)		
	Experiment 1	Experiment 2	Experiment 3
1	43.5	48.9	42.8
2	50.9	58.9	47.2
3	55.3	63.1	48.2
4	68.7	78.5	62.4

Table 5-14 The concentration of the waste protein solution after each sonication during the NoTUCeM.

Sonication	Concentration (%w/v)		
	Experiment 1	Experiment 2	Experiment 3
1	2.3	2.3	2.3
2	1.9	1.6	1.9
3	1.6	1.3	1.7
4	0.7	0.5	1.1

Table 5-15. The final usage and concentration of the protein solution using the initial (multiple stage) NoTUCoM.

Experiment	Protein Used (%)	Concentration (w/v%)
1**	51.0	2.3
2	49.6	2.2
3	48.5	2.2

Table 5-16. The final usage and concentration of the protein solution using the NoTUCoM (v2) feedback method.

Experiment	Protein Used (%)	Concentration (w/v%)
1	55.8	1.89
2	51.5	2.10
3	53.9	1.93

Table 7-4. A table showing a summary of the model for the absorbance results obtained. Produced by the Statistician at Campden BRI and Jermann et al [74].

Analysis of variance

Source	DF	Seq SS	Seq MS	F-value	P-value
Sugar x Sugar	1	0.006217	0.006217	8.56	0.004*
Salt x Salt	1	0.006749	0.006749	9.29	003*
Amplitude x Amplitude	1	0.040853	0.040853	56.23	0.000*
Linear terms					0.104
Sugar (%)	1	0.001949	0.001949	2.68	0.000*
Salt (%)	1	0.030153	0.030153	41.5	
Amplitude (%)	1	0.012286	0.012286	16.91	0.000*
Residence time (%)	1	000018	0.000018	0.02	0.876
Temperature (°C)	1	0.15352	0.15352	211.3	0.000*
Square terms					
Residence time x Residence time	1	0.002486	0.002486	3.42	0.066
Temperature x Temperature	1	0.012261	0.012261	16.88	0.000*
2-way interactions					
Sugar x Salt	1	0.000387	0.000387	0.53	0.467
Sugar x Amplitude	1	0	0	0	0.994
Sugar x Residence time	1	0.000118	0.000118	0.16	688
Sugar x Temperature	1	0.006515	0.006515	8.97	0.003*
Salt x Amplitude	1	0.003756	0.003756	5.17	0.025*
Salt x Residence time	1	0.002651	0.002651	3.65	0.058
Salt x Temperature	1	0.014175	0.014175	19.51	0.000*
Amplitude x Residence time	1	0.000528	0.000528	0.73	0.395
Amplitude x Temperature	1	0	0	0	0.987
Residence time x Temperature	1	0.024886	0.024886	34.25	0.000*

Error			138	0.100264	0.000727		
Lack of fit			97	0.093297	0.000962	5.66	0.000
Pure error	41	0.006967	0.00017	Total	158	0.419772	

Model summary

S	R-sq	R-sq (adj)	R-sq (pred)
0.0269545	76.11	72.65	68.07

* Significant p-values

Table 7-5. A table showing a summary of the model for the energy results obtained. Produced by the Statistician at Campden BRI and Jermann et al. †In this table SS and MS are calculated based on raw data, indicating how much of the variation in energy is fitted by different terms [74].

Analysis of variance

Source	DF	Seq SS	Seq MS	P-Value†
Amplitude (%)	1	484886	484886	0.000*
Residence time (min)	1	520	520	0.107
Temperature (°C)	1	3122	3122	0.000*
Amplitude x Amplitude	1	1457	1457	0.082
Residence time x Residence time	1	468	468	0.014*
Temperature x Temperature	1	101	101	0.920
Amplitude x Residence time	1	468	468	0.069
Amplitude x Temperature	1	135	135	0.538
Residence time x Temperature	1	25	25	0.283
Error	225	6685	30	
Lack of fit 122 4877 40 Pure error 103 1808 18				
Total	234	497867		

Model summary

S	R-sq	R-sq (adj)	R-sq (pred)
5.45095	98.66	98.6	98.44

Mastersizer Raw Data

No	Size (µm)	Mean In%	1*S.D.
1	0.010	0.00	0.00
2	0.011	0.00	0.00
3	0.013	0.00	0.00
4	0.014	0.00	0.00
5	0.016	0.00	0.00
6	0.018	0.00	0.00
7	0.020	0.00	0.00
8	0.022	0.00	0.00
9	0.025	0.00	0.00
10	0.028	0.00	0.00
11	0.032	0.00	0.00
12	0.035	0.00	0.00
13	0.040	0.00	0.00
14	0.045	0.00	0.00
15	0.050	0.00	0.00
16	0.056	0.00	0.00
17	0.063	0.00	0.00
18	0.071	0.00	0.00
19	0.079	0.00	0.00
20	0.089	0.00	0.00
21	0.100	0.00	0.00
22	0.112	0.00	0.00
23	0.126	0.00	0.00
24	0.141	0.05	0.07
25	0.158	0.55	0.27
26	0.178	1.59	0.12
27	0.200	2.43	0.18
28	0.224	3.30	0.16
29	0.251	4.10	0.13
30	0.282	4.72	0.10
31	0.316	5.16	0.04
32	0.355	5.40	0.02
33	0.398	5.44	0.09
34	0.447	5.30	0.15
35	0.501	5.02	0.19
36	0.562	4.63	0.20
37	0.631	4.21	0.18
38	0.708	3.81	0.13
39	0.794	3.49	0.06
40	0.891	3.30	0.00
41	1.000	3.25	0.05
42	1.122	3.32	0.07
43	1.259	3.43	0.05
44	1.413	3.49	0.02
45	1.585	3.48	0.03
46	1.778	3.45	0.06
47	1.995	3.34	0.08
48	2.239	3.09	0.08
49	2.512	2.76	0.07
50	2.818	2.34	0.06
51	3.162	1.88	0.03
52	3.548	1.43	0.01
53	3.981	1.02	0.02
54	4.467	0.67	0.02
55	5.012	0.37	0.07
56	5.623	0.17	0.03
57	6.310	0.02	0.03
58	7.079	0.00	0.00
59	7.943	0.00	0.00
60	8.913	0.00	0.00
61	10.000	0.00	0.00
62	11.220	0.00	0.00
63	12.589	0.00	0.00
64	14.125	0.00	0.00
65	15.849	0.00	0.00
66	17.783	0.00	0.00
67	19.953	0.00	0.00
68	22.387	0.00	0.00
69	25.119	0.00	0.00
70	28.184	0.00	0.00
71	31.623	0.00	0.00
72	35.481	0.00	0.00
73	39.811	0.00	0.00
74	44.668	0.00	0.00
75	50.119	0.00	0.00
76	56.234	0.00	0.00
77	63.096	0.00	0.00
78	70.795	0.00	0.00
79	79.433	0.00	0.00
80	89.125	0.00	0.00
81	100.000	0.00	0.00
82	112.202	0.00	0.00
83	125.893	0.00	0.00
84	141.254	0.00	0.00
85	158.489	0.00	0.00
86	177.828	0.00	0.00
87	199.526	0.00	0.00
88	223.872	0.00	0.00
89	251.189	0.00	0.00
90	281.838	0.00	0.00
91	316.228	0.00	0.00
92	354.813	0.00	0.00
93	398.107	0.00	0.00
94	446.684	0.00	0.00
95	501.187	0.00	0.00
96	562.341	0.00	0.00
97	630.957	0.00	0.00
98	707.946	0.00	0.00
99	794.328	0.00	0.00
100	891.251	0.00	0.00
	1000.000		

Raw Data from the Mastersizer for the STUM HE (ambient) initial sonication.

No	Size (µm)	Mean In%	1*S.D.
1	0.010	0.00	0.00
2	0.011	0.00	0.00
3	0.013	0.00	0.00
4	0.014	0.00	0.00
5	0.016	0.00	0.00
6	0.018	0.00	0.00
7	0.020	0.00	0.00
8	0.022	0.00	0.00
9	0.025	0.00	0.00
10	0.028	0.00	0.00
11	0.032	0.00	0.00
12	0.035	0.00	0.00
13	0.040	0.00	0.00
14	0.045	0.00	0.00
15	0.050	0.00	0.00
16	0.056	0.00	0.00
17	0.063	0.00	0.00
18	0.071	0.00	0.00
19	0.079	0.00	0.00
20	0.089	0.00	0.00
21	0.100	0.02	0.02
22	0.112	0.25	0.20
23	0.126	0.87	0.16
24	0.141	1.59	0.11
25	0.158	2.35	0.09
26	0.178	3.16	0.03
27	0.200	3.93	0.02
28	0.224	4.60	0.07
29	0.251	5.13	0.11
30	0.282	5.47	0.13
31	0.316	5.61	0.14
32	0.355	5.58	0.12
33	0.398	5.39	0.09
34	0.447	5.07	0.05
35	0.501	4.68	0.01
36	0.562	4.24	0.02
37	0.631	3.83	0.03
38	0.708	3.47	0.03
39	0.794	3.22	0.01
40	0.891	3.09	0.01
41	1.000	3.07	0.03
42	1.122	3.11	0.03
43	1.259	3.15	0.03
44	1.413	3.10	0.01
45	1.585	2.96	0.01
46	1.778	2.80	0.02
47	1.995	2.56	0.03
48	2.239	2.22	0.03
49	2.512	1.84	0.02
50	2.818	1.42	0.02
51	3.162	1.01	0.01
52	3.548	0.65	0.01
53	3.981	0.37	0.01
54	4.467	0.13	0.01
55	5.012	0.04	0.00
56	5.623	0.00	0.00
57	6.310	0.00	0.00
58	7.079	0.00	0.00
59	7.943	0.00	0.00
60	8.913	0.00	0.00
61	10.000	0.00	0.00
62	11.220	0.00	0.00
63	12.589	0.00	0.00
64	14.125	0.00	0.00
65	15.849	0.00	0.00
66	17.783	0.00	0.00
67	19.953	0.00	0.00
68	22.387	0.00	0.00
69	25.119	0.00	0.00
70	28.184	0.00	0.00
71	31.623	0.00	0.00
72	35.481	0.00	0.00
73	39.811	0.00	0.00
74	44.668	0.00	0.00
75	50.119	0.00	0.00
76	56.234	0.00	0.00
77	63.096	0.00	0.00
78	70.795	0.00	0.00
79	79.433	0.00	0.00
80	89.125	0.00	0.00
81	100.000	0.00	0.00
82	112.202	0.00	0.00
83	125.893	0.00	0.00
84	141.254	0.00	0.00
85	158.489	0.00	0.00
86	177.828	0.00	0.00
87	199.526	0.00	0.00
88	223.872	0.00	0.00
89	251.189	0.00	0.00
90	281.838	0.00	0.00
91	316.228	0.00	0.00
92	354.813	0.00	0.00
93	398.107	0.00	0.00
94	446.684	0.00	0.00
95	501.187	0.00	0.00
96	562.341	0.00	0.00
97	630.957	0.00	0.00
98	707.946	0.00	0.00
99	794.328	0.00	0.00
100	891.251	0.00	0.00
	1000.000		

Raw Data from the Mastersizer for the STUM HE (ambient) recycle 1.

No	Size (µm)	Mean In%	1*S.D.
1	0.010	0.00	0.00
2	0.011	0.00	0.00
3	0.013	0.00	0.00
4	0.014	0.00	0.00
5	0.016	0.00	0.00
6	0.018	0.00	0.00
7	0.020	0.00	0.00
8	0.022	0.00	0.00
9	0.025	0.00	0.00
10	0.028	0.00	0.00
11	0.032	0.00	0.00
12	0.035	0.00	0.00
13	0.040	0.04	0.02
14	0.045	0.16	0.03
15	0.050	0.24	0.04
16	0.056	0.34	0.05
17	0.063	0.48	0.07
18	0.071	0.68	0.08
19	0.079	0.93	0.09
20	0.089	1.22	0.09
21	0.100	1.54	0.09
22	0.112	1.92	0.08
23	0.126	2.32	0.07
24	0.141	2.74	0.05
25	0.158	3.15	0.03
26	0.178	3.54	0.00
27	0.200	3.87	0.03
28	0.224	4.12	0.05
29	0.251	4.28	0.07
30	0.282	4.32	0.09
31	0.316	4.26	0.09
32	0.355	4.13	0.09
33	0.398	3.93	0.08
34	0.447	3.70	0.06
35	0.501	3.44	0.04
36	0.562	3.18	0.02
37	0.631	2.96	0.00
38	0.708	2.80	0.01
39	0.794	2.73	0.01
40	0.891	2.76	0.00
41	1.000	2.87	0.00
42	1.122	3.02	0.01
43	1.259	3.12	0.01
44	1.413	3.13	0.01
45	1.585	3.05	0.00
46	1.778	2.92	0.00
47	1.995	2.71	0.01
48	2.239	2.40	0.01
49	2.512	2.05	0.02
50	2.818	1.65	0.02
51	3.162	1.26	0.02
52	3.548	0.90	0.02
53	3.981	0.59	0.02
54	4.467	0.36	0.02
55	5.012	0.14	0.02
56	5.623	0.03	0.02
57	6.310	0.00	0.00
58	7.079	0.00	0.00
59	7.943	0.00	0.00
60	8.913	0.00	0.00
61	10.000	0.00	0.00
62	11.220	0.00	0.00
63	12.589	0.00	0.00
64	14.125	0.00	0.00
65	15.849	0.00	0.00
66	17.783	0.00	0.00
67	19.953	0.00	0.00
68	22.387	0.00	0.00
69	25.119	0.00	0.00
70	28.184	0.00	0.00
71	31.623	0.00	0.00
72	35.481	0.00	0.00
73	39.811	0.00	0.00
74	44.668	0.00	0.00
75	50.119	0.00	0.00
76	56.234	0.00	0.00
77	63.096	0.00	0.00
78	70.795	0.00	0.00
79	79.433	0.00	0.00
80	89.125	0.00	0.00
81	100.000	0.00	0.00
82	112.202	0.00	0.00
83	125.893	0.00	0.00
84	141.254	0.00	0.00
85	158.489	0.00	0.00
86	177.828	0.00	0.00
87	199.526	0.00	0.00
88	223.872	0.00	0.00
89	251.189	0.00	0.00
90	281.838	0.00	0.00
91	316.228	0.00	0.00
92	354.813	0.00	0.00
93	398.107	0.00	0.00
94	446.684	0.00	0.00
95	501.187	0.00	0.00
96	562.341	0.00	0.00
97	630.957	0.00	0.00
98	707.946	0.00	0.00
99	794.328	0.00	0.00
100	891.251	0.00	0.00
	1000.000		

Raw Data from the Mastersizer for the STUM HE (ambient) recycle 2.

No	Size (µm)	Mean In%	1*S.D.
1	0.010	0.00	0.00
2	0.011	0.00	0.00
3	0.013	0.00	0.00
4	0.014	0.00	0.00
5	0.016	0.00	0.00
6	0.018	0.00	0.00
7	0.020	0.00	0.00
8	0.022	0.00	0.00
9	0.025	0.00	0.00
10	0.028	0.00	0.00
11	0.032	0.00	0.00
12	0.035	0.00	0.00
13	0.040	0.00	0.00
14	0.045	0.00	0.00
15	0.050	0.00	0.00
16	0.056	0.00	0.00
17	0.063	0.00	0.00
18	0.071	0.01	0.02
19	0.079	0.06	0.08
20	0.089	0.23	0.13
21	0.100	0.56	0.09
22	0.112	0.97	0.11
23	0.126	1.46	0.09
24	0.141	2.02	0.08
25	0.158	2.61	0.06
26	0.178	3.20	0.04
27	0.200	3.76	0.01
28	0.224	4.23	0.02
29	0.251	4.59	0.04
30	0.282	4.82	0.05
31	0.316	4.93	0.06
32	0.355	4.92	0.06
33	0.398	4.82	0.06
34	0.447	4.62	0.05
35	0.501	4.33	0.04
36	0.562	3.96	0.03
37	0.631	3.57	0.03
38	0.708	3.19	0.04
39	0.794	2.91	0.06
40	0.891	2.76	0.07
41	1.000	2.77	0.07
42	1.122	2.91	0.07
43	1.259	3.08	0.07
44	1.413	3.19	0.05
45	1.585	3.20	0.03
46	1.778	3.16	0.01
47	1.995	3.00	0.01
48	2.239	2.69	0.02
49	2.512	2.31	0.03
50	2.818	1.85	0.03
51	3.162	1.38	0.03
52	3.548	0.94	0.03
53	3.981	0.58	0.02
54	4.467	0.32	0.02
55	5.012	0.09	0.01
56	5.623	0.00	0.00
57	6.310	0.00	0.00
58	7.079	0.00	0.00
59	7.943	0.00	0.00
60	8.913	0.00	0.00
61	10.000	0.00	0.00
62	11.220	0.00	0.00
63	12.589	0.00	0.00
64	14.125	0.00	0.00
65	15.849	0.00	0.00
66	17.783	0.00	0.00
67	19.953	0.00	0.00
68	22.387	0.00	0.00
69	25.119	0.00	0.00
70	28.184	0.00	0.00
71	31.623	0.00	0.00
72	35.481	0.00	0.00
73	39.811	0.00	0.00
74	44.668	0.00	0.00
75	50.119	0.00	0.00
76	56.234	0.00	0.00
77	63.096	0.00	0.00
78	70.795	0.00	0.00
79	79.433	0.00	0.00
80	89.125	0.00	0.00
81	100.000	0.00	0.00
82	112.202	0.00	0.00
83	125.893	0.00	0.00
84	141.254	0.00	0.00
85	158.489	0.00	0.00
86	177.828	0.00	0.00
87	199.526	0.00	0.00
88	223.872	0.00	0.00
89	251.189	0.00	0.00
90	281.838	0.00	0.00
91	316.228	0.00	0.00
92	354.813	0.00	0.00
93	398.107	0.00	0.00
94	446.684	0.00	0.00
95	501.187	0.00	0.00
96	562.341	0.00	0.00
97	630.957	0.00	0.00
98	707.946	0.00	0.00
99	794.328	0.00	0.00
100	891.251	0.00	0.00
	1000.000		

Raw Data from the Mastersizer for the STUM HE (ambient) recycle 3.

No	Size (µm)	Mean In%	1*S.D.
1	0.010	0.00	0.00
2	0.011	0.00	0.00
3	0.013	0.00	0.00
4	0.014	0.00	0.00
5	0.016	0.00	0.00
6	0.018	0.00	0.00
7	0.020	0.00	0.00
8	0.022	0.00	0.00
9	0.025	0.00	0.00
10	0.028	0.00	0.00
11	0.032	0.00	0.00
12	0.035	0.00	0.00
13	0.040	0.00	0.00
14	0.045	0.00	0.00
15	0.050	0.00	0.00
16	0.056	0.00	0.00
17	0.063	0.00	0.00
18	0.071	0.00	0.00
19	0.079	0.00	0.00
20	0.089	0.00	0.00
21	0.100	0.00	0.00
22	0.112	0.00	0.00
23	0.126	0.00	0.00
24	0.141	0.08	0.04
25	0.158	0.56	0.19
26	0.178	1.54	0.01
27	0.200	2.35	0.00
28	0.224	3.18	0.04
29	0.251	3.95	0.08
30	0.282	4.57	0.09
31	0.316	5.03	0.10
32	0.355	5.30	0.10
33	0.398	5.40	0.09
34	0.447	5.33	0.07
35	0.501	5.10	0.06
36	0.562	4.74	0.04
37	0.631	4.32	0.02
38	0.708	3.90	0.01
39	0.794	3.54	0.00
40	0.891	3.30	0.01
41	1.000	3.22	0.01
42	1.122	3.27	0.01
43	1.259	3.37	0.01
44	1.413	3.42	0.02
45	1.585	3.42	0.03
46	1.778	3.41	0.03
47	1.995	3.32	0.03
48	2.239	3.09	0.03
49	2.512	2.79	0.03
50	2.818	2.41	0.04
51	3.162	1.97	0.04
52	3.548	1.53	0.04
53	3.981	1.12	0.04
54	4.467	0.75	0.04
55	5.012	0.46	0.04
56	5.623	0.21	0.03
57	6.310	0.05	0.00
58	7.079	0.00	0.00
59	7.943	0.00	0.00
60	8.913	0.00	0.00
61	10.000	0.00	0.00
62	11.220	0.00	0.00
63	12.589	0.00	0.00
64	14.125	0.00	0.00
65	15.849	0.00	0.00
66	17.783	0.00	0.00
67	19.953	0.00	0.00
68	22.387	0.00	0.00
69	25.119	0.00	0.00
70	28.184	0.00	0.00
71	31.623	0.00	0.00
72	35.481	0.00	0.00
73	39.811	0.00	0.00
74	44.668	0.00	0.00
75	50.119	0.00	0.00
76	56.234	0.00	0.00
77	63.096	0.00	0.00
78	70.795	0.00	0.00
79	79.433	0.00	0.00
80	89.125	0.00	0.00
81	100.000	0.00	0.00
82	112.202	0.00	0.00
83	125.893	0.00	0.00
84	141.254	0.00	0.00
85	158.489	0.00	0.00
86	177.828	0.00	0.00
87	199.526	0.00	0.00
88	223.872	0.00	0.00
89	251.189	0.00	0.00
90	281.838	0.00	0.00
91	316.228	0.00	0.00
92	354.813	0.00	0.00
93	398.107	0.00	0.00
94	446.684	0.00	0.00
95	501.187	0.00	0.00
96	562.341	0.00	0.00
97	630.957	0.00	0.00
98	707.946	0.00	0.00
99	794.328	0.00	0.00
100	891.251	0.00	0.00
	1000.000		

Raw Data from the Mastersizer for the STUM HE (cold) initial sonication.

No	Size (µm)	Mean In%	1*S.D.
1	0.010	0.00	0.00
2	0.011	0.00	0.00
3	0.013	0.00	0.00
4	0.014	0.00	0.00
5	0.016	0.00	0.00
6	0.018	0.00	0.00
7	0.020	0.00	0.00
8	0.022	0.00	0.00
9	0.025	0.00	0.00
10	0.028	0.00	0.00
11	0.032	0.00	0.00
12	0.035	0.00	0.00
13	0.040	0.00	0.00
14	0.045	0.00	0.00
15	0.050	0.00	0.00
16	0.056	0.00	0.00
17	0.063	0.00	0.00
18	0.071	0.00	0.00
19	0.079	0.00	0.00
20	0.089	0.00	0.00
21	0.100	0.01	0.00
22	0.112	0.27	0.00
23	0.126	0.89	0.00
24	0.141	1.59	0.00
25	0.158	2.34	0.01
26	0.178	3.13	0.01
27	0.200	3.89	0.01
28	0.224	4.54	0.01
29	0.251	5.07	0.00
30	0.282	5.41	0.01
31	0.316	5.58	0.02
32	0.355	5.57	0.03
33	0.398	5.40	0.04
34	0.447	5.12	0.05
35	0.501	4.75	0.06
36	0.562	4.32	0.07
37	0.631	3.90	0.07
38	0.708	3.53	0.06
39	0.794	3.25	0.05
40	0.891	3.09	0.03
41	1.000	3.05	0.01
42	1.122	3.09	0.01
43	1.259	3.12	0.03
44	1.413	3.08	0.04
45	1.585	2.95	0.04
46	1.778	2.79	0.05
47	1.995	2.56	0.05
48	2.239	2.23	0.05
49	2.512	1.84	0.04
50	2.818	1.43	0.04
51	3.162	1.01	0.04
52	3.548	0.65	0.03
53	3.981	0.37	0.02
54	4.467	0.12	0.02
55	5.012	0.04	0.01
56	5.623	0.00	0.00
57	6.310	0.00	0.00
58	7.079	0.00	0.00
59	7.943	0.00	0.00
60	8.913	0.00	0.00
61	10.000	0.00	0.00
62	11.220	0.00	0.00
63	12.589	0.00	0.00
64	14.125	0.00	0.00
65	15.849	0.00	0.00
66	17.783	0.00	0.00
67	19.953	0.00	0.00
68	22.387	0.00	0.00
69	25.119	0.00	0.00
70	28.184	0.00	0.00
71	31.623	0.00	0.00
72	35.481	0.00	0.00
73	39.811	0.00	0.00
74	44.668	0.00	0.00
75	50.119	0.00	0.00
76	56.234	0.00	0.00
77	63.096	0.00	0.00
78	70.795	0.00	0.00
79	79.433	0.00	0.00
80	89.125	0.00	0.00
81	100.000	0.00	0.00
82	112.202	0.00	0.00
83	125.893	0.00	0.00
84	141.254	0.00	0.00
85	158.489	0.00	0.00
86	177.828	0.00	0.00
87	199.526	0.00	0.00
88	223.872	0.00	0.00
89	251.189	0.00	0.00
90	281.838	0.00	0.00
91	316.228	0.00	0.00
92	354.813	0.00	0.00
93	398.107	0.00	0.00
94	446.684	0.00	0.00
95	501.187	0.00	0.00
96	562.341	0.00	0.00
97	630.957	0.00	0.00
98	707.946	0.00	0.00
99	794.328	0.00	0.00
100	891.251	0.00	0.00
	1000.000		

Raw Data from the Mastersizer for the STUM HE (cold) recycle 1.

No	Size (µm)	Mean In%	1*S.D.
1	0.010	0.00	0.00
2	0.011	0.00	0.00
3	0.013	0.00	0.00
4	0.014	0.00	0.00
5	0.016	0.00	0.00
6	0.018	0.00	0.00
7	0.020	0.00	0.00
8	0.022	0.00	0.00
9	0.025	0.00	0.00
10	0.028	0.00	0.00
11	0.032	0.01	0.01
12	0.035	0.02	0.03
13	0.040	0.05	0.02
14	0.045	0.13	0.04
15	0.050	0.19	0.07
16	0.056	0.25	0.10
17	0.063	0.37	0.13
18	0.071	0.54	0.17
19	0.079	0.77	0.20
20	0.089	1.05	0.22
21	0.100	1.37	0.24
22	0.112	1.75	0.24
23	0.126	2.17	0.23
24	0.141	2.62	0.20
25	0.158	3.07	0.16
26	0.178	3.49	0.11
27	0.200	3.87	0.04
28	0.224	4.16	0.04
29	0.251	4.35	0.12
30	0.282	4.43	0.18
31	0.316	4.39	0.22
32	0.355	4.26	0.23
33	0.398	4.07	0.21
34	0.447	3.83	0.17
35	0.501	3.56	0.12
36	0.562	3.28	0.08
37	0.631	3.03	0.05
38	0.708	2.86	0.03
39	0.794	2.77	0.04
40	0.891	2.79	0.04
41	1.000	2.90	0.05
42	1.122	3.05	0.05
43	1.259	3.16	0.05
44	1.413	3.18	0.06
45	1.585	3.10	0.06
46	1.778	2.97	0.06
47	1.995	2.76	0.06
48	2.239	2.44	0.05
49	2.512	2.07	0.04
50	2.818	1.66	0.02
51	3.162	1.26	0.02
52	3.548	0.89	0.01
53	3.981	0.58	0.01
54	4.467	0.35	0.00
55	5.012	0.13	0.00
56	5.623	0.02	0.00
57	6.310	0.00	0.00
58	7.079	0.00	0.00
59	7.943	0.00	0.00
60	8.913	0.00	0.00
61	10.000	0.00	0.00
62	11.220	0.00	0.00
63	12.589	0.00	0.00
64	14.125	0.00	0.00
65	15.849	0.00	0.00
66	17.783	0.00	0.00
67	19.953	0.00	0.00
68	22.387	0.00	0.00
69	25.119	0.00	0.00
70	28.184	0.00	0.00
71	31.623	0.00	0.00
72	35.481	0.00	0.00
73	39.811	0.00	0.00
74	44.668	0.00	0.00
75	50.119	0.00	0.00
76	56.234	0.00	0.00
77	63.096	0.00	0.00
78	70.795	0.00	0.00
79	79.433	0.00	0.00
80	89.125	0.00	0.00
81	100.000	0.00	0.00
82	112.202	0.00	0.00
83	125.893	0.00	0.00
84	141.254	0.00	0.00
85	158.489	0.00	0.00
86	177.828	0.00	0.00
87	199.526	0.00	0.00
88	223.872	0.00	0.00
89	251.189	0.00	0.00
90	281.838	0.00	0.00
91	316.228	0.00	0.00
92	354.813	0.00	0.00
93	398.107	0.00	0.00
94	446.684	0.00	0.00
95	501.187	0.00	0.00
96	562.341	0.00	0.00
97	630.957	0.00	0.00
98	707.946	0.00	0.00
99	794.328	0.00	0.00
100	891.251	0.00	0.00
	1000.000		

Raw Data from the Mastersizer for the STUM HE (cold) recycle 2.

No	Size (µm)	Mean In%	1*S.D.
1	0.010	0.00	0.00
2	0.011	0.00	0.00
3	0.013	0.00	0.00
4	0.014	0.00	0.00
5	0.016	0.00	0.00
6	0.018	0.00	0.00
7	0.020	0.00	0.00
8	0.022	0.00	0.00
9	0.025	0.00	0.00
10	0.028	0.00	0.00
11	0.032	0.00	0.00
12	0.035	0.00	0.00
13	0.040	0.00	0.00
14	0.045	0.00	0.00
15	0.050	0.00	0.00
16	0.056	0.00	0.00
17	0.063	0.00	0.00
18	0.071	0.00	0.00
19	0.079	0.00	0.00
20	0.089	0.00	0.00
21	0.100	0.00	0.00
22	0.112	0.00	0.00
23	0.126	0.00	0.00
24	0.141	0.19	0.09
25	0.158	1.00	0.16
26	0.178	2.07	0.12
27	0.200	3.07	0.12
28	0.224	4.01	0.10
29	0.251	4.86	0.08
30	0.282	5.53	0.04
31	0.316	6.04	0.01
32	0.355	6.37	0.02
33	0.398	6.52	0.04
34	0.447	6.46	0.06
35	0.501	6.19	0.07
36	0.562	5.69	0.07
37	0.631	5.02	0.07
38	0.708	4.23	0.06
39	0.794	3.44	0.06
40	0.891	2.76	0.05
41	1.000	2.32	0.03
42	1.122	2.14	0.02
43	1.259	2.14	0.01
44	1.413	2.20	0.01
45	1.585	2.28	0.01
46	1.778	2.39	0.02
47	1.995	2.45	0.02
48	2.239	2.37	0.02
49	2.512	2.21	0.02
50	2.818	1.92	0.02
51	3.162	1.55	0.02
52	3.548	1.16	0.01
53	3.981	0.78	0.00
54	4.467	0.48	0.00
55	5.012	0.14	0.00
56	5.623	0.00	0.00
57	6.310	0.00	0.00
58	7.079	0.00	0.00
59	7.943	0.00	0.00
60	8.913	0.00	0.00
61	10.000	0.00	0.00
62	11.220	0.00	0.00
63	12.589	0.00	0.00
64	14.125	0.00	0.00
65	15.849	0.00	0.00
66	17.783	0.00	0.00
67	19.953	0.00	0.00
68	22.387	0.00	0.00
69	25.119	0.00	0.00
70	28.184	0.00	0.00
71	31.623	0.00	0.00
72	35.481	0.00	0.00
73	39.811	0.00	0.00
74	44.668	0.00	0.00
75	50.119	0.00	0.00
76	56.234	0.00	0.00
77	63.096	0.00	0.00
78	70.795	0.00	0.00
79	79.433	0.00	0.00
80	89.125	0.00	0.00
81	100.000	0.00	0.00
82	112.202	0.00	0.00
83	125.893	0.00	0.00
84	141.254	0.00	0.00
85	158.489	0.00	0.00
86	177.828	0.00	0.00
87	199.526	0.00	0.00
88	223.872	0.00	0.00
89	251.189	0.00	0.00
90	281.838	0.00	0.00
91	316.228	0.00	0.00
92	354.813	0.00	0.00
93	398.107	0.00	0.00
94	446.684	0.00	0.00
95	501.187	0.00	0.00
96	562.341	0.00	0.00
97	630.957	0.00	0.00
98	707.946	0.00	0.00
99	794.328	0.00	0.00
100	891.251	0.00	0.00
	1000.000		

Raw Data from the Mastersizer for the NoTUM (NoTUCoM v2) after 1 hour.

No	Size (µm)	Mean In%	1*S.D.
1	0.010	0.00	0.00
2	0.011	0.00	0.00
3	0.013	0.00	0.00
4	0.014	0.00	0.00
5	0.016	0.00	0.00
6	0.018	0.00	0.00
7	0.020	0.00	0.00
8	0.022	0.00	0.00
9	0.025	0.00	0.00
10	0.028	0.00	0.00
11	0.032	0.00	0.00
12	0.035	0.00	0.00
13	0.040	0.00	0.00
14	0.045	0.00	0.00
15	0.050	0.00	0.00
16	0.056	0.00	0.00
17	0.063	0.00	0.00
18	0.071	0.00	0.00
19	0.079	0.00	0.00
20	0.089	0.00	0.00
21	0.100	0.00	0.00
22	0.112	0.00	0.00
23	0.126	0.00	0.00
24	0.141	0.00	0.00
25	0.158	0.22	0.03
26	0.178	1.36	0.12
27	0.200	2.46	0.08
28	0.224	3.51	0.05
29	0.251	4.45	0.03
30	0.282	5.21	0.00
31	0.316	5.84	0.02
32	0.355	6.32	0.02
33	0.398	6.66	0.01
34	0.447	6.78	0.01
35	0.501	6.64	0.03
36	0.562	6.20	0.03
37	0.631	5.48	0.03
38	0.708	4.56	0.02
39	0.794	3.60	0.00
40	0.891	2.76	0.02
41	1.000	2.23	0.03
42	1.122	2.05	0.03
43	1.259	2.11	0.03
44	1.413	2.24	0.04
45	1.585	2.39	0.04
46	1.778	2.58	0.04
47	1.995	2.70	0.04
48	2.239	2.64	0.03
49	2.512	2.46	0.03
50	2.818	2.14	0.02
51	3.162	1.71	0.02
52	3.548	1.25	0.01
53	3.981	0.82	0.01
54	4.467	0.49	0.01
55	5.012	0.14	0.00
56	5.623	0.00	0.00
57	6.310	0.00	0.00
58	7.079	0.00	0.00
59	7.943	0.00	0.00
60	8.913	0.00	0.00
61	10.000	0.00	0.00
62	11.220	0.00	0.00
63	12.589	0.00	0.00
64	14.125	0.00	0.00
65	15.849	0.00	0.00
66	17.783	0.00	0.00
67	19.953	0.00	0.00
68	22.387	0.00	0.00
69	25.119	0.00	0.00
70	28.184	0.00	0.00
71	31.623	0.00	0.00
72	35.481	0.00	0.00
73	39.811	0.00	0.00
74	44.668	0.00	0.00
75	50.119	0.00	0.00
76	56.234	0.00	0.00
77	63.096	0.00	0.00
78	70.795	0.00	0.00
79	79.433	0.00	0.00
80	89.125	0.00	0.00
81	100.000	0.00	0.00
82	112.202	0.00	0.00
83	125.893	0.00	0.00
84	141.254	0.00	0.00
85	158.489	0.00	0.00
86	177.828	0.00	0.00
87	199.526	0.00	0.00
88	223.872	0.00	0.00
89	251.189	0.00	0.00
90	281.838	0.00	0.00
91	316.228	0.00	0.00
92	354.813	0.00	0.00
93	398.107	0.00	0.00
94	446.684	0.00	0.00
95	501.187	0.00	0.00
96	562.341	0.00	0.00
97	630.957	0.00	0.00
98	707.946	0.00	0.00
99	794.328	0.00	0.00
100	891.251	0.00	0.00
	1000.000		

Raw Data from the Mastersizer for the NoTUM (NoTUCoM v2) after 2 hours.

No	Size (µm)	Mean In%	1*S.D.
1	0.010	0.00	0.00
2	0.011	0.00	0.00
3	0.013	0.00	0.00
4	0.014	0.00	0.00
5	0.016	0.00	0.00
6	0.018	0.00	0.00
7	0.020	0.00	0.00
8	0.022	0.00	0.00
9	0.025	0.00	0.00
10	0.028	0.00	0.00
11	0.032	0.00	0.00
12	0.035	0.00	0.00
13	0.040	0.00	0.00
14	0.045	0.00	0.00
15	0.050	0.00	0.00
16	0.056	0.00	0.00
17	0.063	0.00	0.00
18	0.071	0.00	0.00
19	0.079	0.00	0.00
20	0.089	0.00	0.00
21	0.100	0.00	0.00
22	0.112	0.00	0.00
23	0.126	0.00	0.00
24	0.141	0.00	0.00
25	0.158	0.26	0.07
26	0.178	1.53	0.27
27	0.200	2.57	0.15
28	0.224	3.61	0.07
29	0.251	4.55	0.00
30	0.282	5.30	0.07
31	0.316	5.89	0.12
32	0.355	6.31	0.15
33	0.398	6.55	0.15
34	0.447	6.59	0.13
35	0.501	6.39	0.09
36	0.562	5.93	0.05
37	0.631	5.26	0.02
38	0.708	4.43	0.00
39	0.794	3.59	0.02
40	0.891	2.85	0.03
41	1.000	2.38	0.03
42	1.122	2.20	0.03
43	1.259	2.21	0.03
44	1.413	2.28	0.03
45	1.585	2.38	0.03
46	1.778	2.53	0.02
47	1.995	2.63	0.02
48	2.239	2.57	0.02
49	2.512	2.41	0.01
50	2.818	2.11	0.00
51	3.162	1.72	0.00
52	3.548	1.29	0.01
53	3.981	0.88	0.01
54	4.467	0.55	0.01
55	5.012	0.22	0.01
56	5.623	0.05	0.01
57	6.310	0.00	0.00
58	7.079	0.00	0.00
59	7.943	0.00	0.00
60	8.913	0.00	0.00
61	10.000	0.00	0.00
62	11.220	0.00	0.00
63	12.589	0.00	0.00
64	14.125	0.00	0.00
65	15.849	0.00	0.00
66	17.783	0.00	0.00
67	19.953	0.00	0.00
68	22.387	0.00	0.00
69	25.119	0.00	0.00
70	28.184	0.00	0.00
71	31.623	0.00	0.00
72	35.481	0.00	0.00
73	39.811	0.00	0.00
74	44.668	0.00	0.00
75	50.119	0.00	0.00
76	56.234	0.00	0.00
77	63.096	0.00	0.00
78	70.795	0.00	0.00
79	79.433	0.00	0.00
80	89.125	0.00	0.00
81	100.000	0.00	0.00
82	112.202	0.00	0.00
83	125.893	0.00	0.00
84	141.254	0.00	0.00
85	158.489	0.00	0.00
86	177.828	0.00	0.00
87	199.526	0.00	0.00
88	223.872	0.00	0.00
89	251.189	0.00	0.00
90	281.838	0.00	0.00
91	316.228	0.00	0.00
92	354.813	0.00	0.00
93	398.107	0.00	0.00
94	446.684	0.00	0.00
95	501.187	0.00	0.00
96	562.341	0.00	0.00
97	630.957	0.00	0.00
98	707.946	0.00	0.00
99	794.328	0.00	0.00
100	891.251	0.00	0.00
	1000.000		

Raw Data from the Mastersizer for the NoTUM (NoTUCoM v2) after 3 hours.

No	Size (µm)	Mean In%	1*S.D.
1	0.010	0.00	0.00
2	0.011	0.00	0.00
3	0.013	0.00	0.00
4	0.014	0.00	0.00
5	0.016	0.00	0.00
6	0.018	0.00	0.00
7	0.020	0.00	0.00
8	0.022	0.00	0.00
9	0.025	0.00	0.00
10	0.028	0.00	0.00
11	0.032	0.00	0.00
12	0.035	0.00	0.00
13	0.040	0.00	0.00
14	0.045	0.00	0.00
15	0.050	0.00	0.00
16	0.056	0.00	0.00
17	0.063	0.00	0.00
18	0.071	0.00	0.00
19	0.079	0.00	0.00
20	0.089	0.00	0.00
21	0.100	0.00	0.00
22	0.112	0.00	0.00
23	0.126	0.00	0.00
24	0.141	0.00	0.00
25	0.158	0.31	0.09
26	0.178	1.52	0.11
27	0.200	2.49	0.07
28	0.224	3.46	0.03
29	0.251	4.36	0.01
30	0.282	5.10	0.04
31	0.316	5.72	0.06
32	0.355	6.18	0.07
33	0.398	6.49	0.06
34	0.447	6.60	0.04
35	0.501	6.46	0.01
36	0.562	6.04	0.01
37	0.631	5.38	0.02
38	0.708	4.54	0.02
39	0.794	3.65	0.02
40	0.891	2.86	0.01
41	1.000	2.34	0.00
42	1.122	2.13	0.01
43	1.259	2.14	0.01
44	1.413	2.23	0.00
45	1.585	2.36	0.00
46	1.778	2.54	0.00
47	1.995	2.67	0.00
48	2.239	2.64	0.00
49	2.512	2.50	0.00
50	2.818	2.22	0.01
51	3.162	1.82	0.01
52	3.548	1.38	0.01
53	3.981	0.95	0.01
54	4.467	0.60	0.01
55	5.012	0.24	0.00
56	5.623	0.06	0.00
57	6.310	0.00	0.00
58	7.079	0.00	0.00
59	7.943	0.00	0.00
60	8.913	0.00	0.00
61	10.000	0.00	0.00
62	11.220	0.00	0.00
63	12.589	0.00	0.00
64	14.125	0.00	0.00
65	15.849	0.00	0.00
66	17.783	0.00	0.00
67	19.953	0.00	0.00
68	22.387	0.00	0.00
69	25.119	0.00	0.00
70	28.184	0.00	0.00
71	31.623	0.00	0.00
72	35.481	0.00	0.00
73	39.811	0.00	0.00
74	44.668	0.00	0.00
75	50.119	0.00	0.00
76	56.234	0.00	0.00
77	63.096	0.00	0.00
78	70.795	0.00	0.00
79	79.433	0.00	0.00
80	89.125	0.00	0.00
81	100.000	0.00	0.00
82	112.202	0.00	0.00
83	125.893	0.00	0.00
84	141.254	0.00	0.00
85	158.489	0.00	0.00
86	177.828	0.00	0.00
87	199.526	0.00	0.00
88	223.872	0.00	0.00
89	251.189	0.00	0.00
90	281.838	0.00	0.00
91	316.228	0.00	0.00
92	354.813	0.00	0.00
93	398.107	0.00	0.00
94	446.684	0.00	0.00
95	501.187	0.00	0.00
96	562.341	0.00	0.00
97	630.957	0.00	0.00
98	707.946	0.00	0.00
99	794.328	0.00	0.00
100	891.251	0.00	0.00
	1000.000		

Raw Data from the Mastersizer for the NoTUM (NoTUCoM v2) after 4 hours.

No	Size (µm)	Mean In%	1*S.D.
1	0.010	0.00	0.00
2	0.011	0.00	0.00
3	0.013	0.00	0.00
4	0.014	0.00	0.00
5	0.016	0.00	0.00
6	0.018	0.00	0.00
7	0.020	0.00	0.00
8	0.022	0.00	0.00
9	0.025	0.00	0.00
10	0.028	0.00	0.00
11	0.032	0.00	0.00
12	0.035	0.00	0.00
13	0.040	0.00	0.00
14	0.045	0.00	0.00
15	0.050	0.00	0.00
16	0.056	0.00	0.00
17	0.063	0.00	0.00
18	0.071	0.00	0.00
19	0.079	0.00	0.00
20	0.089	0.00	0.00
21	0.100	0.00	0.00
22	0.112	0.00	0.00
23	0.126	0.00	0.00
24	0.141	0.25	0.12
25	0.158	1.10	0.22
26	0.178	2.12	0.17
27	0.200	3.11	0.16
28	0.224	4.04	0.13
29	0.251	4.86	0.09
30	0.282	5.51	0.05
31	0.316	6.01	0.00
32	0.355	6.33	0.03
33	0.398	6.48	0.06
34	0.447	6.42	0.07
35	0.501	6.16	0.08
36	0.562	5.67	0.08
37	0.631	5.01	0.08
38	0.708	4.22	0.07
39	0.794	3.44	0.07
40	0.891	2.76	0.06
41	1.000	2.32	0.05
42	1.122	2.14	0.03
43	1.259	2.14	0.02
44	1.413	2.20	0.02
45	1.585	2.28	0.02
46	1.778	2.39	0.03
47	1.995	2.45	0.03
48	2.239	2.37	0.04
49	2.512	2.20	0.04
50	2.818	1.92	0.03
51	3.162	1.55	0.02
52	3.548	1.15	0.01
53	3.981	0.77	0.01
54	4.467	0.48	0.00
55	5.012	0.14	0.00
56	5.623	0.00	0.00
57	6.310	0.00	0.00
58	7.079	0.00	0.00
59	7.943	0.00	0.00
60	8.913	0.00	0.00
61	10.000	0.00	0.00
62	11.220	0.00	0.00
63	12.589	0.00	0.00
64	14.125	0.00	0.00
65	15.849	0.00	0.00
66	17.783	0.00	0.00
67	19.953	0.00	0.00
68	22.387	0.00	0.00
69	25.119	0.00	0.00
70	28.184	0.00	0.00
71	31.623	0.00	0.00
72	35.481	0.00	0.00
73	39.811	0.00	0.00
74	44.668	0.00	0.00
75	50.119	0.00	0.00
76	56.234	0.00	0.00
77	63.096	0.00	0.00
78	70.795	0.00	0.00
79	79.433	0.00	0.00
80	89.125	0.00	0.00
81	100.000	0.00	0.00
82	112.202	0.00	0.00
83	125.893	0.00	0.00
84	141.254	0.00	0.00
85	158.489	0.00	0.00
86	177.828	0.00	0.00
87	199.526	0.00	0.00
88	223.872	0.00	0.00
89	251.189	0.00	0.00
90	281.838	0.00	0.00
91	316.228	0.00	0.00
92	354.813	0.00	0.00
93	398.107	0.00	0.00
94	446.684	0.00	0.00
95	501.187	0.00	0.00
96	562.341	0.00	0.00
97	630.957	0.00	0.00
98	707.946	0.00	0.00
99	794.328	0.00	0.00
100	891.251	0.00	0.00
	1000.000		

Raw Data from the Mastersizer for the NoTUM- Non Top-Up Centrifugal Method, (NoTUCeM) after 1 hour.

No	Size (µm)	Mean In%	1*S.D.
1	0.010	0.00	0.00
2	0.011	0.00	0.00
3	0.013	0.00	0.00
4	0.014	0.00	0.00
5	0.016	0.00	0.00
6	0.018	0.00	0.00
7	0.020	0.00	0.00
8	0.022	0.00	0.00
9	0.025	0.00	0.00
10	0.028	0.00	0.00
11	0.032	0.00	0.00
12	0.035	0.00	0.00
13	0.040	0.00	0.00
14	0.045	0.00	0.00
15	0.050	0.00	0.00
16	0.056	0.00	0.00
17	0.063	0.00	0.00
18	0.071	0.00	0.00
19	0.079	0.00	0.00
20	0.089	0.00	0.00
21	0.100	0.00	0.00
22	0.112	0.00	0.00
23	0.126	0.00	0.00
24	0.141	0.00	0.00
25	0.158	0.22	0.03
26	0.178	1.36	0.11
27	0.200	2.46	0.07
28	0.224	3.50	0.05
29	0.251	4.44	0.03
30	0.282	5.20	0.00
31	0.316	5.83	0.02
32	0.355	6.31	0.02
33	0.398	6.64	0.01
34	0.447	6.77	0.01
35	0.501	6.63	0.02
36	0.562	6.19	0.03
37	0.631	5.48	0.03
38	0.708	4.56	0.02
39	0.794	3.60	0.00
40	0.891	2.76	0.02
41	1.000	2.24	0.02
42	1.122	2.06	0.03
43	1.259	2.12	0.03
44	1.413	2.25	0.03
45	1.585	2.40	0.04
46	1.778	2.59	0.04
47	1.995	2.71	0.03
48	2.239	2.65	0.03
49	2.512	2.47	0.02
50	2.818	2.14	0.02
51	3.162	1.71	0.02
52	3.548	1.25	0.01
53	3.981	0.82	0.01
54	4.467	0.49	0.01
55	5.012	0.14	0.00
56	5.623	0.00	0.00
57	6.310	0.00	0.00
58	7.079	0.00	0.00
59	7.943	0.00	0.00
60	8.913	0.00	0.00
61	10.000	0.00	0.00
62	11.220	0.00	0.00
63	12.589	0.00	0.00
64	14.125	0.00	0.00
65	15.849	0.00	0.00
66	17.783	0.00	0.00
67	19.953	0.00	0.00
68	22.387	0.00	0.00
69	25.119	0.00	0.00
70	28.184	0.00	0.00
71	31.623	0.00	0.00
72	35.481	0.00	0.00
73	39.811	0.00	0.00
74	44.668	0.00	0.00
75	50.119	0.00	0.00
76	56.234	0.00	0.00
77	63.096	0.00	0.00
78	70.795	0.00	0.00
79	79.433	0.00	0.00
80	89.125	0.00	0.00
81	100.000	0.00	0.00
82	112.202	0.00	0.00
83	125.893	0.00	0.00
84	141.254	0.00	0.00
85	158.489	0.00	0.00
86	177.828	0.00	0.00
87	199.526	0.00	0.00
88	223.872	0.00	0.00
89	251.189	0.00	0.00
90	281.838	0.00	0.00
91	316.228	0.00	0.00
92	354.813	0.00	0.00
93	398.107	0.00	0.00
94	446.684	0.00	0.00
95	501.187	0.00	0.00
96	562.341	0.00	0.00
97	630.957	0.00	0.00
98	707.946	0.00	0.00
99	794.328	0.00	0.00
100	891.251	0.00	0.00
	1000.000		

Raw Data from the Mastersizer for the NoTUM - Non Top-Up Centrifugal Method, (NoTUCeM) after 2 hours.

No	Size (µm)	Mean In%	1*S.D.
1	0.010	0.00	0.00
2	0.011	0.00	0.00
3	0.013	0.00	0.00
4	0.014	0.00	0.00
5	0.016	0.00	0.00
6	0.018	0.00	0.00
7	0.020	0.00	0.00
8	0.022	0.00	0.00
9	0.025	0.00	0.00
10	0.028	0.00	0.00
11	0.032	0.00	0.00
12	0.035	0.00	0.00
13	0.040	0.00	0.00
14	0.045	0.00	0.00
15	0.050	0.00	0.00
16	0.056	0.00	0.00
17	0.063	0.00	0.00
18	0.071	0.00	0.00
19	0.079	0.00	0.00
20	0.089	0.00	0.00
21	0.100	0.00	0.00
22	0.112	0.00	0.00
23	0.126	0.00	0.00
24	0.141	0.00	0.00
25	0.158	0.26	0.06
26	0.178	1.54	0.24
27	0.200	2.57	0.13
28	0.224	3.60	0.08
29	0.251	4.52	0.03
30	0.282	5.26	0.03
31	0.316	5.85	0.08
32	0.355	6.27	0.11
33	0.398	6.53	0.12
34	0.447	6.58	0.11
35	0.501	6.40	0.10
36	0.562	5.95	0.07
37	0.631	5.29	0.05
38	0.708	4.46	0.03
39	0.794	3.61	0.01
40	0.891	2.86	0.01
41	1.000	2.39	0.02
42	1.122	2.20	0.03
43	1.259	2.21	0.03
44	1.413	2.29	0.03
45	1.585	2.38	0.03
46	1.778	2.53	0.03
47	1.995	2.63	0.02
48	2.239	2.57	0.01
49	2.512	2.42	0.01
50	2.818	2.12	0.00
51	3.162	1.72	0.01
52	3.548	1.29	0.01
53	3.981	0.88	0.01
54	4.467	0.55	0.01
55	5.012	0.21	0.01
56	5.623	0.05	0.01
57	6.310	0.00	0.00
58	7.079	0.00	0.00
59	7.943	0.00	0.00
60	8.913	0.00	0.00
61	10.000	0.00	0.00
62	11.220	0.00	0.00
63	12.589	0.00	0.00
64	14.125	0.00	0.00
65	15.849	0.00	0.00
66	17.783	0.00	0.00
67	19.953	0.00	0.00
68	22.387	0.00	0.00
69	25.119	0.00	0.00
70	28.184	0.00	0.00
71	31.623	0.00	0.00
72	35.481	0.00	0.00
73	39.811	0.00	0.00
74	44.668	0.00	0.00
75	50.119	0.00	0.00
76	56.234	0.00	0.00
77	63.096	0.00	0.00
78	70.795	0.00	0.00
79	79.433	0.00	0.00
80	89.125	0.00	0.00
81	100.000	0.00	0.00
82	112.202	0.00	0.00
83	125.893	0.00	0.00
84	141.254	0.00	0.00
85	158.489	0.00	0.00
86	177.828	0.00	0.00
87	199.526	0.00	0.00
88	223.872	0.00	0.00
89	251.189	0.00	0.00
90	281.838	0.00	0.00
91	316.228	0.00	0.00
92	354.813	0.00	0.00
93	398.107	0.00	0.00
94	446.684	0.00	0.00
95	501.187	0.00	0.00
96	562.341	0.00	0.00
97	630.957	0.00	0.00
98	707.946	0.00	0.00
99	794.328	0.00	0.00
100	891.251	0.00	0.00
	1000.000		

Raw Data from the Mastersizer for the NoTUM- Non Top-Up Centrifugal Method, (NoTUCeM) after 3 hours.

No	Size (µm)	Mean In%	1*S.D.
1	0.010	0.00	0.00
2	0.011	0.00	0.00
3	0.013	0.00	0.00
4	0.014	0.00	0.00
5	0.016	0.00	0.00
6	0.018	0.00	0.00
7	0.020	0.00	0.00
8	0.022	0.00	0.00
9	0.025	0.00	0.00
10	0.028	0.00	0.00
11	0.032	0.00	0.00
12	0.035	0.00	0.00
13	0.040	0.00	0.00
14	0.045	0.00	0.00
15	0.050	0.00	0.00
16	0.056	0.00	0.00
17	0.063	0.00	0.00
18	0.071	0.00	0.00
19	0.079	0.00	0.00
20	0.089	0.00	0.00
21	0.100	0.00	0.00
22	0.112	0.00	0.00
23	0.126	0.00	0.00
24	0.141	0.00	0.00
25	0.158	0.29	0.03
26	0.178	1.63	0.12
27	0.200	2.59	0.08
28	0.224	3.59	0.05
29	0.251	4.51	0.02
30	0.282	5.25	0.02
31	0.316	5.86	0.04
32	0.355	6.31	0.05
33	0.398	6.60	0.05
34	0.447	6.68	0.03
35	0.501	6.51	0.01
36	0.562	6.07	0.01
37	0.631	5.39	0.01
38	0.708	4.53	0.01
39	0.794	3.64	0.01
40	0.891	2.85	0.02
41	1.000	2.33	0.03
42	1.122	2.10	0.02
43	1.259	2.10	0.01
44	1.413	2.17	0.00
45	1.585	2.28	0.00
46	1.778	2.44	0.00
47	1.995	2.56	0.01
48	2.239	2.51	0.00
49	2.512	2.38	0.00
50	2.818	2.10	0.00
51	3.162	1.72	0.01
52	3.548	1.30	0.01
53	3.981	0.89	0.01
54	4.467	0.56	0.01
55	5.012	0.22	0.01
56	5.623	0.05	0.01
57	6.310	0.00	0.00
58	7.079	0.00	0.00
59	7.943	0.00	0.00
60	8.913	0.00	0.00
61	10.000	0.00	0.00
62	11.220	0.00	0.00
63	12.589	0.00	0.00
64	14.125	0.00	0.00
65	15.849	0.00	0.00
66	17.783	0.00	0.00
67	19.953	0.00	0.00
68	22.387	0.00	0.00
69	25.119	0.00	0.00
70	28.184	0.00	0.00
71	31.623	0.00	0.00
72	35.481	0.00	0.00
73	39.811	0.00	0.00
74	44.668	0.00	0.00
75	50.119	0.00	0.00
76	56.234	0.00	0.00
77	63.096	0.00	0.00
78	70.795	0.00	0.00
79	79.433	0.00	0.00
80	89.125	0.00	0.00
81	100.000	0.00	0.00
82	112.202	0.00	0.00
83	125.893	0.00	0.00
84	141.254	0.00	0.00
85	158.489	0.00	0.00
86	177.828	0.00	0.00
87	199.526	0.00	0.00
88	223.872	0.00	0.00
89	251.189	0.00	0.00
90	281.838	0.00	0.00
91	316.228	0.00	0.00
92	354.813	0.00	0.00
93	398.107	0.00	0.00
94	446.684	0.00	0.00
95	501.187	0.00	0.00
96	562.341	0.00	0.00
97	630.957	0.00	0.00
98	707.946	0.00	0.00
99	794.328	0.00	0.00
100	891.251	0.00	0.00
	1000.000		

Raw Data from the Mastersizer for the NoTUM- Non Top-Up Centrifugal Method, (NoTUCeM)after 4 hours.

No	Size (µm)	Mean In%	1*S.D.
1	0.010	0.00	0.00
2	0.011	0.00	0.00
3	0.013	0.00	0.00
4	0.014	0.00	0.00
5	0.016	0.00	0.00
6	0.018	0.00	0.00
7	0.020	0.00	0.00
8	0.022	0.00	0.00
9	0.025	0.00	0.00
10	0.028	0.00	0.00
11	0.032	0.00	0.00
12	0.035	0.00	0.00
13	0.040	0.00	0.00
14	0.045	0.00	0.00
15	0.050	0.00	0.00
16	0.056	0.00	0.00
17	0.063	0.00	0.00
18	0.071	0.00	0.00
19	0.079	0.00	0.00
20	0.089	0.00	0.00
21	0.100	0.00	0.00
22	0.112	0.00	0.00
23	0.126	0.00	0.00
24	0.141	0.40	0.17
25	0.158	1.47	0.30
26	0.178	2.56	0.20
27	0.200	3.64	0.17
28	0.224	4.59	0.12
29	0.251	5.41	0.07
30	0.282	6.05	0.02
31	0.316	6.53	0.03
32	0.355	6.87	0.06
33	0.398	7.04	0.08
34	0.447	7.00	0.09
35	0.501	6.71	0.09
36	0.562	6.12	0.08
37	0.631	5.29	0.07
38	0.708	4.26	0.06
39	0.794	3.21	0.05
40	0.891	2.28	0.04
41	1.000	1.68	0.03
42	1.122	1.44	0.02
43	1.259	1.46	0.01
44	1.413	1.55	0.01
45	1.585	1.65	0.01
46	1.778	1.80	0.02
47	1.995	1.91	0.02
48	2.239	1.87	0.03
49	2.512	1.79	0.03
50	2.818	1.60	0.04
51	3.162	1.33	0.04
52	3.548	1.03	0.04
53	3.981	0.73	0.03
54	4.467	0.49	0.02
55	5.012	0.20	0.02
56	5.623	0.06	0.02
57	6.310	0.00	0.00
58	7.079	0.00	0.00
59	7.943	0.00	0.00
60	8.913	0.00	0.00
61	10.000	0.00	0.00
62	11.220	0.00	0.00
63	12.589	0.00	0.00
64	14.125	0.00	0.00
65	15.849	0.00	0.00
66	17.783	0.00	0.00
67	19.953	0.00	0.00
68	22.387	0.00	0.00
69	25.119	0.00	0.00
70	28.184	0.00	0.00
71	31.623	0.00	0.00
72	35.481	0.00	0.00
73	39.811	0.00	0.00
74	44.668	0.00	0.00
75	50.119	0.00	0.00
76	56.234	0.00	0.00
77	63.096	0.00	0.00
78	70.795	0.00	0.00
79	79.433	0.00	0.00
80	89.125	0.00	0.00
81	100.000	0.00	0.00
82	112.202	0.00	0.00
83	125.893	0.00	0.00
84	141.254	0.00	0.00
85	158.489	0.00	0.00
86	177.828	0.00	0.00
87	199.526	0.00	0.00
88	223.872	0.00	0.00
89	251.189	0.00	0.00
90	281.838	0.00	0.00
91	316.228	0.00	0.00
92	354.813	0.00	0.00
93	398.107	0.00	0.00
94	446.684	0.00	0.00
95	501.187	0.00	0.00
96	562.341	0.00	0.00
97	630.957	0.00	0.00
98	707.946	0.00	0.00
99	794.328	0.00	0.00
100	891.251	0.00	0.00
	1000.000		

Raw Data from the Mastersizer for the CFF (2 stages method) - before centrifuge and cross-flow.

No	Size (µm)	Mean In%	1*S.D.
1	0.010	0.00	0.00
2	0.011	0.00	0.00
3	0.013	0.00	0.00
4	0.014	0.00	0.00
5	0.016	0.00	0.00
6	0.018	0.00	0.00
7	0.020	0.00	0.00
8	0.022	0.00	0.00
9	0.025	0.00	0.00
10	0.028	0.00	0.00
11	0.032	0.00	0.00
12	0.035	0.00	0.00
13	0.040	0.00	0.00
14	0.045	0.00	0.00
15	0.050	0.00	0.00
16	0.056	0.00	0.00
17	0.063	0.00	0.00
18	0.071	0.00	0.00
19	0.079	0.00	0.00
20	0.089	0.00	0.00
21	0.100	0.00	0.00
22	0.112	0.00	0.00
23	0.126	0.01	0.02
24	0.141	0.63	0.02
25	0.158	1.80	0.07
26	0.178	2.77	0.09
27	0.200	3.84	0.13
28	0.224	4.79	0.14
29	0.251	5.62	0.14
30	0.282	6.26	0.12
31	0.316	6.74	0.09
32	0.355	7.03	0.07
33	0.398	7.13	0.05
34	0.447	7.01	0.04
35	0.501	6.65	0.03
36	0.562	6.01	0.01
37	0.631	5.17	0.00
38	0.708	4.17	0.02
39	0.794	3.19	0.04
40	0.891	2.33	0.06
41	1.000	1.77	0.07
42	1.122	1.54	0.07
43	1.259	1.52	0.07
44	1.413	1.57	0.07
45	1.585	1.62	0.08
46	1.778	1.72	0.08
47	1.995	1.76	0.08
48	2.239	1.67	0.08
49	2.512	1.54	0.07
50	2.818	1.33	0.06
51	3.162	1.06	0.05
52	3.548	0.78	0.04
53	3.981	0.53	0.02
54	4.467	0.33	0.00
55	5.012	0.10	0.01
56	5.623	0.00	0.00
57	6.310	0.00	0.00
58	7.079	0.00	0.00
59	7.943	0.00	0.00
60	8.913	0.00	0.00
61	10.000	0.00	0.00
62	11.220	0.00	0.00
63	12.589	0.00	0.00
64	14.125	0.00	0.00
65	15.849	0.00	0.00
66	17.783	0.00	0.00
67	19.953	0.00	0.00
68	22.387	0.00	0.00
69	25.119	0.00	0.00
70	28.184	0.00	0.00
71	31.623	0.00	0.00
72	35.481	0.00	0.00
73	39.811	0.00	0.00
74	44.668	0.00	0.00
75	50.119	0.00	0.00
76	56.234	0.00	0.00
77	63.096	0.00	0.00
78	70.795	0.00	0.00
79	79.433	0.00	0.00
80	89.125	0.00	0.00
81	100.000	0.00	0.00
82	112.202	0.00	0.00
83	125.893	0.00	0.00
84	141.254	0.00	0.00
85	158.489	0.00	0.00
86	177.828	0.00	0.00
87	199.526	0.00	0.00
88	223.872	0.00	0.00
89	251.189	0.00	0.00
90	281.838	0.00	0.00
91	316.228	0.00	0.00
92	354.813	0.00	0.00
93	398.107	0.00	0.00
94	446.684	0.00	0.00
95	501.187	0.00	0.00
96	562.341	0.00	0.00
97	630.957	0.00	0.00
98	707.946	0.00	0.00
99	794.328	0.00	0.00
100	891.251	0.00	0.00
	1000.000		

Raw Data from the Mastersizer for the CFF (2 stages method) - after centrifuge , before cross-flow.

No	Size (µm)	Mean In%	1*S.D
1	0.010	0.00	0.00
2	0.011	0.00	0.00
3	0.013	0.00	0.00
4	0.014	0.00	0.00
5	0.016	0.00	0.00
6	0.018	0.00	0.00
7	0.020	0.00	0.00
8	0.022	0.00	0.00
9	0.025	0.00	0.00
10	0.028	0.00	0.00
11	0.032	0.00	0.00
12	0.035	0.00	0.00
13	0.040	0.00	0.00
14	0.045	0.00	0.00
15	0.050	0.00	0.00
16	0.056	0.00	0.00
17	0.063	0.00	0.00
18	0.071	0.00	0.00
19	0.079	0.00	0.00
20	0.089	0.00	0.00
21	0.100	0.00	0.00
22	0.112	0.00	0.00
23	0.126	0.17	0.14
24	0.141	0.95	0.30
25	0.158	2.04	0.20
26	0.178	3.05	0.17
27	0.200	4.07	0.09
28	0.224	4.96	0.01
29	0.251	5.71	0.10
30	0.282	6.26	0.18
31	0.316	6.63	0.23
32	0.355	6.84	0.24
33	0.398	6.87	0.21
34	0.447	6.71	0.15
35	0.501	6.34	0.08
36	0.562	5.72	0.02
37	0.631	4.91	0.03
38	0.708	3.98	0.04
39	0.794	3.06	0.04
40	0.891	2.28	0.02
41	1.000	1.78	0.01
42	1.122	1.58	0.00
43	1.259	1.57	0.00
44	1.413	1.61	0.00
45	1.585	1.66	0.00
46	1.778	1.74	0.01
47	1.995	1.78	0.01
48	2.239	1.69	0.02
49	2.512	1.57	0.02
50	2.818	1.36	0.03
51	3.162	1.10	0.03
52	3.548	0.83	0.02
53	3.981	0.58	0.02
54	4.467	0.38	0.01
55	5.012	0.16	0.01
56	5.623	0.05	0.01
57	6.310	0.00	0.00
58	7.079	0.00	0.00
59	7.943	0.00	0.00
60	8.913	0.00	0.00
61	10.000	0.00	0.00
62	11.220	0.00	0.00
63	12.589	0.00	0.00
64	14.125	0.00	0.00
65	15.849	0.00	0.00
66	17.783	0.00	0.00
67	19.953	0.00	0.00
68	22.387	0.00	0.00
69	25.119	0.00	0.00
70	28.184	0.00	0.00
71	31.623	0.00	0.00
72	35.481	0.00	0.00
73	39.811	0.00	0.00
74	44.668	0.00	0.00
75	50.119	0.00	0.00
76	56.234	0.00	0.00
77	63.096	0.00	0.00
78	70.795	0.00	0.00
79	79.433	0.00	0.00
80	89.125	0.00	0.00
81	100.000	0.00	0.00
82	112.202	0.00	0.00
83	125.893	0.00	0.00
84	141.254	0.00	0.00
85	158.489	0.00	0.00
86	177.828	0.00	0.00
87	199.526	0.00	0.00
88	223.872	0.00	0.00
89	251.189	0.00	0.00
90	281.838	0.00	0.00
91	316.228	0.00	0.00
92	354.813	0.00	0.00
93	398.107	0.00	0.00
94	446.684	0.00	0.00
95	501.187	0.00	0.00
96	562.341	0.00	0.00
97	630.957	0.00	0.00
98	707.946	0.00	0.00
99	794.328	0.00	0.00
100	891.251	0.00	0.00
	1000.000		

Raw Data from the Mastersizer for the CFF (2 stages method) - after centrifuge and cross-flow.

No	Size (µm)	Mean In%	1*S.D.
1	0.010	0.00	0.00
2	0.011	0.00	0.00
3	0.013	0.00	0.00
4	0.014	0.00	0.00
5	0.016	0.00	0.00
6	0.018	0.00	0.00
7	0.020	0.00	0.00
8	0.022	0.00	0.00
9	0.025	0.00	0.00
10	0.028	0.00	0.00
11	0.032	0.00	0.00
12	0.035	0.00	0.00
13	0.040	0.00	0.00
14	0.045	0.00	0.00
15	0.050	0.00	0.00
16	0.056	0.00	0.00
17	0.063	0.00	0.00
18	0.071	0.00	0.00
19	0.079	0.00	0.00
20	0.089	0.00	0.00
21	0.100	0.00	0.00
22	0.112	0.01	0.02
23	0.126	0.36	0.46
24	0.141	1.14	0.52
25	0.158	2.16	0.30
26	0.178	3.07	0.30
27	0.200	3.99	0.18
28	0.224	4.77	0.08
29	0.251	5.41	0.02
30	0.282	5.86	0.12
31	0.316	6.15	0.21
32	0.355	6.27	0.29
33	0.398	6.26	0.35
34	0.447	6.07	0.39
35	0.501	5.72	0.41
36	0.562	5.18	0.39
37	0.631	4.51	0.34
38	0.708	3.74	0.27
39	0.794	3.01	0.17
40	0.891	2.39	0.07
41	1.000	2.02	0.02
42	1.122	1.91	0.07
43	1.259	1.97	0.09
44	1.413	2.06	0.08
45	1.585	2.14	0.06
46	1.778	2.22	0.04
47	1.995	2.25	0.03
48	2.239	2.14	0.04
49	2.512	1.97	0.06
50	2.818	1.69	0.09
51	3.162	1.35	0.12
52	3.548	0.99	0.13
53	3.981	0.66	0.12
54	4.467	0.40	0.11
55	5.012	0.14	0.07
56	5.623	0.02	0.03
57	6.310	0.00	0.00
58	7.079	0.00	0.00
59	7.943	0.00	0.00
60	8.913	0.00	0.00
61	10.000	0.00	0.00
62	11.220	0.00	0.00
63	12.589	0.00	0.00
64	14.125	0.00	0.00
65	15.849	0.00	0.00
66	17.783	0.00	0.00
67	19.953	0.00	0.00
68	22.387	0.00	0.00
69	25.119	0.00	0.00
70	28.184	0.00	0.00
71	31.623	0.00	0.00
72	35.481	0.00	0.00
73	39.811	0.00	0.00
74	44.668	0.00	0.00
75	50.119	0.00	0.00
76	56.234	0.00	0.00
77	63.096	0.00	0.00
78	70.795	0.00	0.00
79	79.433	0.00	0.00
80	89.125	0.00	0.00
81	100.000	0.00	0.00
82	112.202	0.00	0.00
83	125.893	0.00	0.00
84	141.254	0.00	0.00
85	158.489	0.00	0.00
86	177.828	0.00	0.00
87	199.526	0.00	0.00
88	223.872	0.00	0.00
89	251.189	0.00	0.00
90	281.838	0.00	0.00
91	316.228	0.00	0.00
92	354.813	0.00	0.00
93	398.107	0.00	0.00
94	446.684	0.00	0.00
95	501.187	0.00	0.00
96	562.341	0.00	0.00
97	630.957	0.00	0.00
98	707.946	0.00	0.00
99	794.328	0.00	0.00
100	891.251	0.00	0.00
	1000.000		

Raw Data from the Mastersizer for the CFF (1stage method) - before cross-flow.

No	Size (µm)	Mean In%	1*S.D.
1	0.010	0.00	0.00
2	0.011	0.00	0.00
3	0.013	0.00	0.00
4	0.014	0.00	0.00
5	0.016	0.00	0.00
6	0.018	0.00	0.00
7	0.020	0.00	0.00
8	0.022	0.00	0.00
9	0.025	0.00	0.00
10	0.028	0.00	0.00
11	0.032	0.00	0.00
12	0.035	0.00	0.00
13	0.040	0.00	0.00
14	0.045	0.00	0.00
15	0.050	0.00	0.00
16	0.056	0.00	0.00
17	0.063	0.00	0.00
18	0.071	0.00	0.00
19	0.079	0.00	0.00
20	0.089	0.00	0.00
21	0.100	0.00	0.00
22	0.112	0.00	0.00
23	0.126	0.00	0.00
24	0.141	0.49	0.12
25	0.158	1.52	0.22
26	0.178	2.40	0.15
27	0.200	3.32	0.13
28	0.224	4.10	0.08
29	0.251	4.75	0.02
30	0.282	5.25	0.03
31	0.316	5.62	0.06
32	0.355	5.90	0.08
33	0.398	6.07	0.08
34	0.447	6.10	0.06
35	0.501	5.94	0.04
36	0.562	5.56	0.02
37	0.631	4.98	0.00
38	0.708	4.25	0.01
39	0.794	3.50	0.01
40	0.891	2.84	0.00
41	1.000	2.42	0.01
42	1.122	2.27	0.01
43	1.259	2.29	0.02
44	1.413	2.35	0.02
45	1.585	2.42	0.02
46	1.778	2.52	0.02
47	1.995	2.57	0.01
48	2.239	2.46	0.01
49	2.512	2.26	0.02
50	2.818	1.94	0.03
51	3.162	1.53	0.03
52	3.548	1.11	0.04
53	3.981	0.72	0.04
54	4.467	0.42	0.05
55	5.012	0.12	0.02
56	5.623	0.00	0.00
57	6.310	0.00	0.00
58	7.079	0.00	0.00
59	7.943	0.00	0.00
60	8.913	0.00	0.00
61	10.000	0.00	0.00
62	11.220	0.00	0.00
63	12.589	0.00	0.00
64	14.125	0.00	0.00
65	15.849	0.00	0.00
66	17.783	0.00	0.00
67	19.953	0.00	0.00
68	22.387	0.00	0.00
69	25.119	0.00	0.00
70	28.184	0.00	0.00
71	31.623	0.00	0.00
72	35.481	0.00	0.00
73	39.811	0.00	0.00
74	44.668	0.00	0.00
75	50.119	0.00	0.00
76	56.234	0.00	0.00
77	63.096	0.00	0.00
78	70.795	0.00	0.00
79	79.433	0.00	0.00
80	89.125	0.00	0.00
81	100.000	0.00	0.00
82	112.202	0.00	0.00
83	125.893	0.00	0.00
84	141.254	0.00	0.00
85	158.489	0.00	0.00
86	177.828	0.00	0.00
87	199.526	0.00	0.00
88	223.872	0.00	0.00
89	251.189	0.00	0.00
90	281.838	0.00	0.00
91	316.228	0.00	0.00
92	354.813	0.00	0.00
93	398.107	0.00	0.00
94	446.684	0.00	0.00
95	501.187	0.00	0.00
96	562.341	0.00	0.00
97	630.957	0.00	0.00
98	707.946	0.00	0.00
99	794.328	0.00	0.00
100	891.251	0.00	0.00
	1000.000		

Raw Data from the Mastersizer for the CFF (1stage method)- after cross-flow

Dry weight Analysis

Table of Dry Weight Analysis- IPS= Initial Project Studies, STUM-WB=Top Up Recycle Method- Water Bath, STUM-HEA= Top Up Recycle Method- Heat Exchanger (Ambient), STUM-HEC= Top Up Recycle Method- Heat Exchanger (Cold), #= Recycle Number, NoTUCeM- Non Top-Up Centrifugal Method, NoTUCoM- Non Top-Up Continuous Method, CFF1- Cross Flow-Filtration (1 stage), CFF2- Cross Flow-Filtration (2 stages).

Raw data

Method	Weight of Lens	Lens +10ml	Dry Weight
Test Run	173.62	183.67	173.89
IPS-30%	173.60	183.64	173.95
IPS-60%	167.94	176.99	168.13
IPS-100%	161.92	170.72	162.05
STUM-WB-run1	173.57	182.40	173.75
STUM-WB-run1 #1	167.92	177.03	168.27
STUM-WB-run1 #2	113.86	121.87	114.09
STUM-WB-run1 #3	161.89	168.48	162.14
STUM-WB- run2	167.93	176.49	168.17
STUM-WB-run2 #1	167.92	176.12	168.15
STUM-WB-run2 #2	173.58	182.86	173.87
STUM-WB-run2 #3	173.56	182.48	173.93
STUM-WB-run3	167.93	176.34	168.13
STUM-WB-run3 #1	161.90	168.54	162.04
STUM-WB-run3 #2	173.56	182.56	173.87
STUM-WB-run3 #3	167.93	176.30	168.20
STUM-HEA-run1	173.56	181.31	173.74
STUM-HEA-run1 #1	161.91	169.61	162.10
STUM-HEA-run1 #2	161.90	169.57	162.10
STUM-HEA-run1 #3	173.56	180.08	173.74
STUM-HEA-run2	173.56	181.31	173.74
STUM-HEA-run2 #1	161.92	169.45	162.11
STUM-HEA-run2 #2	173.56	179.98	173.70
STUM-HEA-run2 #3	167.93	176.55	168.21
STUM-HEA-run3	161.90	169.85	162.04
STUM-HEA-run3 #1	167.93	176.52	168.19
STUM-HEA-run3 #2	173.56	180.53	173.74
STUM-HEA-run3 #3	173.56	180.67	173.81
STUM-HEC-run1	161.89	169.26	162.06
STUM-HEC-run1 #1	167.93	175.58	168.10
STUM-HEC-run1 #2	161.89	168.87	162.02
STUM-HEC-run2	161.89	169.26	162.06
STUM-HEC-run2 #1	167.93	175.58	168.10
STUM-HEC-run2 #2	161.89	168.87	162.02
STUM-HEC-run3	173.59	181.68	173.78
STUM-HEC-run3 #1	161.89	169.12	162.04
STUM-HEC-run3 #2	55.50	63.20	55.68

NoTUCeM-run1-1	173.60	181.52	173.78
NoTUCeM-run1- 2	167.93	176.38	168.09
NoTUCeM-run1- 3	137.09	145.56	137.23
NoTUCeM-run1 -4	173.59	181.72	173.65
NoTUCeM-run2 -1	167.90	177.20	168.11
NoTUCeM-run2 -2	173.54	181.74	173.65
NoTUCeM-run2 -3	161.88	170.92	162.01
NoTUCeM-run2 -4	167.91	176.81	167.96
NoTUCeM-run3 -1	137.1	145.16	137.28
NoTUCeM-run3 -2	113.86	121.83	114.01
NoTUCeM-run3 -3	55.50	62.80	55.62
NoTUCeM-run3 -4	173.57	181.70	173.66
NoTUCoM-run 1	173.57	183.08	173.78
NoTUCoM-run 2	167.93	176.88	168.12
NoTUCoM-run 3	167.93	176.77	168.12
NoTUCoM v2- run 1	167.93	177.08	168.10
NoTUCoM v2- run 2	173.60	181.90	173.75
NoTUCoM v2- run 3	167.92	176.88	168.09
CFF2- conc AFE	161.90	169.85	162.89
CFF2- EWP soln	173.59	181.75	173.90
CFF1- Conc AFE 1	161.91	169.24	162.36
CFF1- EWP Soln 1	167.93	175.78	168.02
CFF1- Conc AFE 2	173.58	181.65	174.07
CFF1- EWP Soln 2	137.11	145.62	137.20